

Editor-in-Chief B.E.Paton

EDITORIAL BOARD

Yu.S. Borisov,
B.V. Khitrovskaya (*exec. secretary*),
V.F. Khorunov, V.V. Knysh, I.V. Krivtsun,
S.I. Kuchuk-Yatsenko (*vice-chief editor*),
Yu.N. Lankin, V.N. Lipodaev (*vice-chief editor*),
L.M. Lobanov, A.A. Mazur,
O.K. Nazarenko, I.K. Pokhodnya,
V.D. Poznyakov, I.A. Ryabtsev,
K.A. Yushchenko,
A.T. Zelnichenko (*exec. director*)
(*Editorial Board Includes PWI Scientists*)

**INTERNATIONAL EDITORIAL
COUNCIL**

N.P. Alyoshin
N.E. Bauman MSTU, Moscow, Russia
V.G. Fartushny
Welding Society of Ukraine, Kiev, Ukraine
Guan Qiao
Beijing Aeronautical Institute, China
V.I. Lysak
Volgograd State Technical University, Russia
B.E. Paton
PWI, Kiev, Ukraine
Ya. Pilarczyk
Welding Institute, Gliwice, Poland
U. Reisgen
Welding and Joining Institute, Aachen, Germany
O.I. Steklov
Welding Society, Moscow, Russia
G.A. Turichin
St.-Petersburg State Polytechn. Univ., Russia
M. Zinigrad
College of Judea & Samaria, Ariel, Israel
A.S. Zubchenko
OKB «Gidropress», Podolsk, Russia

Founders

E.O. Paton Electric Welding Institute
of the NAS of Ukraine
International Association «Welding»

Publisher

International Association «Welding»

Translators

A.A. Fomin, O.S. Kurochko,
I.N. Kutianova
Editor
N.A. Dmitrieva
Electron galley
D.I. Sereda, T.Yu. Snegiryova

Address

E.O. Paton Electric Welding Institute,
International Association «Welding»
11, Bozhenko Str., 03680, Kyiv, Ukraine
Tel.: (38044) 200 60 16, 200 82 77
Fax: (38044) 200 82 77, 200 81 45
E-mail: journal@paton.kiev.ua
www.patonpublishinghouse.com

State Registration Certificate
KV 4790 of 09.01.2001
ISSN 0957-798X

Subscriptions

\$348, 12 issues per year,
air postage and packaging included.
Back issues available.

All rights reserved.

This publication and each of the articles contained
herein are protected by copyright.
Permission to reproduce material contained in this
journal must be obtained in writing from the
Publisher.

CONTENTS

The 80th Anniversary of the E.O. Paton Electric Welding
Institute of the NAS of Ukraine 2

SCIENTIFIC AND TECHNICAL

*Paton B.E., Lobanov L.M., Lysak V.L., Knysh V.V.,
Pavlovsky V.I., Prilutsky V.P., Timoshenko A.N.,
Goncharov P.V. and Guan Qiao.* Deformation-free
welding of stringer panels of titanium alloy VT20 6

Krikent I.V., Krivtsun I.V. and Demchenko V.F.
Simulation of electric arc with refractory cathode and
evaporating anode 17

*Lankin Yu.N., Ryabtsev I.A., Soloviov V.G., Chernyak
Ya.P. and Zhdanov V.A.* Effect of electric parameters of
arc surfacing using flux-cored wire on process stability
and base metal penetration 25

INDUSTRIAL

*Yushchenko K.A., Kozulin S.M., Lychko I.I. and Kozulin
M.G.* Joining of thick metal by multipass electroslag
welding 30

Korotynsky A.E., Drachenko N.P. and Shapka V.A.
Peculiarities of application of supercapacitors in
devices for pulse welding technologies 34

*Lebedev V.A., Maksimov S.Yu., Pichak V.G. and
Zajnulín D.I.* Automatic machine for wet underwater
welding in confined spaces 39

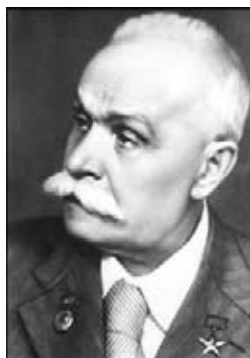
Levchenko O.G., Kuleshov V.A. and Arlamov A.Yu.
Sanitary-hygienic evaluation of noise in manual arc
welding with covered electrodes 45

INFORMATION

The 55th Anniversary of the Experimental Design
Technological Bureau of the E.O. Paton Electric
Welding Institute 49

Paton Turbine Technologies — new name of a
well-known company 51

THE 80th ANNIVERSARY OF THE E.O. PATON ELECTRIC WELDING INSTITUTE OF THE NAS OF UKRAINE



Academician
E.O. Paton

The Institute of Electric Welding was founded as a member of the All-Ukrainian Academy of Sciences by academician Evgeny O. Paton in 1934 on the facility of electric welding laboratory at the Chair of Engineering Constructions of the AUAS and Electric Welding Committee. Formation and all the further activity of the Electric Welding Institute are associated with the name of the

outstanding engineer and scientist. He defined the main scientific trends of the Institute in the field of welding technology and welded structures, which are also urgent nowadays.

E.O. Paton could predict the great progress in the development of technology of electric welding of metals. The convinced confirmation of this scientific prediction is the indisputable fact that welding today is the leading technological process of permanent joining of metallic and non-metallic materials. This was due to the great contribution of the Institute staff during 80 years of its activity.

At the first stage the specialists of the Institute proved the feasibility of manufacture of welded structures, being not inferior to riveted ones as to their strength and reliability and by some characteristics even significantly surpassing them. This served a basis for the further mass application of welding. In the 1930s the conception of arc welding as a metallurgical process was scientifically grounded at the Institute and investigations for its automation were carried out under supervision of E.O. Paton. By 1940 the development of high-efficient process of submerged arc welding was finalized and implementation at plants of the country was started. During the World War II the automatic submerged arc welding conquered the decisive importance. Directly in the tank plant shops in the Urals the Institute specialists developed and implemented the technology of automatic welding of armored steel, which made it possible to create the production line for manufacture of welded bodies of tanks T-34 and to mechanize the welding of other military machinery.

Pre-war and war stages in the Institute activity were the period of establishment of scientific school, the convinced authority of which was confirmed by awarding the Institute with name of Evgeny O. Paton in 1945.

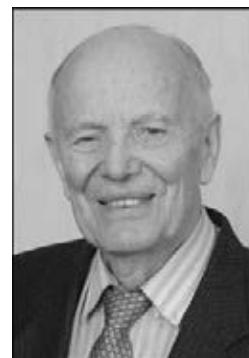
The solution of main problem, i.e. improvement of efficiency and level of mechanization of welding jobs, required the continu-

ous widening of research works at the Institute for searching new methods and techniques of mechanized welding, naturally, without minimizing of works on increasing the rational fields of application of submerged arc welding. Search for feasibility of submerged arc welding of welds located in various spatial positions was finalized by the development under supervision of E.O. Paton of forced formation of weld to start the mechanization of arc welding of welds in vertical plane.

On August 12, 1953 E.O. Paton, the man added a vivid page to the history of national science and technology, died at the 84th year of his life. Since 1953 until now academician Boris E. Paton, his son, is the Director of the Institute.

One of the most significant achievements of the Institute at the beginning of the 1950s became the development of new technology of fusion melting of thick metal, namely an electroslag welding, which changed radically the technology of manufacture of heavy frameworks, boilers, hydraulic units and other unique rolled-welded and cast-welded structures. Its application allowed producing the high-quality welded joints within the wide range of thicknesses.

Later, the CO₂ welding method with thin wire was developed, finding the wide spreading in industry and providing the significant growth in level of mechanization of welding jobs. The further development of gas electric consumable electrode welding became the development of process and equipment for pulsed-arc welding, welding in mixtures of active and inert gases.



Academician
B.E. Paton



At the end of the 1950s the investigations in the field of electron beam welding actively started at the Institute. The efforts of scientists were directed to investigation of physical-metalurgical processes under the action of powerful (up to 100 kW) sharply-focused beam of electrons to thick-sheet (150–200 mm) structural materials. The problem of a particular importance and successfully solved by the Institute concerned the development of technology of closing the circular welds to prevent the root defects in the form of cavities, pores and discontinuities. Over the recent 10 years more than 60 sets of different types of equipment for EBW, including the installations with a volume of vacuum chambers of up to 100 m³, were put into industrial operation.

The next stage in development of the beam technology was its application for welding and cutting by a laser. The systematic investigations are carried out in the field of pulsed and continuous laser welding. During recent years the specialists of the Institute have developed the hybrid laser–arc and laser–plasma sources of heating.

Investigations were progressing on all the main trends of pressure welding, such as flash-butt welding and resistance welding, spot welding, friction and diffusion welding.

Physical and technological peculiarities of new technological processes of flash-butt welding were studied, the systems of automatic control and diagnostics of quality of joints were developed. On the basis of new technologies the manufacture of several generations of specialized and universal machines for flash-butt welding of a large assortment of parts of cross-section area of up to 200,000 mm² of low-alloy and high-strength steels, as well as of aluminium, titanium, chromium and copper alloys, was organized and mastered. Machines for welding of rails of various categories under field and stationary conditions,

serially manufactured at Kakhovka Plant of Electric Welding Equipment, machines for welding of pipes of diameter from 150 up to 1420 mm in construction of main pipelines, installations for welding of elements of aerospace engineering structures found the widest spreading. Equipment for flash-butt welding of rails is exported to many countries of the world.

Over many years the Institute carries out investigations on space welding. In 1969, V. Kubasov, the pilot-cosmonaut, performed the first in the world unique experiment on the board of spaceship «Soyuz-6» for welding by electron beam, plasma and consumable electrode in the unit «Vulkan», designed and manufactured at the PWI. Thus, the beginning of the space technology was started, having the great importance in the program of space exploration. In 1984 the extremely important experiment, prepared by the PWI, was carried out on the board of orbital station in open space. Cosmonauts S. Savitskaya and V. Dzhanibekov performed for the first time welding, brazing, cutting and spraying in open space by using the hand electron beam tool.

In parallel, such a complex problem was solved at the Institute as mechanization of underwater arc welding, which acquired a great importance in exploration of the World ocean shelf. Specialists of the Institute designed the equipment for mechanized arc welding and cutting by a special flux-cored wire at depths of up to 200 m.

The intensive growth of the advanced engineering is accompanied by a continuous widening of assortment of structural metals and alloys for welded structures. During investigations for study of processes proceeding in the weld the new welding consumables were developed: electrodes, metal and flux-cored wires, fluxes and gas mixtures.

Investigations and research works in the field of strength of welded joints and structures are



the traditional directions in the Institute research area, started by E.O. Paton. Today, these investigations are of an integrated nature, making it possible to develop the new effective methods of improvement of reliability of critical engineering structures at static and cyclic loading. The problem of manufacture of reliable welded structures covers also the problems of selection of materials, rational design solutions, technologies of manufacture and erection, reduction of metal intensity, which are solved successfully by the Institute in collaboration with many industrial organizations and enterprises. During recently, the intensive works are carried out for improvement of reliability, durability and service life of welded structures, as well as development of effective methods of their diagnostics.

At the present time the systems of continuous monitoring, developed at the Institute, are successfully operated at a number of petrochemical enterprises with use of Internet system of communication. This allows developing the monitoring and controlling systems, which give the opportunity to observe the state of structure from a common specialized diagnostic center independently of its location site.

Since the 1950s by the initiative of academician Boris E. Paton the searching investigations and experimental developments were started for revealing the feasibility of applying the welding sources of heating for producing metals and alloys of ultra-high quality and reliability, on the basis of which one more basic scientific direction in the Institute activity was formed — a special electrometallurgy. Efforts and successes of the Institute team in this new field provided the noticeable progress in the development of the advanced quality metallurgy.

The new electrometallurgical processes include, first of all, the electroslag remelting of consumable electrode into a water-cooled mould. Fundamental studies of the electroslag process, its physical-chemical, metallurgical and electro-technical features provided the advanced positions of the Institute in the development and application of electroslag technology, including remelting, surfacing, casting, hot topping, etc.

During recent years, a complex of research works was carried out at the Institute, serving as a base for the development of new generation of electroslag technologies, based on producing ingots and billets directly from molten metal without remelting of consumable electrodes. These technologies are patented in Ukraine and abroad and realized in industry. In particular, a unique complex for production of bimetal mill rolls was manufac-

tured at Novo-Kramatorsk Machine-Building Works on the basis of these technologies.

Two more electrometallurgical technologies were developed at the Institute: plasma-arc and electron beam. Development of technique and technology of these remelting processes was carried out in parallel with fundamental investigations of physical-metallurgical peculiarities of refining in controllable atmosphere or vacuum and processes of crystallization of steels, complexly-alloyed alloys, non-ferrous and refractory metals.

Due to systematic investigations of high-temperature gas-metal systems the plasma-arc remelting opened up the wide opportunities for production of the new class of structural materials, namely the high-nitrogen steels. Design of powerful plasmatrons for metallurgy allowed the Institute «to enter» the great metallurgy: new designs of units of ladle-furnace type of up to 100 t capacity were developed. The quality of metal, produced in these units, is not inferior to electroslag one.

Using the joint efforts of the Institute scientists, industry research institutes and manufacturers the advanced electron beam equipment was designed, and the technology of electron beam remelting in vacuum became indispensable process for producing the ultra-quality materials in metallurgy and machine building. The works in this direction are concentrated at the RE Center «Titan», established at the Institute.

Investigations of process of evaporation in vacuum of metallic and non-metallic materials and their subsequent condensation as a basis for vapor-phase metallurgy opened up the feasibility of producing coatings of different materials, including heat-resistant, refractory and composite ones with regulation of composition, structure and properties of deposited layers. Thickness of deposited layers is regulated, depending on purpose, from tens of micrometers up to several millimeters.

At the beginning of the 1980s the new scientific direction was formed at the Institute, dealing with the development of new processes and improvement of existing processes of thermal spraying of protective and wear-resistant coatings. At present, the Institute is developing almost all the advanced processes of spraying of protective and strengthening coatings. Technology and equipment have been developed for plasma-arc spraying of wear-resistant coatings, as well as installations for detonation spraying, which can operate with applying different working gases (acetylene, propane, hydrogen).

Result of investigations and developments in the field of building welded structures, made by

the PWI scientists, became the building of famous constructions, among them, first of all, the unique all-welded bridge, named after E.O. Paton, across the Dnieper river. Principles, approaches and design-technological solutions, used in its designing and construction, gave the way to a wide application of welding in bridge construction. This bridge was recognized by the American Welding Society as the outstanding welded structure of the XX century. The experience in construction of E.O. Paton bridge was used in construction of bridges across the Dnieper river in Kiev (Yuzhny, Moskovsky, Gavansky, Podolsko-Voskresensky, road and railway bridges) and bridges in Dnepropetrovsk and Zaporozhie, as well as bridge across the Smotrich river in Kamenetsk-Podolsk. In collaboration with Research Institute «Ukrproektstalkonstruktziya» the projects and technologies of construction have been worked out, which were realized successfully in construction of unique TV towers in Kiev, St.-Petersburg, Erevan, Tbilisi, Vitebsk, Kharkov. Technologies of welding, developed at the PWI, were applied successfully in construction of huge monument «Motherland», as well as in construction of objects of Euro-2012 in Kiev.

Over the recent years the great attention is paid to the realization of achievements of advanced science and technology in practical medicine. In the 1990s B.E. Paton gave an idea to apply welding for joining of live tissues and organized a creative team of scientists of the PWI, A.A. Shalimov Institute of Surgery and Transplantation, Central Hospital of Security Services of Ukraine and other medical institutions. This cooperation allowed developing the new method of joining (welding) of soft live tissues. At the PWI the advanced equipment of several generations for welding of live tissues has been designed and manufactured already in industry. Method of electric welding of live tissues is applied in more than 50 clinics of Ukraine. Since 2001 more than 100,000 surgical operations of different profiles were made and more than 130 new surgical procedures have been developed and used in practice.

Owing to the combination of purposeful fundamental theoretical investigations with engineering-applied developments, close creative relations with industrial enterprises in realization of technological innovations the Institute transformed for the past 80 years of its activity into the largest center in the field welding and related technologies in the country and world.

Today, the PWI staff is 1560 persons. The scientific potential of the Institute is 440 scientists, among which 8 academicians and 4 corresponding members of the NAS of Ukraine, 72 Dr. of Techn. Sci. and more than 200 Candidates of Techn. Sci.

Results of works of the Institute are confirmed by licenses and received patents, more than 150 licenses have been sold to the USA, Germany, Japan, Russia, Sweden, France, China, etc. About 2600 patents of Ukraine and near and far foreign countries, as well as more than 6500 Author's Certificates were received.

For the years of the PWI activity more than 60 most outstanding developments, fulfilled and implemented in national economy by the Institute specialists in collaboration with industrial teams, were awarded by the Lenin and State Prizes, and also by various Prizes of Ukraine.

The Institute supports international relations with leading welding centers in Europe, USA, Asia and is the member of the International Institute of Welding and European Federation of Welding.

Results of investigations of scientists of the Institute are published in journals «Avtomaticheskaya Svarka», «Tekhnicheskaya Diagnostika i Nerazrushayushchy Kontrol», «Sovremennaya Elektrometallurgiya», «The Paton Welding Journal», which have a wide reading audience. Monographs, subject collections, proceedings of the conferences, handbooks and other book products are also published at the Institute. Specialized councils are working at the PWI for defending the theses for degrees of Dr. or Candidate of Techn. Sci. The associates of the Institute defended more than 139 theses for Dr. of Techn. Sci. and about 720 theses for Candidate of Techn. Sci. The Institute organizes different conferences, seminars, exhibitions and takes part in the national and international exhibitions.

Due to implementation of the PWI developments in industry, the production of welding consumables and equipment has been created in Ukraine, that allows recognizing the welding as one of the few branches of economy having a stable positive foreign trade balance.

Over 80 years the Institute team has passed a glorious path. Today, this is a team of confederates, increasing the achievements of the Paton scientific school, which has the world recognition. All the activity is directed for the further progress of welding and related processes, as well for the solution of basic problems of industrial production.



DEFORMATION-FREE WELDING OF STRINGER PANELS OF TITANIUM ALLOY VT20

B.E. PATON¹, L.M. LOBANOV¹, V.L. LYSAK¹, V.V. KNYSH¹, V.I. PAVLOVSKY¹,
V.P. PRILUTSKY¹, A.N. TIMOSHENKO¹, P.V. GONCHAROV¹ and GUAN QIAO²

¹E.O. Paton Electric Welding Institute, NASU

11 Bozhenko Str., 03680, Kiev, Ukraine. E-mail: office@paton.kiev.ua

²BAMTRI, Beijing, China. E-mail: guang@cae.cn

Presented are the results of complex of carried out investigations on development of technology for welding by penetration welds of stringer panels of titanium alloy VT20 providing minimum residual stresses and deformations and also high values of their life at cyclic loads. On the full-scale specimens, simulating stringer panels, the penetration welds of T-joints were produced using three methods: electron beam, automatic argon-arc nonconsumable-electrode welding over the layer of activating flux, and automatic argon-arc nonconsumable-electrode welding with immersed arc. To prevent the residual welding stresses and deformations, preliminary elastic deformation of elements being welded was applied. The fatigue tests of all the types of specimens at longitudinal cyclic tension were carried out. The effect of heat treatment, impact mechanical treatment and repair-welding technologies on their fatigue life was also determined. Basing on the results of investigations of full-scale specimens the batches of stringer panels of 1200 mm length were manufactured and tested. The penetration welds, made by argon arc non-consumable electrode welding over the layer of activating flux using preliminary elastic deformation and high-frequency mechanical peening of welds, provide the higher values of fatigue life of welded stringer panels of high-strength titanium alloy VT20 as compared to electron beam welding and argon arc non-consumable electrode welding with immersed arc. The developed technology can be accepted for industrial production of welded stringer panels of high-strength titanium alloys. 14 Ref., 1 Table, 13 Figures.

Keywords: *thin-sheet welded structures, stringer stiffened panels, T-joints, penetration weld, residual stresses and deformations, preliminary elastic deformation, fatigue strength, high-frequency mechanical peening*

Stringer panels of light alloys find ever wider application in aircraft, aerospace engineering, shipbuilding and other fields of industry. The leading aircraft companies pay increased attention to designing of new and updating of existing technologies for manufacture of load-carrying thin-walled panels of high-strength titanium alloys. The characteristic example is application of stringer panels of titanium alloy VT20 of 2.5 mm thickness and up to 2000 mm length with argon-arc welded-on stiffeners of up to 25 mm height in the fighters of the Company «Sukhoi». After welding, the panels in a jig of stainless steel are subjected to thermal annealing in electric vacuum furnace for relieving the residual stresses and deformations [1].

In the Langley Research Center (NASA) for manufacture of such structures the method of braze-welding was developed. Using this method, at first Z-shaped stiffeners of titanium alloy are welded-on to the titanium sheet by spots through the interlayer of aluminium brazing alloy, and then the as-assembled structure of the

panel is placed to the vacuum chamber where brazing process takes place [1].

The structures of fighter F-14 of titanium alloy are manufactured using EBW providing high properties of a joint and process efficiency [2].

In any case, notwithstanding whether it refers to structures of titanium or other alloys, in thriving of aircraft builders to replace the riveted or milled thin-sheet stiffened structures by the structures with welded-on stiffeners, the technologists encounter the necessity to minimize the influence of such negative factors as residual stresses and deformations, which are present during welding process and greatly decrease the service characteristics of a product, first of all, accuracy and life [3].

To solve the problems of increasing the accuracy and fatigue characteristics of welded thin-sheet structures, such methods were developed at the E.O. Paton Electric Welding Institute as preliminary elastic deforming (PED) [4–7] and high-frequency mechanical peening (HFMP) [8], which are nowadays successfully applied for shipbuilding structures of aluminium alloys and steels [9]. It should be noted that unlike other methods of surface plastic deformation, for example, using shot blast treatment, HFMP is dis-



tinguished by its influence on a narrow fusion zone of 4–7 mm width. It forms compressive residual stresses in the surface layer of fusion zone and decreases concentration of stresses due to smoothing of transition from weld to base metal.

In work [9] the efficiency of PED application to control residual stresses and strains in welding of thin-sheet structures of titanium alloys was experimentally confirmed.

As a rule, in thin-sheet structures the joining of sheet with stiffeners is performed using fusion welding on the side of stiffener. Here, in most cases two-sided fillet welds are used, made by automatic argon-arc welding with tungsten electrode (TIG), EBW or laser welding. The technology of producing penetration welds in the structures, when T-joint is made by one pass only on the side of sheet by its penetration across the thickness and partial penetration of stiffener, is challenging and at the same time more complicated.

However, in arc welding the processes of weld pool formation, heating of near-weld zone and penetration of metal depend greatly on heat transfer and, respectively, heat conductivity of metal. Therefore, in the conventional arc welding the problems of producing the quality penetration welds of relatively large depth, narrow zones of residual tensile stresses and minimum distortions are obvious.

The processes of formation of penetration weld as compared to the butt weld are considerably different. This problem is essentially complicated in use of titanium alloys due to their thermal physical and physical-mechanical properties.

It is known that the main type of metallurgical defects of welded joints of titanium alloys, made both by arc as well as by beam welding methods, are pores. The pore formation in weld metal can be essentially decreased by a careful pre-welding preparation of surfaces of metal in the welding zone. According to the statistic data on defects in welded T-joints of titanium alloy VT20, the most frequent problem occurs with pores of a small size (0.1–0.4 mm).

The presence of pores in welds scarcely influences the behavior of welded joints at static loads, but considerably decreases life of their operation under the conditions of cyclic loads, sharply decreasing the fatigue strength. In cyclic tensile loads the sources of fracture of titanium alloys mostly arise from the inner weld defects. The longest life is observed in welds with carefully treated smooth transitions from reinforcement to base metal.

It is known that the process of deformation at cyclic loads causes the directed diffusion of

hydrogen into the zone, adjacent to pore, with increased stress. The origin of cracks can occur not only from the inner surface of pore but also in the nearest zone. Moreover, the growth of concentration of hydrogen at the surface of developing crack near the pore is by one order higher than at some distance from the pore.

The life of welds is mainly influenced not so significantly by the size of pores, but by their location zone. The pores far from the stress concentrators decrease the life by 2–3 times, whereas pores in the zone of stress concentration decrease the life by one order [10].

It was noted that application of surface cold working arrests the development of fatigue fracture sources from the defects close to the surface and increases the life of welded joint.

The successful application of welding technology with penetration welds in the panel structures is impossible without development of special measures, which could provide necessary strength and fatigue characteristics of welded joints and structures, low residual welding deformations and stresses, high accuracy of product manufacture alongside with high quality of welds.

The aim of this investigation was the development of technology for manufacture of welded stringer panels of titanium alloy VT20 providing their high accuracy and fatigue characteristics.

Titanium alloy VT20 relates to a pseudo- α' -alloys with the following content of alloying elements, %: 5.5–7.0 Al, 1.5–2.5 Zr, 0.5–2.0 Mo, 0.8–2.5 V. The coefficient of stability of β -phase in this alloy in annealed state depending on the content of alloying elements amounts to 5–7 %.

Phase transformations in the alloy during cooling in the process of welding are proceeding according to the martensite kinetics, $\beta \rightarrow \alpha$ transformation is observed. The increase in cooling rate results in refining of α' -phase formed in weld metal and HAZ, however this does not considerably influence the properties of joints at static tests.

The formed α' -structure is slightly alloyed by β -stabilizers, therefore, it is close by its properties to the common α' -structure with the corresponding alloying. The structure is not changed also in the process of long low-temperature heating. Therefore, annealing for the purposes of stabilizing of structure and hardening postweld heat treatment are not efficient. It is rationally to conduct annealing for relieving residual welding stresses, decreasing concentrations in the site of transition from the base metal to weld.

It should be noted that at the present time at the enterprises producing welded structures of titanium alloys, annealing remains the main

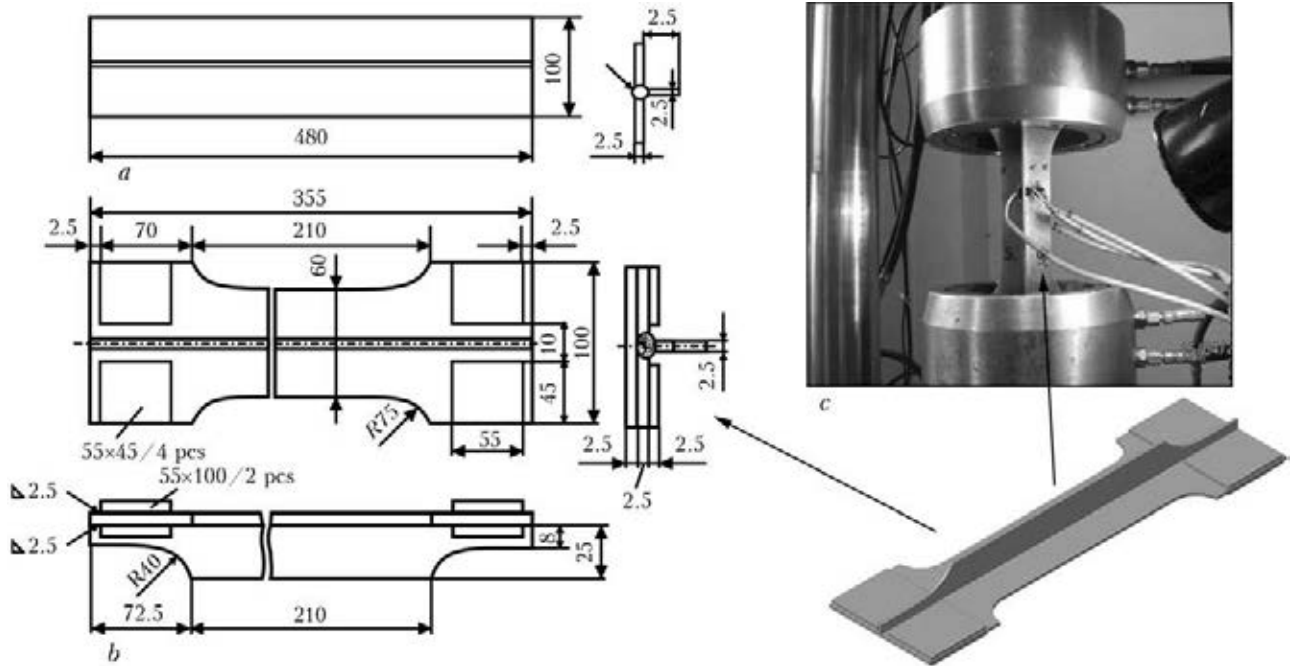


Figure 1. Welded T-specimen of VT20 alloy for the first stage of investigations: *a* – sketch of specimen; *b* – sketch of specimen of blade type; *c* – specimen for fatigue tests clamped in the machine

method used for prevention of residual stresses and deformations. Here, the main disadvantages of this technological process are great energy losses, restricted application due to the sizes of the treated parts and also high material capacity of the rigging, applied for fastening of annealed structures. In this connection, in the present investigations the additional aim was followed, i.e. a search of the alternative for the annealing operation.

The strength properties of weld metal in welding of alloy VT20 are close to the properties of base metal, and slight decrease in ductility is connected with the peculiarity of formation of cast structure. The size of grains in weld metal depends on the energy input introduced in welding. During slow cooling of joint after welding the ductility of cast metal decreases as a result of increase in grains size. At the same time, the high rates of cooling result in decrease of ductility because of formation of fine-acicular β -structure where α' -phase is absent [11].

The development of technology of deformation-free welding of stringer panels of alloy VT20 was carried out in two stages. At the first stage, on the experimented T-welded specimens the possible methods of welding-on of stiffener to the sheet by penetration weld in combination with different technological procedures, directed to improvement of accuracy of producing T-joints, were investigated. At the second stage, on the base of mastered technological variants the batch of stiffened panels was manufactured, which were subjected to tests at cyclic tension to confirm the possibility of producing large-size air-

craft panels, meeting the operation requirements without heat treatment application.

Welded T-joint specimens and stiffened panels for investigations had geometric parameters corresponding to the parameters of structures applied in the aircraft construction. During performance of tasks of the first stage the welding of T-specimens with one stiffener (Figure 1, *a*) was performed, of which specimens of blade type were cut out (Figure 1, *b*) for fatigue tests.

The design of stiffened panel for the second stage of investigations with four welded-on stringers, and specimen of blade type of it for fatigue tests, are given in Figure 2.

The load-carrying assembly rigging (Figure 3) of the first stage of works is designed for manufacture of T-specimens and provides a possibility of preliminary elastic tension of sheet and stiffeners being welded and also simultaneous sheet bending in the transverse direction. It was composed of three functional units: tension of sheet, tension of stiffener, and berth. The unit of tension of T-specimen sheet (see Figure 3, *b*) was designed according to the principle of a breaking lever, the length of which exceeds the distance between the edges of opposite clamps for the value of required tension of sheet.

The application of the breaking lever in the load-carrying rigging design allowed providing its minimum sizes and weight, due to which it was easily mated without additional resetting with welding equipment for different welding methods. Moreover, the rigging allowed performing nondestructive testing of quality of weld and

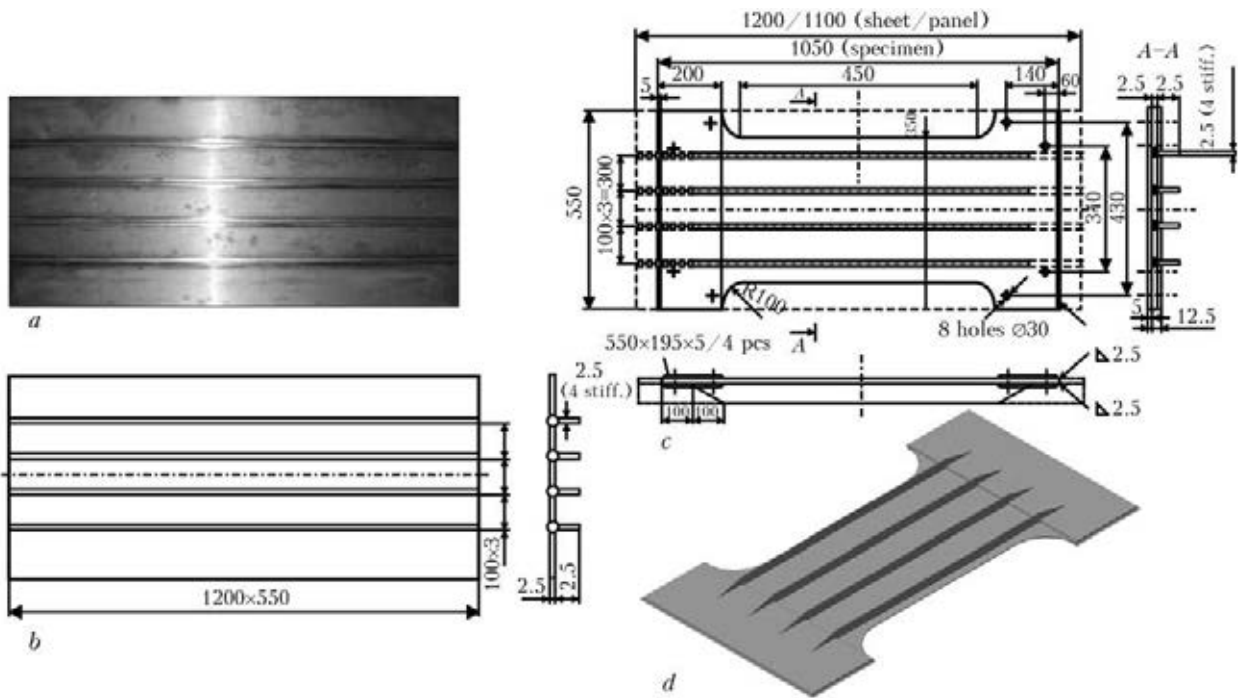


Figure 2. Welded stiffened panel of alloy VT20 for the second stage of investigations: *a* – general view; *b* – sketch of panel; *c* – sketch of specimen of blade type; *d* – appearance of specimen for fatigue tests

its simultaneous repair at detection of defect directly after welding without disassembly and in tensile state.

In the unit of tension of T-specimen stiffener (see Figure 3, *c*) the stiffener under tension is located between two traverses, receiving the load, and the tension of specimen is created by a screw jack and transmitted to the stiffener through its clamps.

The unit of berth (Figure 3, *d*) is manufactured in the form a rigid basement with raising lodgement, which serves as a support for units of tension and has a shape of reverse bending of sheet in the transverse direction, and its longitudinal guides are rectilinear.

In the position for welding the sheet was tightly pressed to the lodgement, and stiffener – to the sheet. Moreover, copper water-cooled backings were pressed to sheet and stiffener, which served for formation of fillets of weld root and its gas protection.

Load-carrying welding rigging of the second stage of works, designed for manufacture of stringer panels, is similar and composed of the same units as the rigging for specimens, but with the only difference that there are four units for tension of stiffeners in its composition, which are simultaneously installed below the panel sheet.

The laboratory equipment for argon-arc welding using penetration welds of stiffened specimens and panels under the conditions of PED (Figure 4) was also applied. In welding installation the power source Fronius Magic Ware 3300

was used and also welding head with improved gas protection of arc and cooling weld area, which was moved by a three-coordinate manipulator. The control of welding installation was performed by a programmable controller. The installation included also water cooling and gas cylinder equipment.

At the first stage of investigations, three methods of welding were selected: automatic argon-arc nonconsumable-electrode welding over the layer of flux (TIG-F), automatic argon-arc nonconsumable-electrode welding with immersed arc (TIG-I), and EBW. The selection of these methods was determined considering the experience of the PWI works on welding of titanium alloys and need in providing the complete penetration of the sheet, its reliable fusion with the stiffener, uniform formation of fillet transitions on the side of stiffener and also producing the weld reinforcement on the face side without undercuts.

In connection with some physical properties of titanium, certain difficulties in welding occur connected with providing quality formation of penetration weld root on both sides of stiffener with smooth mating of surfaces of stiffener and sheet. It is predetermined, on the one hand, by a high coefficient of surface tension of molten titanium (1.5 times higher than that of aluminium), which hinders a free sagging and formation of solidifying metal on the backing. On the other hand, a low viscosity of molten titanium facilitates the intensification of hydraulic processes in weld pool, that can not only influence

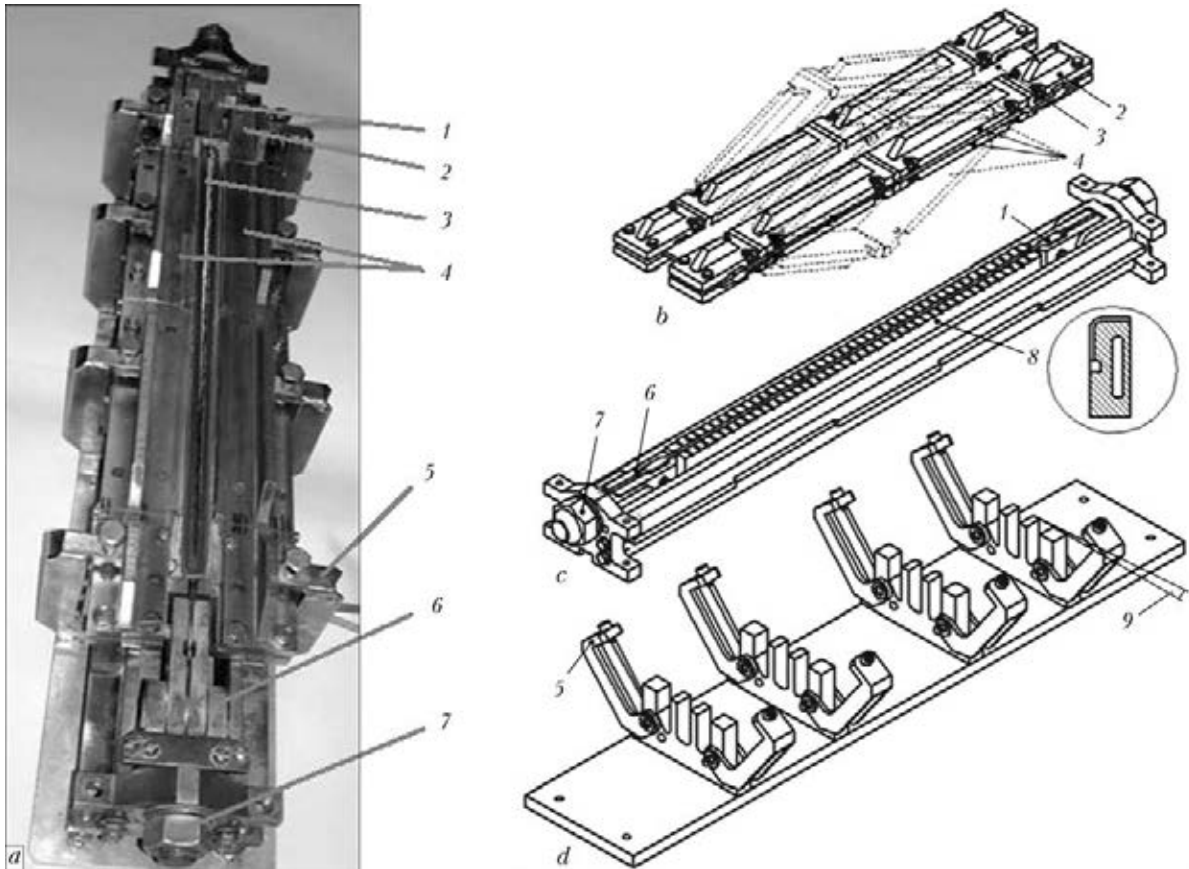


Figure 3. Load-carrying assembly rigging for welding of T-specimens under the conditions of PED: *a* – general view of rigging with specimen after welding; *b* – unit of sheet tension; *c* – unit of stiffener tension; *d* – unit of birth; 1, 2 – clamping of stiffener and sheet, respectively; 3 – sheet of T-specimen; 4 – breaking lever; 5 – clamps; 6 – jack rod; 7 – jack nut; 8 – copper water-cooled backing; 9 – angle of transverse bending of sheet

the structure of weld and formation of pores in it, but also influence the arc penetrability.

Therefore, in TIG welding of titanium by the surface arc a low coefficient of heat conductivity of titanium and low heat power factor predetermine producing of wide welds with undesirably small coefficient of weld shape (relation of pene-

tration width to weld depth). To produce the required complete penetration of joint using this method, the considerable increase in welding current and high heat input are required.

The TIG-I welding method is intended to increase the depth of penetration and differs from the method with surface arc by a peculiarity that the arc and also the electrode tip are submerged into the pool lower than the surface of sheet, which considerably complicates the welded joint formation. The conditions of burning of the arc itself and movement of metal in the pool are principally differed from the welding by surface arc. Actually, the whole arc is burning in a conical depression, the walls of which are washed by molten metal flows. It is transferred mostly from the front part of pool to its rear part, where its cooling takes place. In welding by immersed arc the molten metal of weld pool is not sufficiently involved to the total stirring, thus influencing the processes of shape and pores formation.

Using immersion the maximum efficiency of welding arc heat is attained, hydrodynamic processes and heat exchange in weld pool are intensified, however, heat and current loads on the electrode tip are abruptly increased. At decreased values of current or increased speeds the process

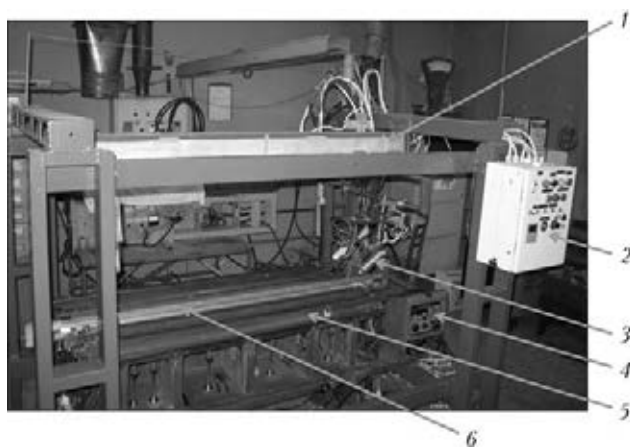


Figure 4. Laboratory equipment for argon-arc welding of stiffened panels under the conditions of PED: 1 – gentry with carriage for movement of welding head; 2 – control unit; 3 – welding head; 4 – power source; 5 – load-carrying assembly stand for PED of parts being welded; 6 – welded panel



of welding is characterized by frequent short-period short circuits and, respectively, sharp current fluctuations. They cause changes in the shape of electrode due to current erosion of its tip. Due to this the unpredicted jumps of welding process parameters and non-quality formations of welded T-joint occur. The width of weld and depth of penetration are changed. As the arc moves forward, the frequency of short circuits grows and total voltage drops. During this method there is a high probability of getting the unstable result at the same conditions of assembly and welding condition parameters. The process is very sensitive to the temporary welding deformations and it is used to stop because of common short circuiting, arc extinction and «freezing» of electrode at negligible deplanations of sheet, as a rule. Due to that the use of TIG-I welding in manufacture of structures with long welds is restricted.

The EBW method is characterized by comparatively high concentration of energy and, as a rule, is applied for joining of large thicknesses. While producing penetrated T-joints electron beam cuts through the sheet metal quite easily unlike the arc, providing the guaranteed melting of stiffener, which is under the sheet [12]. At the same time, the necessity in formation of radii of fillets (up to 2 mm) from below the sheet on both sides of stiffener imposes quite severe restrictions for selection of modes, as this leads to widening the pool on the joint face side. It is difficult to maintain in balance the wide pool on sheet and, as a result, the flaky surface of weld is formed with undercuts. The tendency to burn-outs and pores is also high near the root weld. To eliminate the defects in this case the additional smoothing of weld by repeated pass of unfocused beam is necessary.

The analysis of results of selection of EBW mode parameters for T-joints of VT20 alloy with penetration welds shows the following. The better conditions for formation of smooth fillets on the weld bottom are achieved during the modes with deep penetration of beam to the stiffener and high heat inputs, which are close to the process of sheet cutting. However, the better formation of weld surface on the face side is achieved at modes close to the process of smoothing. The

selection of optimal mode consists in finding the grounded compromise between these processes.

The method of TIG-F welding is designed for producing welds on titanium alloys of 0.8–6.0 mm thickness [13]. Before welding a layer of flux is deposited on the surface of parts being welded. The welding is performed in one pass without preparation of edges both with filler wire and also without it. The adding of halogenide fluxes into the welding zone causes constriction of arc, predetermined by physical processes, which occur in the arc column. Here the conditions of welded joint formation are changed in principle and technological capabilities of TIG-F welding are widened as compared to welding using surface arc.

The main advantages of TIG-F welding are increase of penetration depth at negligible decrease of input energy, decrease in width of weld and HAZ, prevention of porosity. Thus, input energy is 1.5–2 times decreased, width of welds is characterized by the small coefficient of weld shape. Metallurgical treatment of metal of weld pool by a liquid slag almost completely prevents the formation of pores in joint in welding of different titanium alloys. It is connected with the fact that as a result of metallurgical reactions occurred in a weld pool between flux and titanium the chemical binding of hydrogen occurs. Hydrogen, dissolved in weld pool molten metal, is bonded by fluorine to hydride-fluorides remaining in weld metal as microscopic slag inclusions. As the mechanical properties of weld metal are determined by the state of α' - and β -phases and not by interphase interlayers, then TIG-F welding provides sufficiently high level of properties of joints.

Besides, during this method the welding current is increased by 20–25 % above the optimum one, thus leading to the growth of width of reverse formation (by 30–50 %) at negligible increase (by 7–12 %) of weld width. This feature allows efficiently using this method to produce T-welded joints by through penetration of sheet with simultaneous melting of the stiffener.

Carrying out the first stage of investigations on the T-joint specimens with penetration welds the optimal modes of welding process were practiced. The mentioned modes for each of three methods of welding of alloy VT20 are given in the Table.

Method of welding	Welding speed, m/h	Filler diameter, mm	Protection	Beam current, mA	Accelerating voltage, kV	Focusing current, mA	Scanning amplitude, mm	Scanning frequency, Hz	Welding current, A	Arc voltage, V
EBW	14	1	Vacuum (10^{-5})	70	28	80	8	380	–	–
TIG-F	18	1	Argon	–	–	–	–	–	195	14.0–14.5
TIG-I	17	1	Same	–	–	–	–	–	250	11.2–11.5

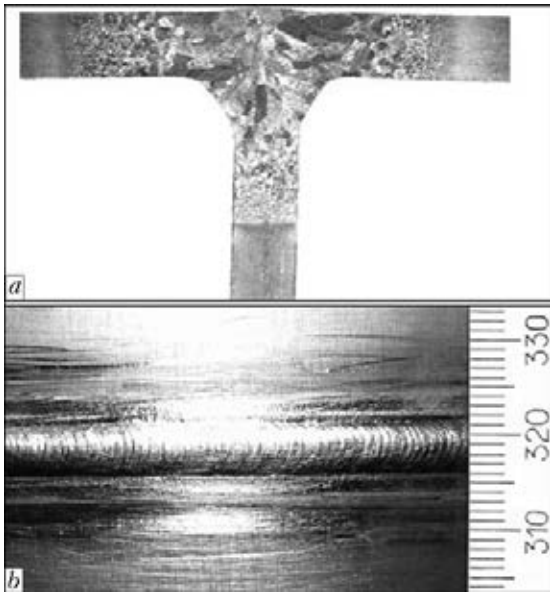


Figure 5. Macrosection (a) and appearance (b) of the face side of VT20 welded T-joint of 2.5 mm thickness of elements (TIG-F welding, flux ANT-25A)

Microstructures of welded joints produced using mentioned methods are quite of the same type. As is seen from Figure 5, microcracks and pores in weld and HAZ metal are absent. It should be noted that the length of HAZ is varied in the ranges of 2.5–3 mm, the weld width amounts to 6–7 mm. In the weld from the fusion zone to the center of welded joint the non-uniaxial grains are solidified, mostly columnar crystallites, elongated to the direction of heat removal. In the central part of joint the crystallites are formed, close to uniaxial shape, which grow together along the axis of weld at the angles of about 60–90°. The grains in weld are uniform by their size.

To strengthen the weld, filler wire VT1-00 (commercial titanium) of 1.0 mm diameter was used. In the experiments of the first stage the influence of adding of this filler wire to weld pool for decrease of content of alloyed elements in welded joint was investigated. The quantita-

tive evaluation of change in level of weld metal alloying was carried out using X-ray spectral analysis. The content of alloying elements, determined in the single spots, changed in the following ranges, %: 5.91–6.33 Al; 1.65–1.84 Zr; 0.77–1.24 Mo; 1.06–1.17 V, that corresponds to the content of alloying elements in alloy VT20.

To decrease welding stresses and deformations the PED of elements to be welded was applied. The sheet and stiffener were subjected to longitudinal tension at a preset level of stresses. Besides, the sheet was subjected to bending in the transverse direction as regards to angular welding deformations.

To set the optimal parameters of PED, the experiments on determination of dependence of residual stress-strain state of the specimen on the preliminary stresses of tension of sheet and stiffener were determined. It is seen from Figure 6 that residual welding stresses are considerably decreased with increase of preliminary tensile stresses to $0.5\sigma_{0.2}$. The residual welding deformations of shape changing in welded T-joints are also decreased during increase of initial tensile stresses. Reaching the level of initial stresses $(0.30\text{--}0.35)\sigma_{0.2}$ the residual welding distortions almost correspond to the values of deformations of initial sheets.

The reverse transverse bending of sheet is applied to eliminate completely the angular residual deformations. The reverse bending, determined experimentally, amounted to 0.75 of the value of residual angular deformations produced in welding of specimen in a free state.

In T-welded specimens (Figure 7), produced using EBW without application of PED at optimal parameters, the significant torsional deformations are seen and also those of longitudinal and transverse bending, while on the specimens applying PED the mentioned deformations are absent. In welding of specimens using TIG-I and

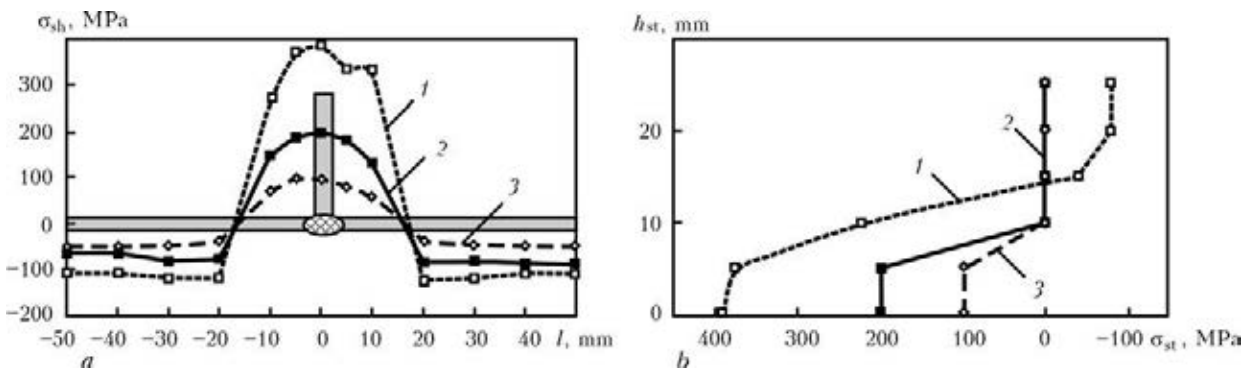


Figure 6. Diagrams of distribution of longitudinal residual stresses in the transverse section of EB-welded T-specimens of alloy VT20 with penetration weld in plate (a) and stiffener (b): 1 – welding of specimen in the rigging without tension; 2 – welding of specimen under the conditions of PED at $\sigma_{sh} = 220$ and $\sigma_{st} = 250$ MPa; 3 – welding of specimen under the conditions of PED at $\sigma_{sh} = \sigma_{st} = 450$ MPa



TIG-F methods under PED conditions and without it, the similar results were obtained.

Five specimens, produced applying three welding technologies, were subjected to PWHT. According to the recommendations accepted during manufacture of elements of welded aircraft structures of titanium alloys, PWHT was carried out in electric furnace in vacuum with automatic control of temperature (Figure 8). To prevent distortions of specimens during treatment the fixing rigging of stainless steel was applied. The applied mode was the following: heating to 650 °C in vacuum $1.33 \cdot 10^{-1}$ MPa for 2 h, furnace cooling in vacuum. Then all the specimens were treated by HFMP to increase the fatigue resistance (Figure 9). HFMP of specimens consisted in peening of fusion zones of welded joint both along the sheet as well as along the stiffener using ultrasonic impact tool, where hard-alloy strikers with radius rounding at the ends were used as the working part.

The challenging task in manufacture of thin-sheet structures of light alloys is the development of repair-welding technologies and evaluation of their influence on strength and life of welded joints. For T-joints, made with penetration weld, two types of defects are peculiar: absence of smooth transition (fillets) from sheet to stiffener, and also the presence of inner weld defects (pores, inclusions, microcracks). In this connection the evaluation of efficiency of two repair technologies was carried out. To eliminate the first type of defects, smoothing of the fillet using argon-arc nonconsumable-electrode welding was performed, and to eliminate the second one the defects were drilled

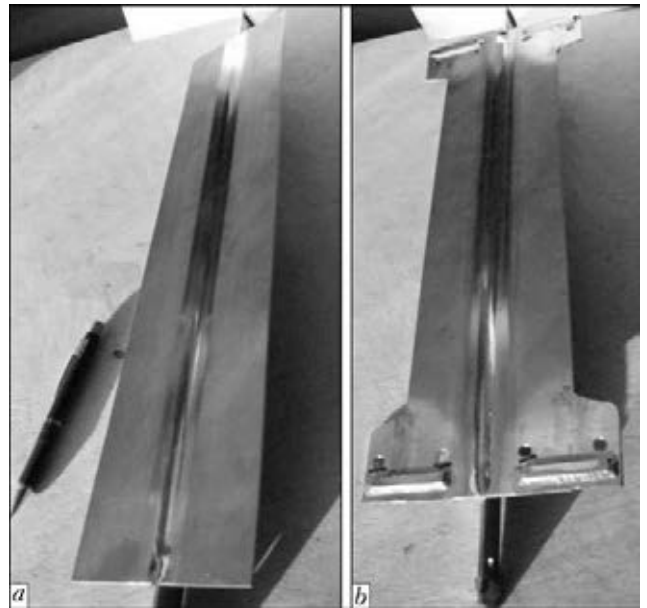


Figure 7. Appearance of T-specimens manufactured using EBW without (a) and with (b) PED of sheet at $\sigma_{sh} = 220$ and $\sigma_{st} = 250$ MPa

out, at first, on the face part of weld, and then they were filled by argon-arc welding using filler wire VT20 of 2.0 mm diameter. The repair welding was performed in special rigging providing fixation of the specimen and gas protection of surfaces of sheet and stiffener. After the repair HFMP of welded joints was performed.

For fatigue tests the specimens were fixed in clamps of testing machine URS-20 along the flat areas near the edges (without clamping of stiffener) (see Figure 1, a) and loaded by longitudinal tensile cyclic load with asymmetry of cycle $R_{\sigma} = 0.1$ at frequency of 7 Hz. The preset tensile

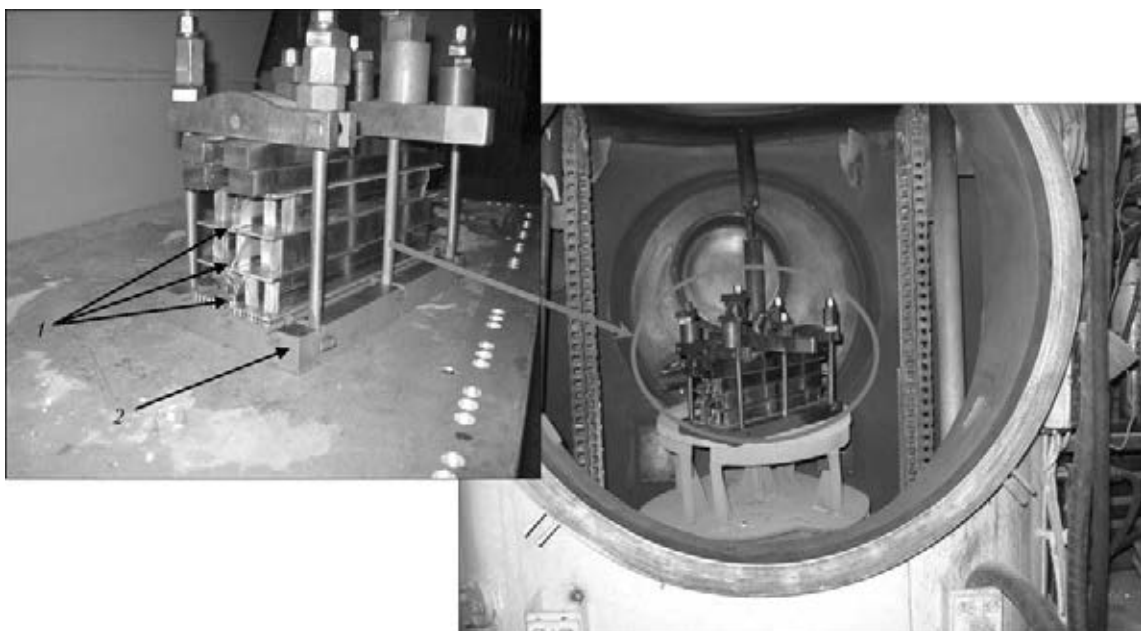


Figure 8. Heat treatment of welded specimens of alloy VT20 in electric vacuum furnace: 1 – T-specimens; 2 – rigging for annealing in furnace

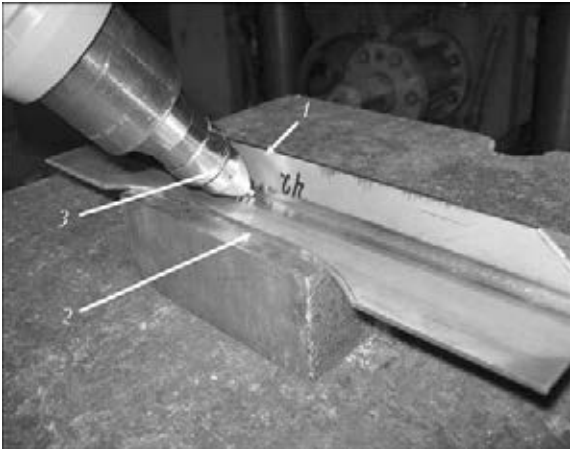


Figure 9. HFMP of specimen of VT20 alloy T-welded joint by hand impact tool: 1 – specimen; 2 – backing; 3 – working head of impact tool

force was selected so that the calculation level of maximum stresses of the cycle in specimen sheet part (not considering the stiffener) amounted to $0.5\sigma_{0.2}$ for alloy VT20. However, at the given scheme of loading the welded-on stiffener was subjected to the certain part of applied loading. As a result, the maximum cycle stresses in T-joint net-section were lower than calculated ones. To determine the real stresses, the strain gauges were used. The measurements performed by them showed that maximum stresses in the middle section of sheet amounted to 350 MPa.

The fatigue tests of specimens were carried out until their complete fracture, and corresponding amount of stresses was taken as a criterion for evaluation of investigated variant of welding technology and treatment.

In the summarized diagram in Figure 10 the test results for T-specimens, used in the experiments of the first type, are given. During tests the specimens were mainly fractured in the working sections 60 mm width. Here the fatigue crack was initiated in the sheet in the transition zone from weld to base metal and further was propagated to both directions until the complete fracture. The microfractographic examinations of the surface of fatigue fractures showed that the character of fracture in the zone of penetration weld was mostly tough-brittle and tough-quasi-brittle.

As the base variants, T-joints produced using one of three welding methods (specimens TIG-I-1, TIG-F-1, EBW-1) without PED were fatigue tested (see Figure 10). As is seen, welding method influences the level of life of tested specimens. The shortest life is observed in EBW and it is increased in TIG-I and TIG-F welding.

PED results in increase of cyclic life of welded specimens (TIG-I-2, TIG-F-2, EBW-2) up to twice as compared to the base variants.

Smoothing of weld legs decreases cyclic life of welded specimens, produced under the conditions of PED, at all the welding methods (specimens TIG-I-3, TIG-F-3, EBW-3).

HFMP by ultrasonic impact tool of welds produced using PED, greatly increases their load-carrying capacity, especially in TIG-F welding (specimens TIG-I-4, TIG-F-4, EBW-4).

The fatigue properties of welded specimens (TIG-I-5, TIG-F-5, EBW-5) sharply decrease as a result of repair of defect by surface arc on the side of sheet.

The heat-treated specimens (TIG-I-6, TIG-F-6, EBW-6) showed a considerable increase in cyclic life in case of welding over the activating flux. However it should be noted that PWHT is less efficient as compared to mechanical peening of welds using ultrasonic impact tool.

Thus, the fatigue tests of specimens showed that the highest load-carrying capacity of T-welded joints with penetration weld can be obtained in TIG-F and TIG-I welding applying PED and HFMP.

At the second stage the welding of groups of panels was performed using two methods: TIG-I and TIG-F (Figure 11). Technological modes of welding of panels corresponded to the modes of welding of T-specimens. The welding of panels was performed applying PED of sheet and stiffeners at the level $\sigma_{sh} = \sigma_{st} = 220$ MPa and reverse bend with the arrow of bend of 14 mm. Welded joints of all the panels were treated by HFMP using the tool and technology, which were mastered at the first stage of investigations.

It should be noted that as a result of application of PED of sheet and stiffeners the residual shape changes of panels after welding were less than initial bends of sheet plates.

The quality control of welded joints was performed using the method developed at the PWI based on the application of electron shearography [14], which allows operative determination of defect areas of welds without disassembly of load-carrying rigging and, if necessary, starting the repair immediately. Thus, welding and repair were joined in one technological process, that facilitated the improvement of the quality of panels.

According to the results of quality control on two panels manufactured using TIG-I welding, the defects as a chain of pores of 2 mm diameter were corrected applying mechanical preparation of the weld. On two panels corresponding to TIG-F welding the repair smoothing of leg area was performed.

To carry out the fatigue tests of welded panels the large-size specimens of blade type with test

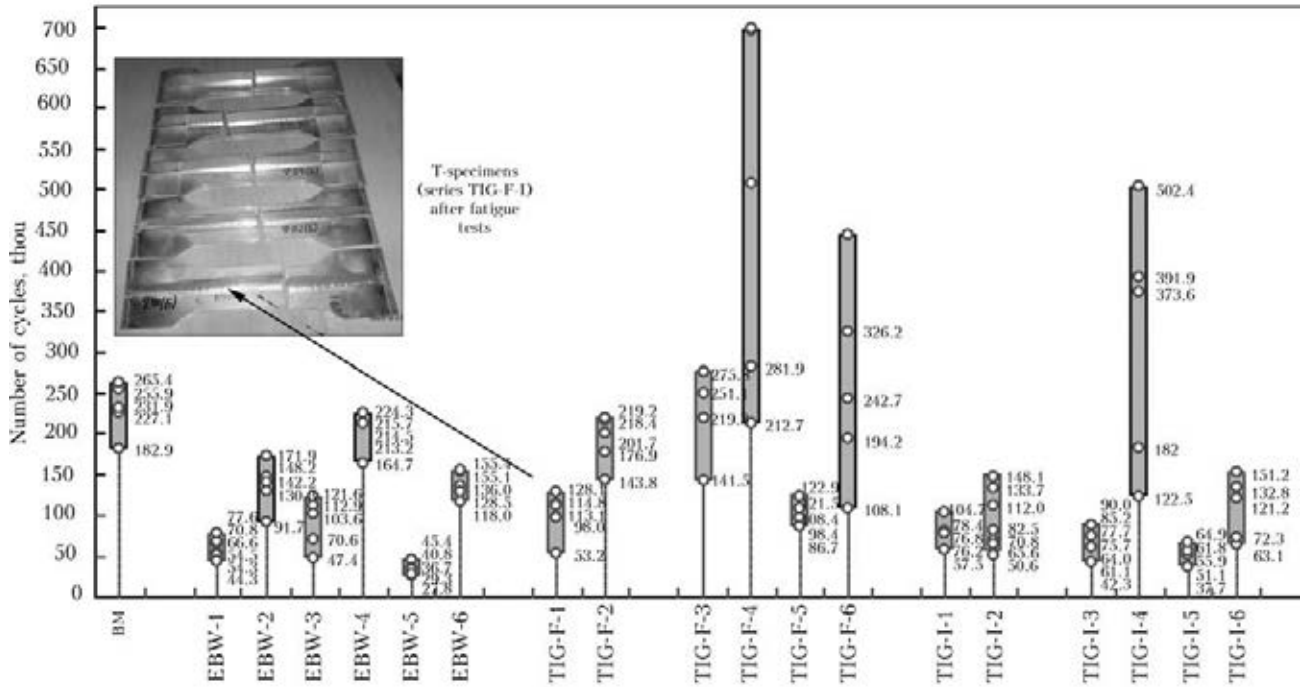


Figure 10. Results of fatigue tests at cyclic longitudinal tension of T-welded specimens of alloy VT20 (indicated using method of welding: 1 – specimens rigidly clamped in the rigging without tension in welding; 2 – produced applying PED; 3 – with smoothing of weld leg; 4 – treated using ultrasonic impact tool; 5 – with repair of defect atop (or repair simulation); 6 – after heat treatment)

part of 450 × 350 × 2.5 mm and grinded edges were manufactured (see Figure 2, c). The tests were carried out in the modernized universal servohydraulic testing machine HydroPuls-Schenk with maximum tensile force of 100 t, the control was performed by 4-channel digital controller MTC Flex Test GT.

For evaluation of the real level of stresses in the test section of the specimen and check up of its correct disposition in the clamps of testing machine the set-up tensometry was carried out for each specimen. For this purpose, strain gauges KF 5 P1-200 connected to tensomeasuring system SIIT-2 were glued in the test part of sheet and stiffeners of specimen in three sections along the length (Figure 12).

In the process of set-up tensometry the panel specimen was loaded stepwise with a pitch of

50 kN up to maximum tensile loading. At each step of loading the level of stresses was measured according to the strain gauges. Uniformity and maximum stresses on strain gauges were evaluated and, when necessary, maximum test load was corrected to approximate the test conditions of each panel. As a result, maximum test load was set individually for each panel in the limits from 300 to 320 kN.

At the fatigue tests the loading of specimens was performed by cyclic loading at the frequency of 0.5 Hz and the coefficient of cycle asymmetry $R_\sigma = 0.1$.

The test results of panels manufactured at the second stage of works are presented in Figure 13. As is seen from the diagram, fatigue life of specimens, where the repair of defects of welds is carried



Figure 11. TIG-F- (a) and TIG-I- (b) welded stringer panels of alloy VT20 after fatigue tests



Figure 12. Panel with glued strain gauges installed in the clamps of machine for fatigue tests

out, drops sharply. The higher fatigue life belongs to panels, manufactured applying technology of welding over the layer of activating flux.

The results of the second stage of investigations showed that the technology of argon-arc welding by penetration welds over the layer of activating flux applying PED of the elements being welded and further HFMP of welds can serve as a basis for industrial production of stringer panels of high-strength titanium alloy VT20.

Conclusions

1. It was established that producing of penetration welds using argon-arc welding by non-consumable electrode over the layer of activating flux, PED and HFMP of welds provides higher values of fatigue life of welded stringer panels of high-strength titanium alloy VT20 as compared to EBW and argon-arc nonconsumable-electrode welding with immersion arc.

2. The application of PED at the level lower than $0.25\sigma_{0.2}$ in welding of large-size stringer panels of alloy VT20 gives a possibility to eliminate welding distortions and improve the conditions of welding process in automatic mode.

3. The postweld HFMP of welds noticeably increases the fatigue life of structure of titanium alloys.

4. The technology of manufacture of welded stringer panels of alloy VT20 without PWHT was offered.

1. Matvienko, S.V., Astafiev, A.R., Karasyov, I.G. (2003) Welding and related technologies in aircraft construction. Tendencies of development. *Svarka v Sibiri*, **2**, 36–40.

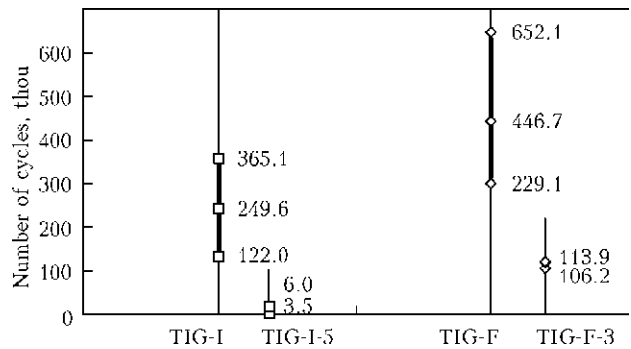


Figure 13. Results of fatigue tests at cyclic longitudinal tension of alloy VT20 welded panels (designated using method of welding: TIG-I-5, TIG-F-3 – panels with repair of weld defect, respectively, with preparation of its face side and smoothing of leg from the weld back side)

2. Robert, W., Messler, J.R. (2007) The greatest story never told: EB welding on the F-14. *Welding J.*, May, 41–47.
3. Bratukhin, A.G., Dmitriev, O.N., Kovalkov, Yu.A. (1997) *Stamping, welding, brazing and heat treatment of titanium and its alloys in aircraft construction*. Moscow: Mashinostroenie.
4. Paton, B.E. (1992) Advanced trends in improvement of welded structures. In: *Welding and Surf. Rev.*, Vol. 2., 1–8. Amsterdam: Harwood Acad. Publ.
5. Paton, B.E., Utkin, V.F., Lobanov, L.M. et al. (1989) Fabrication of welded large-sized panels from high-strength aluminium alloys. *Avtomatich. Svarka*, **10**, 37–45.
6. Lobanov, L.M., Pavlovsky, V.I., Lysak, V.V. (1987) Elastische Vorspannung beim Schweißen von Duennblechen aus Aluminiumlegierungen. *Schweistechnik*, **10**, 443, 447–449.
7. Lobanov, L.M., Pavlovsky, V.I., Pivtorak, V.A. (1992) Optical methods of studying and means of controlling welding strains and stresses. In: *Welding and Surf. Rev.* Amsterdam: Harwood Acad. Publ.
8. Lobanov, L.M., Kirian, V.I., Knysh, V.V. et al. (2006) Improvement of fatigue resistance of welded joints in metal structures by high-frequency mechanical peening (Review). *The Paton Welding J.*, **9**, 2–8.
9. Stanhope, F., Hasellhurs, R.H. (1972) Welding airframe structures in titanium alloys using tensile loading as a means of overcoming distortion. In: *Proc. of Int. Conf. on Welding and Fabrication of Non-Ferrous Metals* (Eastbourne, 1972), Vol. 1, 72–82.
10. Muraviov, V.I. (1986) Specifics of fabrication and quality evaluation of large-sized thin welded structures of VT20 alloy. *Avtomatich. Svarka*, **8**, 15–18.
11. Zamkov, V.N., Prilutsky, V.P., Petrichenko, I.I. et al. (2001) Effect of the method of fusion welding on properties of welded joints in alloy Ti–6Al–4V. *The Paton Welding J.*, **4**, 2–6.
12. Savitsky, V.A., Shevelev, A.D., Zamkov, V.N. et al. (1989) Electron beam welding of stiffened panel elements in VT20 titanium alloy. *Avtomatich. Svarka*, **4**, 55–57.
13. Paton, B.E., Zamkov, V.N., Prilutsky, V.P. et al. (2000) Contraction of the welding arc caused by the flux in tungsten-electrode argon-arc welding. *The Paton Welding J.*, **1**, 5–11.
14. Lobanov, L.M., Pivtorak, V.A., Savitskaya, E.M. et al. (2011) In-process quality control of welded panels of alloy VT20 using method of electron shearography. *Ibid.*, **11**, 22–27.

Received 03.12.2013



SIMULATION OF ELECTRIC ARC WITH REFRACTORY CATHODE AND EVAPORATING ANODE

I.V. KRIKENT¹, I.V. KRIVTSUN² and V.F. DEMCHENKO²

¹Dneprodzerzhinsk State Technical University

2 Dneprostroevskaya Str., 51918, Dneprodzerzhinsk, Ukraine. E-mail: science@dstu.dp.ua

²E.O. Paton Electric Welding Institute, NASU

11 Bozhenko Str., 03680, Kiev, Ukraine. E-mail: office@paton.kiev.ua

Equation of convective diffusion of ionized metal vapour in arc plasma, allowing for the difference in coefficients of diffusion of atoms, single- and double-charged metal ions, presence of thermodiffusion flows of metal particles, as well as ion drift in the electric field, was proposed to more precisely define the earlier developed complex model of the processes of energy, mass and charge transfer in the column and anode region of electric arc with refractory cathode and evaporating anode, running in inert gas. Based on the thus precised complex mathematical model, numerical analysis of the influence of diffusion-induced evaporation of anode material (Fe) on heat, gas-dynamic and electromagnetic characteristics of multicomponent plasma of the column and anode region of stationary electric arc with refractory cathode (W) at its running in inert gas (Ar) was performed. An essential influence of metal surface temperature distribution in the region of anode binding of the arc on distribution of temperature and electric current density in near-anode plasma, as well as on distributed and integral characteristics of its thermal impact on evaporating anode surface, is shown. 18 Ref., 12 Figures.

Keywords: *electric arc, refractory cathode, evaporating anode, arc column, anode region, multicomponent plasma, metal vapour, diffusion, mathematical simulation*

Electric arc plasma in inert-gas nonconsumable-electrode welding, as a rule, is multicomponent, as alongside shielding gas particles, it contains atoms and ions of metal vapour coming to the arc gap due to evaporation of anode metal from weld pool surface. Presence of an even small amount of metal component in inert gas arc plasma has an essential influence on its ionization composition, thermodynamic, transport and optical properties. It leads to a significant difference of heat, electromagnetic and gas-dynamic characteristics of plasma in near-anode zone of arc column in nonconsumable-electrode welding from respective characteristics of arc discharge with refractory cathode and nonevaporating, for instance, water-cooled anode. Characteristics of welding arc anode region, determining the conditions of thermal and electromagnetic interaction of the arc with metal being welded and, consequently, nature of its penetration, are also different [1].

In the first publications, devoted to mathematical simulation of the processes of heat, mass and charge transfer in refractory cathode arcs [2–10], arc plasma was assumed to be single-com-

ponent, i.e. containing atoms and ions of just the shielding gas. Such idealization did not incorporate any conditions of running of real welding arcs, and required further improvement of mathematical models of the arc, in order to allow for a number of additional physical factors, related to multicomponent nature of arc plasma. Publications devoted to allowing for evaporation of anode material in simulation of nonconsumable-electrode welding arc, appeared in the world scientific literature comparatively recently [11–13]. When describing diffusion of ionized metal vapour in arc plasma, however, these works do not differentiate between vapour atoms and ions, having diffusion coefficients, differing significantly by their magnitude [1]. The integrated mathematical model of nonconsumable-electrode welding arc proposed in [14] is an attempt to allow for the difference in the above coefficients. However, when writing the equation of convective diffusion of evaporated anode metal in arc column plasma, thermodiffusion of atoms and ions of metal vapour, as well as metal drift in the electric field, were not allowed for. Therefore, the objective of this work is improvement of the model of convective diffusion of metal vapour in arc plasma and applying the precised integrated mathematical model [14] for numerical analysis of characteristics of multicomponent plasma of the column and anode region of sta-



tionary electric arc with refractory (W) cathode and evaporating (Fe) anode at its running in inert gas (Ar).

Equation of metal vapour transfer in arc plasma. A specific feature of metal vapour diffusion in arc plasma is that metal atoms evaporated from molten anode surface, may ionize, forming single- and double-charged ions, whose coefficients of diffusion differ significantly from the respective coefficients for neutral particles. More over, processes of ionization and recombination of particles in arc plasma column proceed much faster than those of transfer of substance and thermal energy [15, 16]. Therefore, we will assume that concentrations of all the particles of multicomponent plasma of the considered arc column (electrons, atoms and single-charged ions of argon, atoms, single- and double-charged ions of iron) differ only slightly from equilibrium values determined by the principle of detailed equilibrium. We will also assume that arc column plasma is in the state of local thermodynamic equilibrium at electron temperature equal to that of heavy particles (single-temperature model).

In the general case the equation of diffusion for atoms, single- and double-charged metal ions in inert gas plasma can be expressed as follows:

$$\frac{\partial n_{m0}}{\partial t} = -\text{div} (n_{m0} \vec{w}_{m0}) - \dot{n}_{m0}; \quad (1)$$

$$\frac{\partial n_{m1}}{\partial t} = -\text{div} (n_{m1} \vec{w}_{m1}) - \dot{n}_{m1} + \dot{n}_{m0}; \quad (2)$$

$$\frac{\partial n_{m2}}{\partial t} = -\text{div} (n_{m2} \vec{w}_{m2}) + \dot{n}_{m1}; \quad (3)$$

where n_{m0} , n_{m1} , n_{m2} are the concentrations of atoms, single- and double-charged metal ions; \vec{w}_{m0} , \vec{w}_{m1} , \vec{w}_{m2} are the rates of their directed motion; \dot{n}_{mZ} ($Z = 0, 1$) are the reaction rates of first and second ionization, respectively.

Let us represent the rate \vec{w}_{m0} of metal atom motion in the form of a sum of mean velocity \vec{w}_C of plasma particle motion and diffusion rate of neutral metal particles \vec{w}_{D0} :

$$\vec{w}_{m0} = \vec{w}_C + \vec{w}_{D0}. \quad (4)$$

If atomic masses of all the plasma components are the same, then average velocity of particle motion coincides with average mass (gas dynamic) velocity of plasma motion \vec{W} . Otherwise, \vec{w}_C value can be determined from the following balance relationship:

$$\rho \vec{W} = \rho \vec{w}_C + M_m \vec{Y}_{m0} + \bar{M}_{m0} \vec{Y}_{\bar{m}0}, \quad (5)$$

where ρ is the plasma velocity; M_m is the mass of metal atoms; \vec{Y}_{m0} is the density of diffusion flow of metal atoms; $\vec{Y}_{\bar{m}0}$, \bar{M}_{m0} is the density of diffusion flow and average statistical mass of particles, substituting metal atoms.

As diffusion processes do not have any essential influence on pressure distribution in arc plasma, we can assume that it is determined, mainly, by gas-dynamic factors. For the considered here stationary free-running arc the pressure in its column differs only slightly from the atmospheric one [17]. Therefore, metal vapour diffusion in such an arc can with a high degree of accuracy be considered as a process running at constant (atmospheric) pressure. In this case, the result of diffusion is plasma-forming particles exchanging their places. It follows from here that specific diffusion flows \vec{Y}_{m0} and $\vec{Y}_{\bar{m}0}$ compensate each other, i.e. condition $\vec{Y}_{m0} = -\vec{Y}_{\bar{m}0}$ is fulfilled. Then, equation (5) yields the following expression for determination of mean velocity of particle motion:

$$\vec{w}_C = \vec{W} - \frac{M_m - \bar{M}_{m0}}{\rho} \vec{Y}_{m0}. \quad (6)$$

Average statistical weight of particles substituting metal atoms, can be approximately calculated by the following formula:

$$\bar{M}_{m0} = \frac{\rho - M_m n_{m0}}{n_0 - n_{m0}}.$$

Here $n_0 = p_0/kT$ is the total concentration of particles in arc column plasma assumed to be isothermal; p_0 is the atmospheric pressure; T is the plasma temperature; k is the Boltzmann constant. In terms of the above approach, the sum of specific mass flows of atoms of metal and other particles, forming the plasma, is equal to total density of plasma mass flow. This is indicative of consistent description of gas-dynamic and diffusion processes.

Diffusion rate \vec{w}_{D0} of metal atoms is connected with their concentration n_{m0} and diffusion flow density \vec{Y}_{m0} as follows:

$$\vec{w}_{D0} = \frac{Y_{m0}}{n_{m0}},$$

where \vec{Y}_{m0} value in the simplest case can be determined from the following relationship [1]:

$$\vec{Y}_{m0} = -\frac{D_0}{T} \text{grad} (n_{m0}T), \quad (7)$$

where D_0 is the coefficient of metal atom diffusion in plasma.



Substituting (4), (6), (7) into equation (1), we obtain

$$\frac{dn_{m0}}{dt} = \text{div} [G_0 \text{grad} (n_{m0}T)] - n_{m0} \text{div} \vec{W} - \dot{n}_{m0}, \quad (8)$$

where dn_{m0}/dt is the substantial derivative;

$$G_0 = \frac{D_0}{T} \left(1 - n_{m0} \frac{M_m - \bar{M}_{m0}}{\rho} \right).$$

We will perform similar transformations with equations (2), (3) and will additionally allow for drift of charged metal particles (single- and double-charged ions) in the electric field. As a result we will have

$$\frac{dn_{m1}}{dt} = \text{div} [G_1 \text{grad} (n_{m1}T) + b_1 n_{m1} \text{grad} \varphi] - n_{m1} \text{div} \vec{W} - \dot{n}_{m1} + \dot{n}_{m0}, \quad (9)$$

$$\frac{dn_{m2}}{dt} = \text{div} [G_2 \text{grad} (n_{m2}T) + b_2 n_{m2} \text{grad} \varphi] - n_{m2} \text{div} \vec{W} + \dot{n}_{m1}. \quad (10)$$

Here, $G_Z = \frac{D_Z}{T} \left(1 - n_{mZ} \frac{M_m - \bar{M}_{mZ}}{\rho} \right)$; D_Z are the coefficients of diffusion of metal ions with charge number Z ($Z = 1, 2$);

$$\bar{M}_{mZ} = \frac{\rho - M_m n_{mZ}}{n_0 - n_{mZ}};$$

$b_Z = \frac{eZ}{k} G_Z$ are the mobilities of metal ions in the electric field; e is the electron charge; φ is the scalar potential of electric field in the arc column.

Summing up equations (8)–(10), we obtain the equation of metal particle transfer in arc plasma

$$\begin{aligned} \frac{dn_m}{dt} = & \text{div} [G_0 \text{grad} (n_m T) + \\ & + (G_1 - G_0) \text{grad} (n_{m1} T) + \\ & + (G_2 - G_0) \text{grad} (n_{m2} T) + \\ & + (b_1 n_{m1} + b_2 n_{m2}) \text{grad} \varphi] - n_m \text{div} \vec{W}, \end{aligned} \quad (11)$$

where $n_m = n_{m0} + n_{m1} + n_{m2}$ is the total concentration of heavy particles of metal vapour.

Let us express the concentrations of metal ions n_{mZ} ($Z = 1, 2$) through total concentration of metal particles in the plasma: $n_{mZ} = K_Z n_m$, where coefficients K_Z correspond to first ($Z = 1$) and second ($Z = 2$) ionization of metal atoms. Considering the assumption of local thermodynamic equilibrium of arc column plasma, coefficients

K_Z can be determined for equilibrium plasma of specified composition and temperature.

Introducing $\bar{G}_1 = G_1 - G_0$; $\bar{G}_2 = G_2 - G_0$ designations, we will rewrite equation (11) for total concentration of metal particles in the plasma:

$$\begin{aligned} \frac{dn_m}{dt} + n_m \text{div} \vec{W} = & \text{div} [G_0 \text{grad} (n_m T) + \\ & + \bar{G}_1 \text{grad} (K_1 n_m T) + \bar{G}_2 \text{grad} (K_2 n_m T)] + \\ & + \text{div} [b_1 K_1 + b_2 K_2] n_m \text{grad} \varphi. \end{aligned} \quad (12)$$

Equation (12) describes the following kinds of transfer of heavy particles of metal vapour in arc plasma: convective transfer, concentration diffusion, thermodiffusion, as well as vapour ion drift in the electric field. Knowing the solution of this equation, n_m and considering the taken assumption of local thermodynamic equilibrium of arc column plasma, its ionization composition can be determined through application of the respective system of Saha's equations, law of partial pressures and condition of plasma quasineutrality [14]. The thus calculated concentrations of particles of multicomponent arc column plasma can be used for calculation of its thermodynamic and transport properties [18], included into complex model equations [14].

We will define boundary conditions for diffusion equation (12). Assuming that the arc column is characterized by axial symmetry, we will introduce the cylindrical system of coordinates (r, z) and consider design region $\Omega = \{0 < r < R, 0 < z < L\}$, shown in Figure 1.

Considering the direction of movement of shielding gas and plasma in near-cathode zone of arc column [17], we will assume that particles of evaporated anode metal do not reach plane

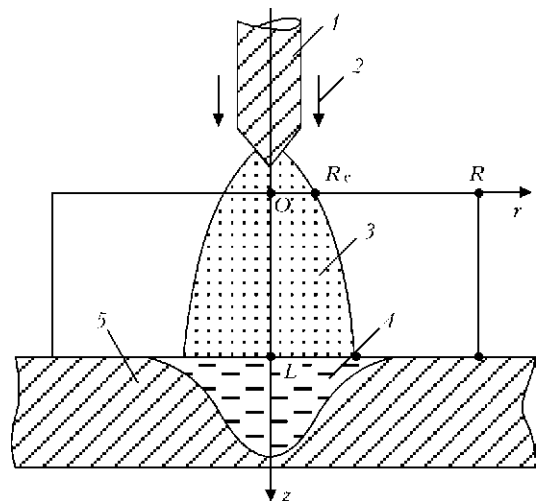


Figure 1. Schematic for mathematical description of arc plasma: 1 – refractory cathode; 2 – shielding gas, 3 – arc column plasma; 4 – molten (evaporating) metal; 5 – anode



$z = 0$ (see Figure 1), i.e. on upper limit of design region we will set

$$n_m|_{z=0} = 0. \tag{13}$$

On the arc axis (at $r = 0$) we will assume the following conditions of symmetry:

$$\frac{\partial n_m}{\partial r}|_{r=0} = 0. \tag{14}$$

On the outer limit of design region (at $r = R$) we will assign «soft» boundary conditions

$$\begin{aligned} n_m|_{r=R} = 0 \text{ at } W_r(R, z) \leq 0; \\ \frac{dn_m}{dt}|_{r=R} = 0 \text{ at } W_r(R, z) > 0, \end{aligned} \tag{15}$$

where $W_r(r, z)$ is the radial component of the vector of average mass velocity of plasma.

On the boundary of multicomponent plasma with anode layer (at $z = L$) we can write the boundary condition in the following form:

$$n_m|_{z=L} = n_{m0}^L(r) + n_{m1}^L(r) + n_{m2}^L(r), \tag{16}$$

where $n_{mZ}^L(r) = n_{mZ}(r, L)$ are the respective distributions of concentration of metal vapour particles, being in charge state Z , which can be determined according to model of anode region of the arc with evaporating anode [14], depending on local values of near-anode plasma temperature and anode surface temperature, its evaporation mode, as well as kind of shielding gas. Limiting further consideration to diffusion evaporation mode, it can be assumed with sufficient accuracy that local values of partial pressure of atoms and ions of metal component of plasma p_m on the above boundary are equal to pressure of saturated vapour of anode metal at the respective value of temperature on its surface T_a :

$$p_m|_{z=L} = p_0 \exp \left\{ \frac{\lambda_v}{k} \left[\frac{1}{T_B} - \frac{1}{T_a(r)} \right] \right\}, \tag{17}$$

where λ_v is the energy consumed for transition of one metal particle from the liquid into the vapour phase; T_B is the boiling temperature of anode metal.

Model of convective diffusion of ionized metal vapour (12)–(17) is a component part of complex model of processes of energy, pulse, mass and charge transfer in multicomponent plasma of the column and anode region of electric arc in inert-gas nonconsumable-electrode welding [14]. For numerical simulation of heat, gas-dynamic and electromagnetic processes in such plasma we will use equations of single-temperature model [17]. When allowing for evaporation of anode metal

on the boundary of condensed phase with arc plasma, there exists a diffusion flow of metal vapour, as a result of which the axial component of plasma velocity vector on this boundary is not equal to zero (unlike the condition of «sticking», used in [17] for the case of water-cooled anode). Considering the fact that atoms and ions of shielding gas, which is inert, cannot accumulate on the anode surface, the resulting flow of heavy particles of gas near the anode surface can be considered to be equal to zero. Then, allowing for diffusion and convective mechanisms of metal vapour particle transfer, the boundary condition for axial component of vector of average mass velocity of plasma on the boundary of arc column with the anode region (at $z = L$) can be written in the following form:

$$W_{zL} = \frac{M_m[Y_{m0z}^L(r) + Y_{m1z}^L(r) + Y_{m2z}^L(r)]}{\rho(r, L) - M_m[n_{m0}^L(r) + n_{m1}^L(r) + n_{m2}^L(r)]}. \tag{18}$$

Here $Y_{mZ}^L(r)$ are the respective distributions of axial components of densities of diffusion flows of metal atoms and ions, which are in charged state Z .

Simulation results and their discussion. For numerical analysis of the influence of diffusion evaporation of anode metal on processes of energy, mass and charge transfer in anode region and column of the considered arc we will assign anode surface temperature distribution by normal-circular law $T_a(r) = (T_{a0} - T_\infty) \exp(-a^2 r^2) + T_\infty$, where T_{a0} is the temperature on the axis of the region of arc anode binding; T_∞ is the temperature of metal surface at a distance from the above region. We will select coefficient of concentration a so that diameter of molten zone on anode surface was 5 mm. Characteristic profiles of $T_a(r)$ distribution at $T_\infty = 500$ K are shown in Figure 2.

Numerical simulation of characteristics of multicomponent plasma of the column and anode region of electric arc with tungsten cathode and evaporating anode from low-carbon steel was conducted at the following parameters: arc length $L = 2.9$ mm; arc current $I = 200$ A; shielding gas is argon, and evaporating element is iron. Initial distributions of arc column plasma characteristics, required to solve the non-stationary problem [17], together with equation (12), were assigned as specified in [17]; initial concentration of metal vapour in the arc gap was also taken to be zero. Calculations were performed right up to establishment of steady state of arc plasma.

We will introduce $\gamma = n_m / (n_g + n_m)$ designation, where $n_g = n_{g0} + n_{g1}$ is the total concentra-



tion of heavy particles (atoms and ions) of shielding gas, and will consider the distribution of the fraction of heavy metal particles γ in arc column plasma for two variants of distribution of evaporating anode surface temperature, which correspond to $T_{a0} = 2600$ K (Figure 3, *a*) and $T_{a0} = 3065$ K (Figure 3, *b*). At 2500–2600 K temperature of molten anode metal, evaporated metal particles appear above its surface, their content reaching 10 % (see Figure 3, *a*). At increase of temperature in the center of the region of arc anode binding above 3000 K, mass flow of vapour from anode surface into arc column increases, that results in formation of a region of arc plasma with high (up to 80 %) content of metal vapour (Figure 3, *b*).

Field of concentration of evaporated metal particles n_m in near-anode plasma forms as a result of interaction of the following four factors: diffusion and convective transfer of metal particles from anode surface into arc column; arc plasma flow with low content of metal vapour, moving over the anode; transfer of metal vapour particles towards the anode due to thermodiffusion; drift of charged metal particles (single- and double-charged ions) in the electric field. Distribution of the fraction of heavy iron particles in the considered arc plasma, presented in Figure 3, is the result of competing interaction of the above-mentioned four transfer mechanisms. Two characteristic features of evaporated metal particle distribution in near-anode plasma can be singled out. On the one hand, convective flow of plasma from near-cathode region of the column, containing practically no metal vapour, is trying to oust metal vapours from evaporation zone in the radial direction. As a result, width of near-surface plasma layer, containing a noticeable quantity of metal vapour ($\gamma > 3\%$), turns out to be 1.5–2 times greater than the radius of molten zone on anode surface, and thickness of

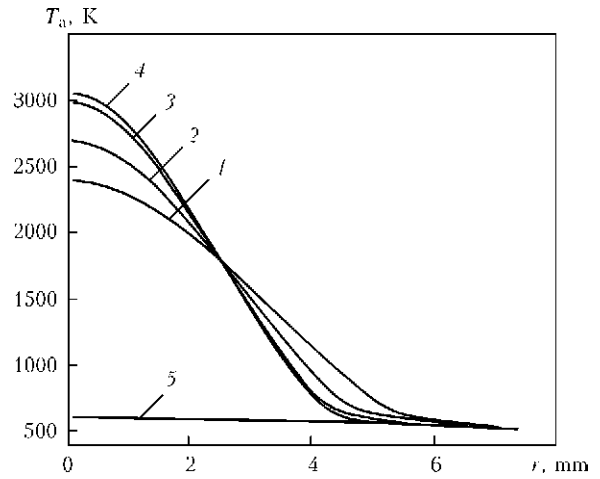


Figure 2. Temperature distribution of anode surface in the region of arc anode binding (here and in Figures 4–7: 1 – $T_{a0} = 2400$ K; 2 – 2700; 3 – 3000; 4 – 3065; 5 – water-cooled (nonevaporating) anode)

this layer is 0.3–0.5 mm. As thickness of the region taken up by vapour is small compared to arc length, influence of evaporated metal in the considered case is limited to just near-anode region of the arc and practically does not affect the processes of heat, mass and charge transfer in it is column. At the same time, region of near-anode plasma, the most enriched in iron vapours, turns out to be «cut off» from the anode surface. This effect can be explained as follows. Ionization composition of metal vapour, which comes to near-anode region of arc column and is further on transported into the region with higher plasma temperature, undergoes changes due to intensive ionization of metal atoms. On the other hand, because of low diffusion mobility of metal ions, they accumulate in the above region, that is exactly what causes formation of a zone of maximum content of metal vapour, localized at a certain distance from anode surface.

Diffusion evaporation of anode metal has the greatest influence on such characteristics of anode region of the considered arc as fraction of iron

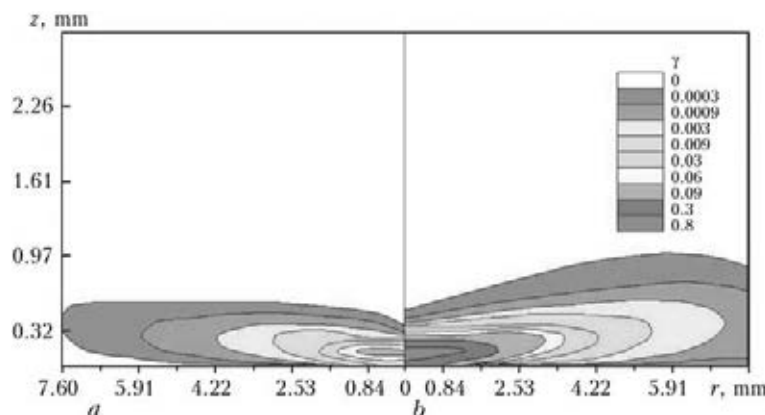


Figure 3. Distribution of fraction of heavy iron particles in near-anode region of arc plasma column: *a* – $T_{a0} = 2600$ K; *b* – 3065

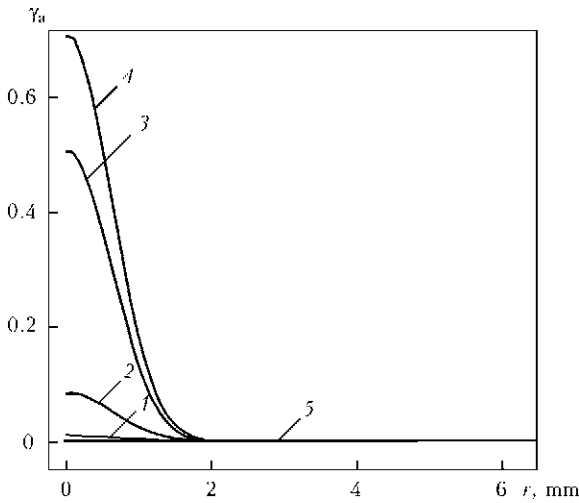


Figure 4. Radial distribution of fraction of heavy iron particles in multicomponent near-anode plasma

particles in near-anode plasma $\gamma_a(r) = \gamma(r, L)$ and its temperature $T_{pa}(r) = T(r, L)$, electric current density $j_a(r)$ and heat flow density $q_a(r)$ on anode surface. Let us consider the influence of temperature on evaporating anode surface on distribution of the above characteristics in the region of anode binding of the arc. Figures 4–7 give the results of calculations of γ_a , T_{pa} , j_a and q_a for different thermal states of anode surface.

Maximum content of metal vapour is reached on the axis of near-anode plasma layer, increasing with temperature rise on anode surface in the center of the region of arc anode binding (see Figure 4). Here, maximum value of average mass velocity of vapour motion $|W_z(0, L)|$ near anode surface also rises at increase of the above temperature. So, for instance, at $T_{a0} = 3065$ K this velocity can reach more than 10 m/s. Such intensive flow of relatively cold vapour, moving from anode surface into arc column, causes local freezing of near-anode plasma. This effect is manifested in that part of anode region, which is lo-

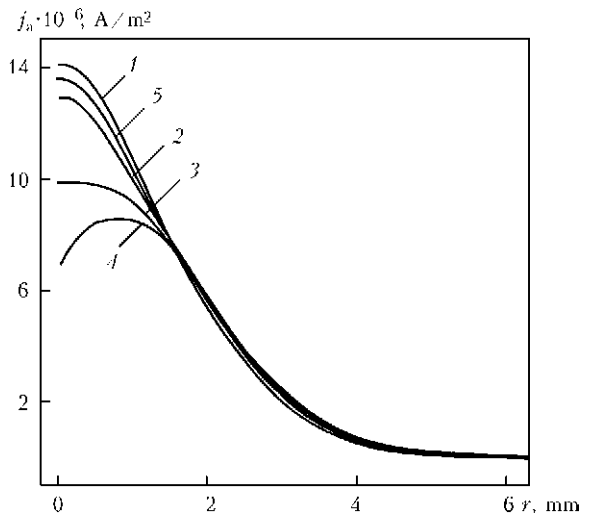


Figure 6. Radial distributions of electric current density on anode surface

cated above the most heated zone of molten anode metal surface, and the more so, the higher the surface temperature in this zone (see Figure 5).

Despite the fact that increase of concentration of easily ionized (compared to argon) metal vapour in multicomponent plasma with T_{a0} rise should lead to increase of its electric conductivity σ , the above-noted effect of local freezing of near-anode plasma by vapour flow has a more significant role, leading to lowering of σ and of electric current density in near-axis zone of the region of arc anode binding, respectively (see Figure 6).

Density of heat flow, applied by the arc to evaporating anode, behaves in a similar fashion (see Figure 7). Considerable lowering of q_a value at high values of anode metal surface temperature is related to reduction of convective energy flow from arc column, as a result of respective variation of gas-dynamic and electromagnetic situation in near-anode region of arc plasma, as well as reduction of heat flow transported to the anode

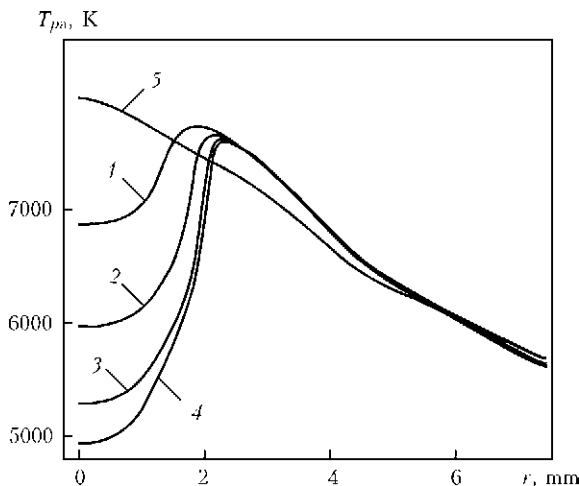


Figure 5. Radial distribution of arc column plasma temperature on the interface with anode region

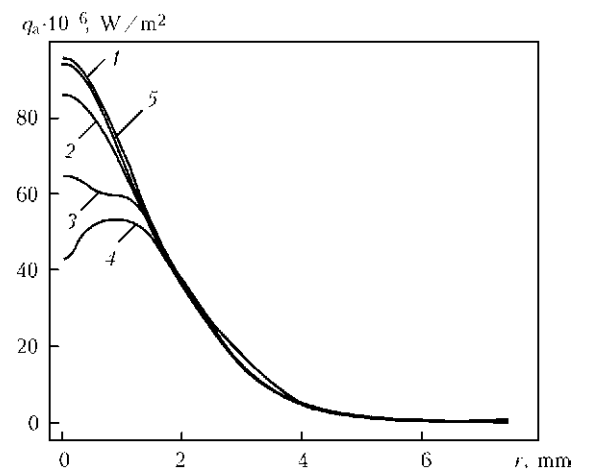


Figure 7. Radial distributions of density of heat flow applied by the arc to the anode

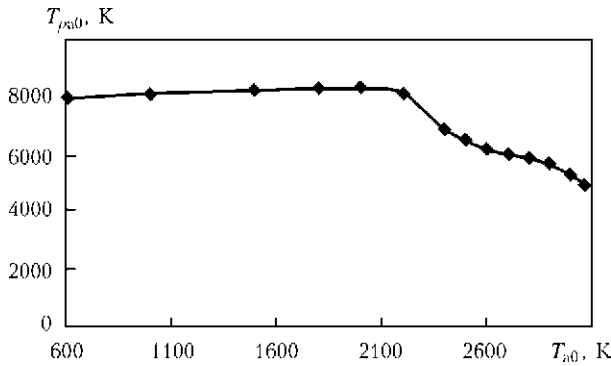


Figure 8. Dependence of axial value of arc plasma temperature on anode region interface on anode surface temperature in the center of the region of arc anode binding

by charged particles, at the expense of respective reduction of j_a (see Figure 6).

Now let us analyze dependencies of axial values of the considered characteristics on anode surface temperature in the center of the region of arc anode binding. Variation of $T_{pa0} = T(0, L)$, $j_{a0} = j_a(0, L)$ and $q_{a0} = q_a(0, L)$ with T_{a0} rise is shown in Figures 8–10. Range of variation of maximum surface temperature of molten anode metal studied in this work can be conditionally divided into two intervals: $T_{a0} < 2400$ K – corresponds to nonevaporating anode; 2400 K $< T_{a0} < 3100$ K – corresponds to diffusion mode of anode metal evaporation. In the first temperature range all the characteristics of arc anode region weakly depend on T_{a0} , whereas in the second range an essential lowering of T_{pa0} takes place. As regards j_{a0} and q_{a0} , they behave non-monotonically (see Figures 9 and 10). Initially observed reduction of electric current density and density of heat flow entering the anode on the axis of the region of arc anode binding is replaced by their certain increase, so that at $T_{a0} \approx 2800$ K these values reach their local maximums. Their further lowering proceeds the faster, the more intensive is anode metal evaporation. The noted peculiarity is the most pronounced in the behaviour of such an integral characteristic of thermal interaction of arc plasma with anode metal as

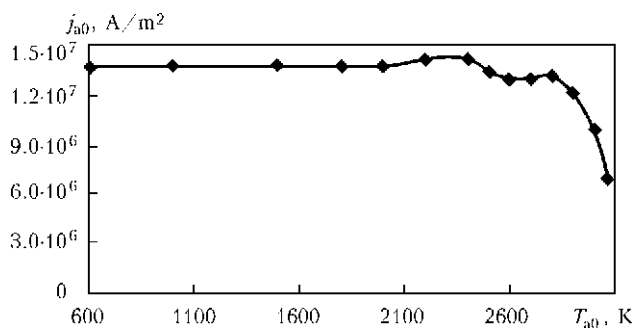


Figure 9. Dependence of axial value of density of electric current on the anode on its surface temperature in the center of the region of arc anode binding

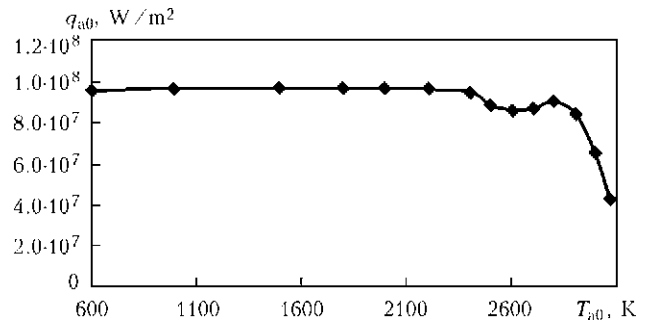


Figure 10. Dependence of axial value of density of heat flow to the anode on its surface temperature in the center of the region of arc anode binding

complete heat power P applied by the arc (Figure 11).

Dependence of density of heat losses of anode metal for evaporation in near-axis zone of the region of the arc anode binding q_{e0} on its surface temperature in this zone is shown in Figure 12. As follows from calculation data given in this Figure, at T_{a0} rise up to 3000 K, the above value can be equal to about 25 % of the respective value of heat flow applied by arc plasma to evaporating anode (compare Figures 10 and 12), and it should be taken into account at determination of energy balance of its surface.

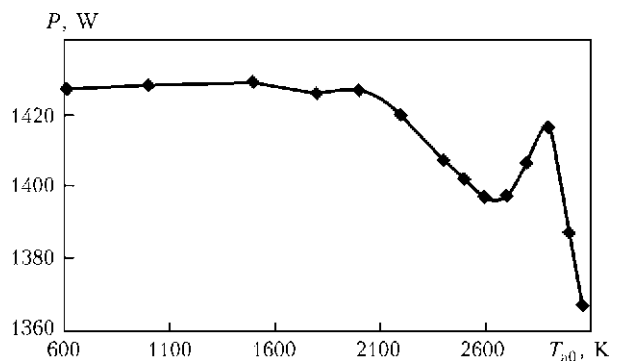


Figure 11. Dependence of heat power applied by the arc to the anode on anode surface temperature in the center of the region of arc anode binding

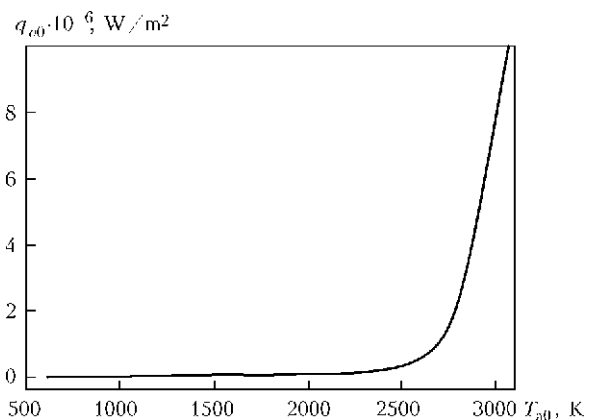


Figure 12. Dependence of axial value of density of energy losses for anode metal evaporation on its surface temperature in the center of the region of arc anode binding



On the whole, numerical analysis of the influence of diffusion evaporation of anode metal on characteristics of the column and anode region of the arc with refractory cathode, running in inert gas, which was conducted in this work, leads to the following conclusions:

1. In the case of inert-gas nonconsumable-electrode arc welding the influence of evaporated anode material on characteristics of arc column plasma is manifested only in thin (just up to 0.5 mm) layer adjacent to anode region. As regards arc plasma characteristics in the rest of arc column, they practically do not change, compared to the arc running to water-cooled (nonevaporating) anode.

2. Evaporation of metal being welded leads to an essential restructuring of spatial distributions of plasma characteristics of anode region of welding arc with nonconsumable electrode, as well as characteristics of its thermal and electromagnetic interaction with weld pool surface. In particular, with increase of melt surface temperature in the center of the region of arc anode binding, density of heat flow applied by the arc to the item being welded and density of electric current on its surface decrease. Alongside losses of molten metal energy for evaporation, this leads to lowering of effectiveness of arc heating of the metal being welded.

1. Murphy, Ant.B. (2010) The effects of metal vapour in arc welding. *J. Phys. D: Appl. Phys.*, **43**.
2. Hsu, K.C., Etemadi, K., Pfender, E. (1983) Study of the free-burning high-intensity argon arc. *J. Appl. Phys.*, **54**(3), 1293–1301.
3. Hsu, K.C., Pfender, E. (1983) Two-temperature modeling of the free-burning high-intensity arc. *Ibid.*, **54**(8), 4359–4366.
4. Engelsht, V.S., Gurovich, V.Ts., Desyatkov, G.A. et al. (1990) *Low-temperature plasma*. Vol. 1: Theory of electric arc column. Novosibirsk: Nauka.
5. Zhu, P., Lowke, J.J., Morrow, R. et al. (1995) Prediction of anode temperatures of free burning arcs. *J. Phys. D: Appl. Phys.*, **28**, 1369–1376.
6. Jenista, J., Heberlein, J.V.R., Pfender, E. (1997) Numerical model of the anode region of high-current electric arcs. *IEEE Transact. on Plasma Science*, **25**(5), 883–890.
7. Lowke, J.J., Morrow, R., Haidar, J. (1997) A simplified unified theory of arcs and their electrodes. *J. Phys. D: Appl. Phys.*, **30**, 2033–2042.
8. Haidar, J. (1999) Non-equilibrium modeling of transferred arcs. *Ibid.*, **32**, 263–272.
9. Sansonnets, L., Haidar, J., Lowke, J.J. (2000) Prediction of properties of free burning arcs including effects of ambipolar diffusion. *Ibid.*, **33**, 148–157.
10. Nishiyama, H., Sawada, T., Takana, H. et al. (2006) Computational simulation of arc melting process with complex interactions. *ISIJ Int.*, **46**(5), 705–711.
11. Lago, F., Gonzalez, J.J., Freton, P. et al. (2004) A numerical modeling of an electric arc and its interaction with the anode. Pt 1: The two-dimensional model. *Ibid.*, **37**, 883–897.
12. Tanaka, M., Yamamoto, K., Tashiro, S. et al. (2008) Metal vapour behaviour in gas tungsten arc thermal plasma during welding. *Welding in the World*, **52**(11/12), 82–88.
13. Mougnot, J., Gonzalez, J.J., Freton, P. et al. (2013) Plasma-weld pool interaction in tungsten inert-gas configuration. *J. Phys. D: Appl. Phys.*, **46**, 135–206.
14. Krivtsun, I.V., Demchenko, V.F., Krikent, I.V. (2010) Model of the processes of heat-, mass- and charge transfer in the anode region and column of the welding arc with refractory cathode. *The Paton Welding J.*, **6**, 2–9.
15. Almeida, R.M.S., Benilov, M.S., Naidis, G.V. (2000) Simulation of the layer of non-equilibrium ionization in a high-pressure argon plasma with multiply-charged ions. *J. Phys. D: Appl. Phys.*, **33**, 960–967.
16. Krivtsun, I.V., Krikent, I.V., Demchenko, V.F. (2013) Modelling of dynamic characteristics of a pulsed arc with refractory cathode. *The Paton Welding J.*, **7**, 13–23.
17. Krikent, I.V., Krivtsun, I.V., Demchenko, V.F. (2012) Modelling of processes of heat-, mass- and electric transfer in column and anode region of arc with refractory cathode. *Ibid.*, **3**, 2–6.
18. Krivtsun, I.V., Porytsky, P., Demchenko, V. et al. (2010) On the application of the theory of Lorentzian plasma to calculation of transport properties of multicomponent arc plasmas. *Europ. Phys. J. D*, **57**, 77–85.

Received 17.04.2014



EFFECT OF ELECTRIC PARAMETERS OF ARC SURFACING USING FLUX-CORED WIRE ON PROCESS STABILITY AND BASE METAL PENETRATION

Yu.N. LANKIN, I.A. RYABTSEV, V.G. SOLOVIOV, Ya.P. CHERNYAK and V.A. ZHDANOV

E.O. Paton Electric Welding Institute, NASU

11 Bozhenko Str., 03680, Kiev, Ukraine. E-mail: office@paton.kiev.ua

Effect of electric parameters of arc surfacing using self-shielding flux-cored wires on process stability and base metal penetration was investigated. The experiments were carried out with computer registration of electric parameters of surfacing. The results of oscillogram processing were used for plotting of I_w and U_w diagrams with outlined areas of stable process of surfacing, short circuits and arc extinctions. Coefficient of process instability γ was derived from received real parameters of arc surfacing using flux-cored wire. It is determined that voltage has the largest effect on stability indices and its rise improves process stability. Effect of modes of surfacing on penetration and portion of base metal in the deposited metal was investigated. 3D chart was plotted on estimation results. An area of optimum modes, providing sufficient stability of the process at minimum penetration and good formation of deposited beads, is outlined. 4 Ref., 2 Tables, 7 Figures.

Keywords: arc surfacing, flux-cored wire, stability of surfacing process, instability coefficient, base metal penetration, portion of base metal

Necessary composition of the deposited metal in multilayer arc surfacing can be obtained only in the third or fourth layer [1] due to its mixing with the base metal. Five layers as minimum should be surfaced, if machining of part is necessary after surfacing. The problem becomes more complicated due to the fact that rise of thickness of the deposited layer promotes for growth of residual shearing stresses and, simultaneously, increases the possibility of appearance in the deposited layer of different type defects, which reduce its service properties, including fatigue life under cyclic loading [2, 3]. Thus, one of the most important characteristics for surfacing is a portion of base metal (PBM) in the deposited metal proportional to base metal penetration other things equal. Reduction of the base metal penetration not only decreases consumption of expensive consumables, but improves quality and service properties of the parts to be surfaced.

Aim of the present work is a study of effect of electric parameters of flux-cored arc surfacing, in particular, stability of these indices on characteristics of the base metal penetration.

Consumables and equipment. Self-shielding flux-cored wire PP-AN130 was used for investigations. It provides for production of surfaced metal of tool steel 25Kh5FMS type. Gas-slag-

forming system of the flux-cored wire, which would provide the best welding-technological properties, was preliminary selected. Four self-shielding flux-cored wires PP-AN130 of 2 mm diameter having different systems of gas-slag-forming components, namely $\text{CaO} + \text{TiO}_2 + \text{MgO} + \text{CaF}_2 + \text{Al}_2\text{O}_3$ (wire with reference designation PP-AN130-1); $\text{CaO} + \text{MgO} + \text{CaF}_2 + \text{Al}_2\text{O}_3$ (PP-AN130-2); $\text{CaO} + \text{CaF}_2 + \text{Al}_2\text{O}_3$ (PP-AN130-3); $\text{CaO} + \text{CaF}_2 + \text{Al}_2\text{O}_3 + \text{starch}$ (PP-AN130-4), were manufactured for this purpose.

Expert estimation (5 examiners) of the welding-technological properties of all four wire types (nature of metal transfer, slag coating of the deposited beads, presence of pores) was carried out. The following system of the expert estimations was used for that. The transfer was marked by the following digits, namely 1 – fine-drop; 2 – globular; 3 – mixed; level of slag coating was estimated in percents; porosity – using two-point system: pores are present (yes) or absent (no). The preference was given to fine-drop transfer, 100 % slag coating of the deposited beads and absence of pores in the deposited metal.

Surfacing of the specimens was carried out using 230–250 A current and 20 m/h rate. Voltage has the key effect on pore formation in flux-cored wire surfacing [4], therefore it was varied from 24 V and higher up to pore formation in the deposited metal for each type of flux-cored wire (Table 1).

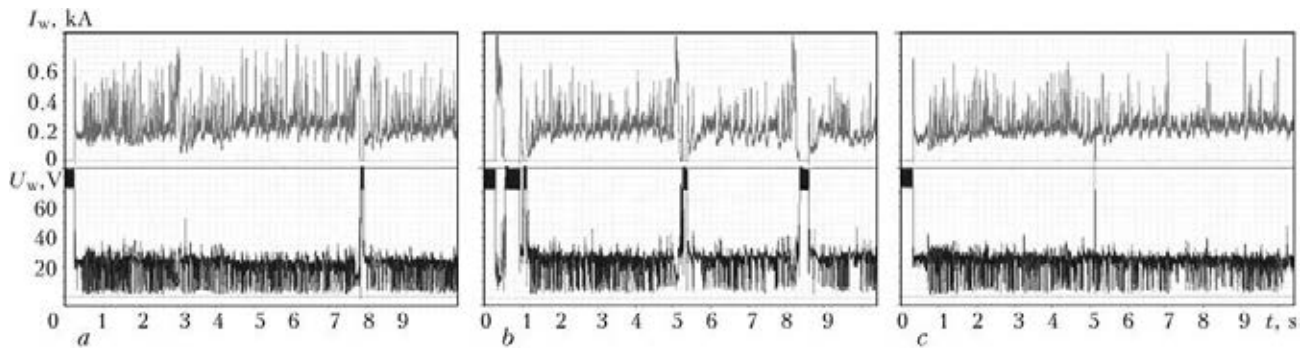


Figure 1. Oscillograms of current and voltage in surfacing using PP-AN130-1 flux-cored wire at different modes: *a-c* – experiments 2, 5 and 8, respectively, according to Table 2

According to expert estimation flux-cored wire PP-AN130-1 has the best welding-technological properties and it was selected for further experiments.

AD-231 automatic surfacing machine with VDU 506 rectifier was used for surfacing experiments. Surfacing was made on sheets from steel St.3 of 15 mm thickness. Surfacing current and voltage were registered with the help of computer data measurement system. Instrument shunt 75ShS-450-05 was used as a primary measuring welding current converter, and resistor divider 10:1 was applied for voltage determination. Measuring voltage converter L-Card E14-440 with imbedded 14-row 16-channel AD converter having conversion frequency up to 440 kHz was used for digitization and enter of data of primary converters in the computer. Registration of the parameters in our experiments was performed at 20 kHz frequency, which is sufficient enough for accurate study of high-rate processes in the arc,

Table 1. Results of estimation of welding-technological properties of flux-cored wires of PP-AN130 type

Designation of flux-cored wire	Voltage, V	Slag coating, %	Presence of pores	Character of transfer, point
PP-AN130-1	24	100	No	3
	28	100	Same	3
	32	100	Yes	2
PP-AN130-2	24	100	No	3
	28	80	Yes	3
	32	60	Same	2
PP-AN130-3	24	100	No	3
	28	100	Same	3
	32	80	Yes	2
PP-AN130-4	24	90	No	1
	28	90	Same	3
	32	90	»	3
	34	90	»	3
	36	90	Yes	3

for example, arc gap short-circuiting. Figure 1 and Table 2 provide for current and voltage oscillograms of surfacing at different modes using self-shielding flux-cored wire PP-AN130-1.

Data processing was carried out using specially-designed software in Visual Studio.NET, PowerGraph3.3 and MATLAB 7 media. Current condition of process being studied (arc ignition, arc extinction, short circuiting of arc gap, period of arcing) is automatically identified on data entered in the computer, and parameters of current and voltage for corresponding condition of surfacing process are calculated.

Results. A full-factorial experiment was carried out in order to determine the effect of surfacing current and voltage on process instability and PBM in the deposited metal. Current and voltage (factors) were varied at three levels, that give the possibility to construct a second-order model, providing more adequate description of the process being studied. The currents were set at 200, 250 and 300 A levels, voltage – at 22, 24 and 26 V. Surfacing rate in all cases was constant and made 20 m/h. Table 2 gives measured and calculated process parameters.

3D diagrams of distribution of U_w and I_w joint probability density only for surfacing process without period of initial arc ignition are shown in Figure 2. Probability p of appearance of specific combination of current and voltage in corresponding section of (I_w-U_w) plane is plotted along the vertical axis. The areas of arcing and short circuiting are outlined on the diagrams. Since arc extinctions in surfacing are rare and their duration is short, the probability density is also very small and being indistinguishable on the diagrams.

Figure 2 and Table 2 show that rise of arc voltage promotes for process stabilizing, i.e. number and duration of short circuits and arc extinctions is reduced. Short circuits and arc extinctions are virtually absent at 26 V voltage. However, appearance of pores in the deposited metal is shown with rise of voltage and, respectively,



Table 2. Parameters of process of arc surfacing using self-shielding flux-cored wire PP-AN130-1

Parameter	Number of experiment								
	1	2	3	4	5	6	7	8	9
U_w, V	22.4	21.8	20.8	23.7	24.8	23.5	25.3	24.4	26
$V(U_w)$	0.50	0.32	0.68	0.22	0.31	0.19	0.17	0.18	0.11
I_w, A	188	256.7	293.7	181.9	243.5	288.1	193.5	241.2	277.9
$V(I_w)$	0.54	0.45	0.69	0.39	0.35	0.31	0.29	0.27	0.22
I_a, A	174.5	239.4	235.3	175.4	241.1	280.7	190.4	237.8	277.2
$V(I_a)$	0.41	0.37	0.48	0.32	0.30	0.26	0.25	0.25	0.22
U_a, V	23.6	23.3	23.7	24.6	24.9	24.1	25.7	24.8	26.1
$V(U_a)$	0.17	0.15	0.21	0.12	0.15	0.12	0.11	0.13	0.10
$I_{sh.c}, A$	369.5	433.5	528.8	325	493.4	485.3	328.5	385.6	435.4
$V(I_{sh.c})$	0.39	0.33	0.27	0.37	0.34	0.28	0.36	0.32	0.29
$U_{sh.c}, V$	6.6	6.2	9.2	4.6	7.9	6.7	5.5	6.1	7.3
$V(U_{sh.c})$	0.61	0.44	0.40	0.41	0.49	0.37	0.69	0.38	0.33
$t_a, \%$	90.76	90.81	77.23	95.62	97.59	96.40	97.70	97.65	99.57
$t_{sh.c}, \%$	6.60	8.94	19.57	4.38	1	3.60	2.30	2.28	0.43
$t_{ex}, \%$	2.60	0.25	3.20	0	1.41	0	0	0.07	0
$F_{sh.c}, Hz$	13.29	19.25	13.75	14.58	2.49	8.21	9.91	8.38	1.99
T_{ig}, s	0	0	0.45	0	0.83	0	0	0	0
T_w, s	42.33	41.12	43.85	39.98	41.41	41.51	40.13	39.99	42.03
N_{ex}	10	3	21	0	6	0	0	1	0
$N_{sh.c.ig}$	1	1	5	1	7	1	1	1	1
$\gamma, rel. un.$	1.03	0.607	1.78	0.47	0.59	0.41	0.38	0.39	0.32
$g_0, \%$	34.75	24.10	20.60	39.10	30.20	330	42.35	29.10	33.10

Note. U_w, I_w – average values of voltage and current during surfacing; $V(U_w), V(I_w)$ – coefficients of variation of voltage and current during surfacing, where coefficient of variation is the relationship of root-mean-square value of parameter to its average value; $I_a, U_a, V(I_a), V(U_a)$ – average values of current, voltage, coefficient of current and voltage variation during arcing (without periods of initial arc excitation); $I_{sh.c}, U_{sh.c}, V(I_{sh.c}), V(U_{sh.c})$ – average values of current, voltage, coefficient of current and voltage variation during arc gap short circuiting (without periods of initial arc excitation); t_a – specific duration of arcing, equal total duration of periods of arcing and total time of welding without period of arc ignition; $t_{sh.c}$ – specific duration of short circuits, equal total duration of periods of short circuits and total time of welding without arc ignition period; t_{ex} – specific duration of arc extinctions, equal relationship of total duration of periods of arc extinction to total duration of surfacing; $F_{sh.c}$ – frequency of arc gap short circuiting without period of arc ignition; T_{ig}, T_w – duration of time of initial arc excitation and total duration of surfacing; $N_{sh.s.ig}$ – quantity of short circuits during the period of initial arc excitation; N_{ex} – number of extinctions during T_w ; γ – coefficient of process instability; g_0 – PBM in deposited metal.

arc length in self-shielding flux-cored wire surfacing.

Coefficient of instability γ was used for estimation of instability of process of flux-cored arc surfacing:

$$\gamma = [V(U_a) + V(I_a)]t_a + [V(U_{sh.c}) + V(I_{sh.c})]t_{sh.c} + t_{ex}N_{ex} \quad (1)$$

It is the sum of coefficients of variation of arcing current and voltage, coefficients of variations of current and voltage of arc gap short circuiting, number of arc extinctions multiplied by weight coefficients. Specific durations of arcing, arc gap short circuiting and arc extinctions

were taken as weight coefficients (for designations see Table 2).

Dependence of instability coefficient of surfacing process on current and voltage was received on formula (1) and data from Table 2 in a form of regression second-order model. Figure 3 shows geometric representation of this model (response surface). Lines of constant value of instability coefficient (lines of equi-response) are also shown in $(I_w - U_w)$ plane. The minimum number of arc extinctions and short circuits is observed at 25 V voltage. The coefficient of instability γ lies in the ranges from 0.50 to 0.32 and arcing is more stable at this current and voltage, changing

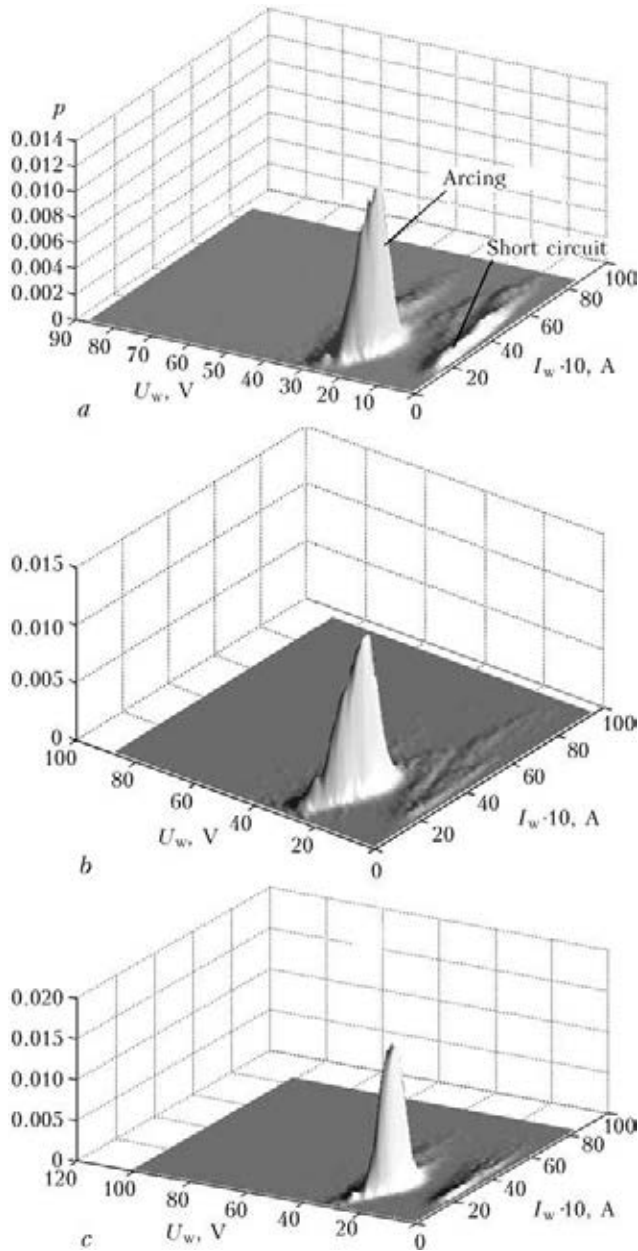


Figure 2. Distribution of joint probability density of surfacing current and arc voltage calculated for oscillograms in Figure 1

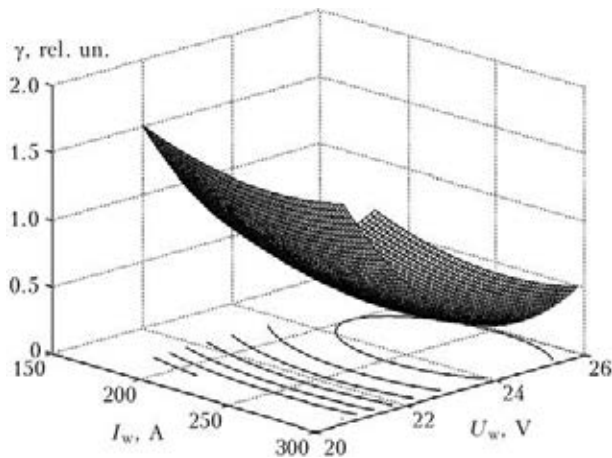


Figure 3. Dependence of coefficient of instability of arc process on surfacing current and arc voltage in surfacing using self-shielding flux-cored wire PP-AN130-1

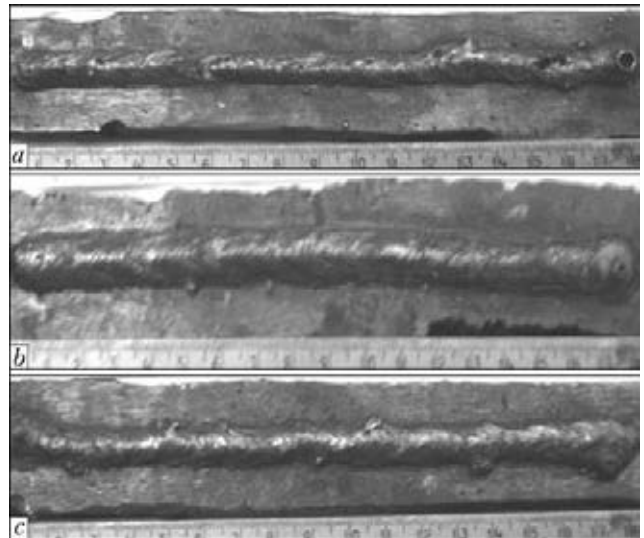


Figure 4. Appearance of beads deposited by flux-cored wire PP-AN130-1 at 200 (a), 250 (b) and 300 (c) A, 22 V and 20 m/h

in the ranges from 200–300 A. The coefficient of instability rises up to 0.9–1.0 in voltage reduction to 22 V and at the same currents.

Specimens deposited using the modes given above were also used for investigation of effect of surfacing modes on penetration and PBM in the deposited metal. As an example, Figure 4 shows the appearance of beads, deposited using different currents at 22 V and 20 m/h, and Figure 5 represents transverse macrosections of these beads.

Cutting of all specimens across the deposited beads was carried out after surfacing. Eight macrosections were manufactured from each specimen. They were used for determination of average from eight measurements of PMB in the deposited metal g_0 (see Table 2).

The calculation was carried out on expression

$$g_0 = \frac{F_0}{F_0 + F_d} 100 \%, \quad (2)$$

where F_0 is the cross-section of molten base metal; F_d is the cross-section of deposited metal.

Regression equation of g_0 dependence on current and voltage was received as for instability coefficient. Figure 6 shows respective response

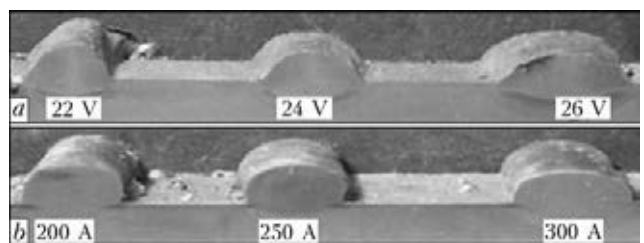


Figure 5. Macrosections of beads deposited using flux-cored wire PP-AN130-1 at different voltages, 250 A (a), and different currents, 24 V (b)

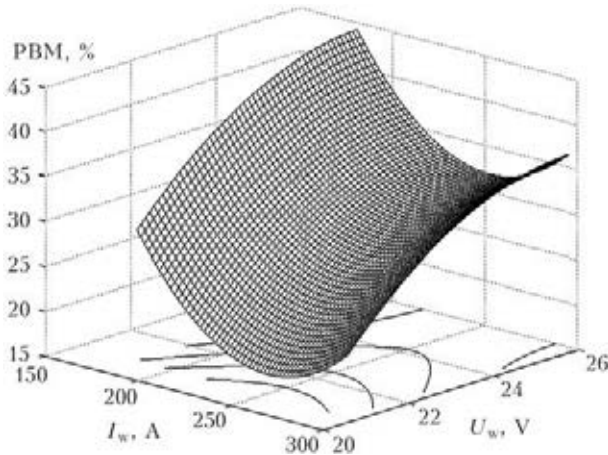


Figure 6. Dependence of PBM in the deposited metal on current and arc voltage

surface. Tendency to PBM decrease is observed in rise of surfacing current. It is related with the fact that the increase of surfacing current is directly connected with the rise of wire feed rate. This increases quantity of the deposited metal per unit of weld length at constant rate of surfacing. Rise of voltage from 22 to 24 V results in some increase of g_0 index at all values of surfacing current. However, this index does not change at further increase of voltage up to 26 V.

Relationship between quality of deposited bead formation, PBM in the deposited metal and indices of stability of surfacing process were also estimated. Figure 7 gives the combined 2D sections of the response surface for instability coefficient and PBM in the deposited metal. Area of optimum modes, providing sufficient process stability at minimum penetration and good formation of the deposited beads, is outlined by grey color. This area includes such modes of surfacing of specific part, selecting of which to the utmost fulfill conditions of its operation, structure of part and requirements to the deposited metal. In particular, if structure of the part requires surfacing of layers of large thickness in several passes, then more intensive mode of surfacing with sufficiently large penetration in the first pass can be selected. Surfacing of thin layer requires using the modes from area of surfacing process minimum stability with large bridging of the neighbor beads.

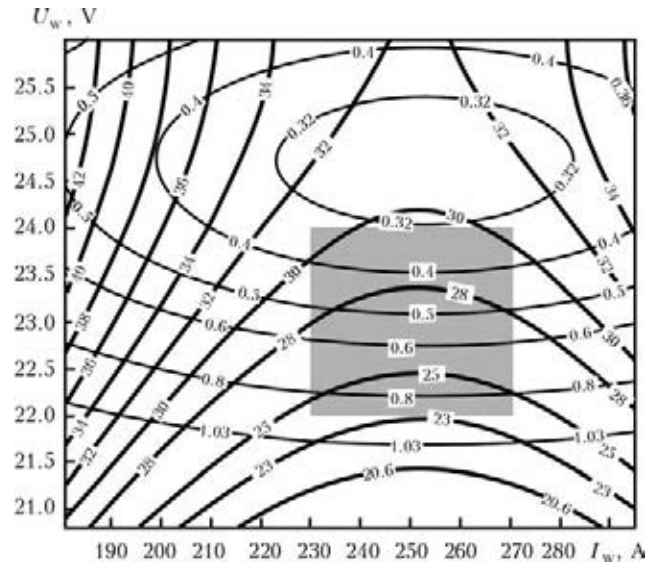


Figure 7. Contour curves of instability coefficient of arcing and PBM in the deposited metal

Conclusions

1. It is determined that wire having $\text{CaO} + \text{TiO}_2 + \text{MgO} + \text{CaF}_2 + \text{Al}_2\text{O}_3$ gas-slag-forming system has the best welding-technological properties among the experimental self-shielding flux-core wires of PP-AN130-1 type.

2. Instability of arcing depends, first of all, on voltage and reduces with its rise. Coefficient of instability reaches the minimum at 25 V in the carried experiments with use of self-shielding flux-cored wire of 2 mm diameter. Current has significantly smaller effect on arcing instability. The minimum instability coefficient for indicated wire is observed at 250–260 A.

3. Area of optimum surfacing modes, providing sufficient stability of the process ($\gamma = 0.32$ – 0.80) at satisfactory penetration ($g_0 = 23$ – 30%), lies in 230–270 A current and 22–24 V voltage change range.

1. Frumin, I.I. (1961) *Automatic electric arc surfacing*. Kharkov: Metallurgizdat.
2. Ryabtsev, I.A., Kondratiev, I.A., Babinets, A.A. et al. (2012) Effect of high-temperature thermal cycling on deposited metal of the type of heat-resistant die steels. *The Paton Welding J.*, 2, 22–24.
3. Senchenkov, I.K., Chervinko, O.P., Ryabtsev, I.A. et al. (2013) Determination of service resource of surfaced parts under cyclic, thermal and mechanic loads. *Svarochn. Proizvodstvo*, 1, 8–3.
4. Yuzvenko, Yu.A., Kirilyuk, G.A. (1973) *Surfacing with flux-cored wire*. Moscow: Mashinostroenie.

Received 06.03.2014

JOINING OF THICK METAL BY MULTIPASS ELECTROSLAG WELDING

K.A. YUSHCHENKO¹, S.M. KOZULIN¹, I.I. LYCHKO¹ and M.G. KOZULIN²

¹E.O. Paton Electric Welding Institute, NASU

11 Bozhenko Str., 03680, Kiev, Ukraine. E-mail: office@paton.kiev.ua

²Toliatti State University

14 Belorusskaya Str., Toliatti, RF. E-mail: office@tetsu.ru

Nonstandard schemes of ESW (multi-layer, well-like etc.) are mostly used for reconstruction repair of large-sized parts of heavy machine building. Through-thickness cracks are the most often type of fracture and they take place mainly in heavy-loaded machine parts being operated under alternating load. Such defects differ by large branching and twisting of the cracks as well as impressive sizes of fracture sections $(2.5-6.8) \cdot 10^5 \text{ mm}^2$. A method of multipass consumable nozzle electroslag welding (MCNESW) is the most appropriate for performance of repair works. Science-based combination of developed technical and technological approaches in MCNESW realizing provides for weld metal with high ductility, homogeneous structure and hardness, absence of hardening structures in HAZ and defects in fusion zone. The method of repair of large through-thickness cracks in large-sized parts directly at operation site is successfully implemented at six enterprises. Technical scheme, workup level and versatile of technological process of MCNESW performance allows also recommending it for joining of thick metal during production of new welded metal structures. 16 Ref., 4 Figures.

Keywords: *multipass electroslag welding, consumable nozzle, repair, large-sized parts, through-thickness cracks*

Single-pass electroslag welding (ESW) is mostly carried out by three main means, i.e. wire electrodes, consumable nozzle and large-section electrodes. These means can be used for production of virtually all existing types of butt, fillet and tee-welded joints, obtaining at that longitudinal and circumferential welds as well as welds of complex profile [1]. Elements of the welded joints are classified on shape of weld longitudinal section according to GOST 15164-95 and DSTU 3490-96. Surfaces of edges being welded, forming an assembly gap, are produced by machining, flame and plasma cutting as well as after rolling. Efficiency of application of single-pass ESW in manufacture of new large-sized metal structures is provided by correct selection of welding equipment and complex solving of issues of technique and technology of weld performance.

Refining of structure of the welded joint metal and reduction of the level of residual stresses require application of a postweld expensive high-temperature treatment (HTT). Therefore, any decision on rejection or, at least, decrease of volumes of its application, is always a priority [2].

One of the ways of approaching of full-strength joint to base metal without HTT is performance of ESW using the schemes differing

from traditional ones, for example, by means of joining of thick metal with the help of multilayer welds [3-5]. Efficiency of ESW application in joining of bi-metal billets rises, if the joint is welded by two welds in sequence [6].

Nonstandard schemes of ESW are mostly used for reconstruction repair of the large-sized parts of heavy-machine building, including, directly at operation site. Work [7] generalizes accumulated scientific-production experience of organizing and performance of such works and technological recommendations, used by corresponding engineering services of many enterprises and organizations, are proposed.

Mineral resource industry, metallurgy, power engineering and other branches have a variety of different large-sized parts in the units, fractured during operation. This requires realizing of individual approach in organizing of repair work for each specific case. It can be caused, first of all, by geometry parameters and spatial position of a fracture place as well as technical supply of working place and conditions of repair.

This work is dedicated to generalization of the results of testing, development and implementation of effective techniques of ESW repair of the through-thickness cracks, appearing mainly in heavy-loaded machine parts. The typical example of such objects are the solid rectangular and profiled cross-section bearing bands of rotary kilns,

which often fracture in operation due to through-thickness cracks [8]. Most of the bands, cross-section sizes of which make $(355-500) \times (900-1350)$ mm, are manufactured from medium-carbon steels of 35L type using traditional casting in sand molds or electroslag casting (steel 34L-ESh). Peculiarity of repair of such defects is related to significant extent with large branching and twisting of the cracks as well as impressive size of fracture sections (Figure 1), area of which can make $(2.5-6.8) \cdot 10^5$ mm². At that, the wide gaps, 2-5 times exceeding standard ones, are inevitably formed after welding edge preparation and volume of the removed defective metal can make 0.3-0.4 m³. Rough oxidized surface of the edges (after removal of damaged metal by oxygen cutting) creates new difficulties for providing of quality fusion during ESW.

Methods of repair of through-thickness cracks in the bands at operation site using electric-arc methods of welding differ by extremely low efficiency and do not always provide the quality welded joints as well as required occupational hygiene conditions [8]. Application of ESW traditional methods is also ineffective due to large expenditure of time for delivery of large-sized welding equipment, complexity of assembly and operation of multielectrode machines at great height (more than 20 m), and impossibility to receive guaranteed fusion of base metal edges with the weld in the beginning of welding, etc.

Application of some untraditional ESW methods [8-10] is complicated, mainly, due to impossibility of complete removal of the defect, having branching (spatial) character, providing of guaranteed fusion of edges being welded and low hot crack formation resistance of the welds.

Development of repair method to the maximum free of indicated disadvantages was necessary for solving of the issues of organizing of

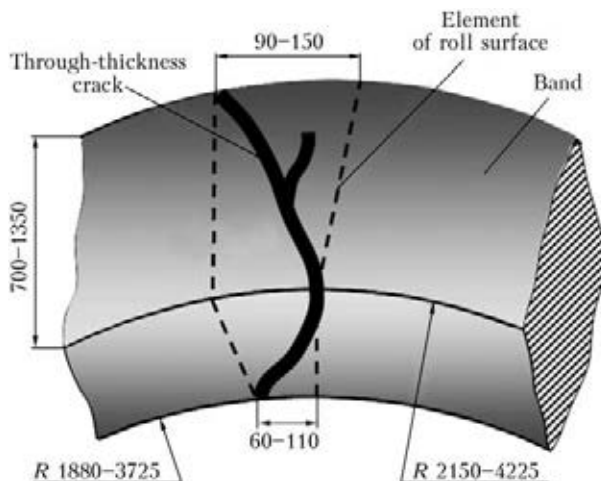


Figure 1. Scheme of typical positioning of crack in fractured band of rotary kiln

on-line repair of equipment with the through-thickness fractures at operation site.

In the best way these requirements are fulfilled by the method of multipass consumable nozzle electroslag welding (MCNESW) (Figure 2) [11].

Metallurgical, energy and technical issues, related with specifics of reconstruction works, were investigated for development of MCNESW principle technology.

The following was determined as the results:

- mechanisms of defect-free formation of welded joint in a wide gap;
- conditions of guaranteed fusion and quality formation of weld;
- energy peculiarities of process from point of view of its stability and absence of defects in welded joints;
- conditions for prevention hot cracks in welds;
- effect of process thermal cycle on structure and mechanical properties of welded joint metal.

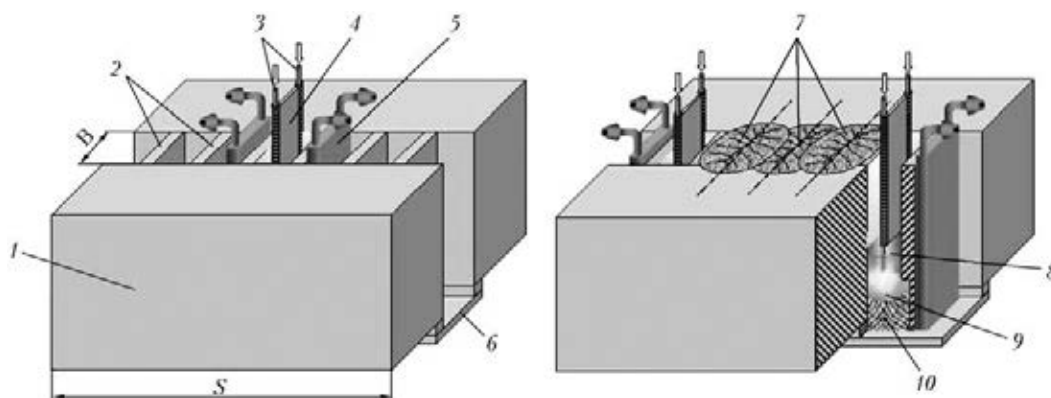


Figure 2. Scheme of the method of multipass ESW of big parts with large cross-section of elements being joined: 1 – part being welded; 2 – forming inserts; 3 – electrode wire; 4 – consumable nozzle; 5 – water-cooled device; 6 – hopper; 7 – welds; 8 – slag pool; 9 – metal pool; 10 – deposited metal; S – thickness of metal being welded; B – welding gap

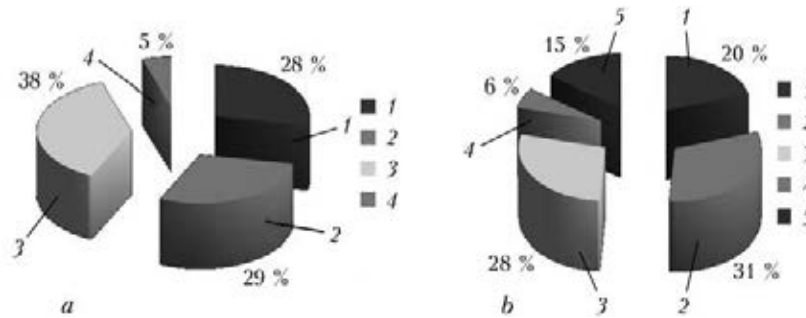


Figure 3. Portion of insert metal in composition of weld metal in MCNESW of the first (central) pass (a) and adjacent passes (b): 1 – base metal; 2 – electrode wires; 3 – metal of inserts; 4 – plate of consumable nozzle; 5 – metal of adjacent weld

Required depth of base metal penetration and width of melting of forming insert for real gaps of 60–150 mm, formed in area of occurrence of the through-thickness crack after removal of defective metal, are provided at values of welding process specific energy in the range of 220–340 kJ/cm².

Technological strength of welded joint metal is provided by set of measures, preventing hot crack formation [12, 13, 14], namely:

- reduction of weld metal shrinkage due to performance of multisection permanent joint by separate welds;
- positioning of weld plane in direction being in close agreement with tensile stress vector;
- reduction of level of tensile stresses in the period of solidification of metal pool due to flexibility of assembly separating inserts;
- selection of parameters of welding mode for each pass with weld shape coefficient in 5–8 range;

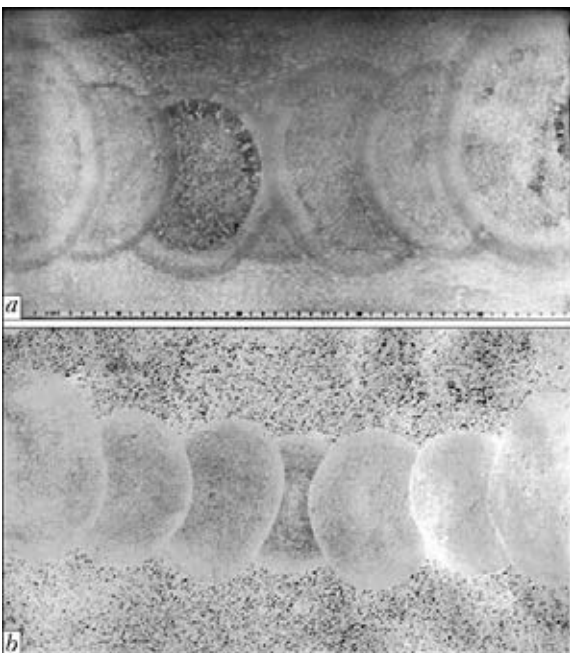


Figure 4. Transverse macrosection (a) and sulphur print (b) of 480 mm thick welded joint produced by new MCNESW method

- distribution of stress field density by means of symmetric welding-up of separate sections of the assembly.

This process is characterized by such a type of welding thermal cycle, at which cooling rates of HAZ metal are very low (0.2–0.8 °C/s), and time of staying of cooling metal in the range of the lowest stability of austenite is so long that conditions for HAZ structure formation can be considered closed to equilibrium [15].

Combination of welding wires of general designation with increased manganese content (for example, Sv-08G2 and Sv-10G2) and fused fluxes of SiO₂–MnO–CaF₂ system (AN-8M and AN-9U) during MCNESW of cast carbon steels of 35L type provides for required mechanical properties under conditions that material of assembly forming inserts will contain not less than 1 % Mn at low content of carbon and make 28–38 wt.% from the deposited weld metal (Figure 3).

Sufficient strength of reconstructed metal of the welded joints in heavily-loaded assemblies of the structures from medium-carbon cast steels of 35L type under conditions of static and impact loading as well as high long-term strength at alternating load are provided [15] due to high ductility of weld metal, homogeneity of its structure and hardness, absence of hardening structures in HAZ and defects in the fusion zone (Figure 4).

Technology for repair of the parts of unique equipment without its disassembly and specialized welding equipment [16] were currently developed using new MCNESW method. The technology was realized in repair of the through-thickness cracks of bands of rotary kilns at six enterprises. Experience of many years of operation of the reconstructed bands showed that long-term strength of the welded joints, produced by MCNESW under conditions of alternating loads, makes not less than 10⁷ cycles. Application of the developed technology in repair of the through-thickness cracks in bands of rotary kilns allowed 3 times reduction of the total time of

repair works in comparison with repair using automatic submerged twin-arc welding.

Conclusions

1. MCNESW is the efficient method of repair of the through-thickness coarse cracks in large-sized parts, immediately at operation site, that is indicated by results of its successful implementation at six enterprises.

2. Science-based combination of the developed technologies and techniques during realizing of MCNESW provides for high ductility of weld metal, homogeneity of its structure and hardness, absence of hardening structures in HAZ and defects in fusion zone.

3. Versatile of technological process and procedure of MCNESW allows also recommending it for joining of thick metal in production of new welded metal structures.

1. (1980) *Electroslag welding and surfacing*. Ed. by B.E. Paton. Moscow: Mashinostroenie.
2. Paton, B.E. (1971) Some predictions on welding development. *Avtomatich. Svarka*, **5**.
3. (1959) *Electroslag welding*. Ed. by B.E. Paton. Moscow; Kiev.
4. Anders, W., Maushake, W. *Verfahren zum Verschweissen von Groessen Querschnitten mittels Elektroschlackeschweissung*. Veroeff. 06.10.61.
5. Khoruzhik, G.I., Sushchuk-Slyusarenko, I.I., Andrianov, G.G. et al. *Forming device for vertical welding*. USSR author's cert. 284224. Int. Cl. B 23 K 25/00. Fil. 22.01.78. Regist. 21.03.80.
6. Sushchuk-Slyusarenko, I.I., Lychko, I.I., Khrundzhe, V.M. et al. *Forming device for vertical welding*. USSR author's cert. 747659. Regist. 23.01.78.
7. Sushchuk-Slyusarenko, I.I., Lychko, I.I., Kozulin, M.G. et al. (1989) *Electroslag welding and surfacing in repair works*. Kiev: Naukova Dumka.
8. Kozulin, S.M., Lychko, I.I., Kozulin, M.G. (2007) Methods of reconditioning rotary kilns (Review). *The Paton Welding J.*, **10**, 33–39.
9. Sushchuk-Slyusarenko, I.I. (1977) *Electroslag welding and surfacing*. Vol. 9. Moscow: Svarka.
10. Filchenkov, D.I., Kozulin, M.G., Sushchuk-Slyusarenko, I.I. (1982) Repair of defects of cast products from 30GSL steel by multilayer electroslag welding. *Svarochn. Proizvodstvo*, **9**, 19–20.
11. Kozulin, M.G., Kozulin, S.M. (1992) *Method of multilayer electroslag welding*. USSR author's cert. 1756074. Int. Cl. B23K 25/00. 33/00.
12. Kozulin, S.M. (2011) Selection of the groove shape for repair of through cracks by multilayer electroslag welding. *The Paton Welding J.*, **3**, 32–35.
13. Kozulin, S.M., Lychko, I.I., Kozulin, M.G. (2010) Increase of resistance of welds to formation of crystalline cracks in repair of bands of kiln furnaces using electroslag welding. *Ibid.*, **1**, 32–34.
14. Kozulin, S.M., Lychko, I.I. (2011) Deformations of welded joints in multilayer electroslag welding. *Ibid.*, **1**, 23–27.
15. Kozulin, S.M., Lychko, I.I., Podyma, G.S. (2013) Structure and properties of steel 35L welded joints produced using multilayer electroslag welding. *Ibid.*, **8**, 7–12.
16. Yushchenko, K.A., Lychko, I.I., Kozulin, S.M. et al. (2012) Portable apparatus for consumable-nozzle electroslag welding. *Ibid.*, **8**, 45–46.

Received 14.07.2014

PECULIARITIES OF APPLICATION OF SUPERCAPACITORS IN DEVICES FOR PULSE WELDING TECHNOLOGIES

A.E. KOROTYNSKY, N.P. DRACHENKO and V.A. SHAPKA
 E.O. Paton Electric Welding Institute, NASU
 11 Bozhenko Str., 03680, Kiev, Ukraine. E-mail: office@paton.kiev.ua

The prospective areas of application of supercapacitors (SC) are resistance spot welding, resistance butt welding as well as pulse-arc welding, where they can be used as slope controllers. Main technical characteristics of SC and bank of SC (BSC), based on series connection of separate SC, are given. Provided are the main calculation relationships, designed for evaluation of electric parameters of BSC, charge-discharge characteristics for developed BSC are experimentally determined. It is shown that the main disadvantage of series connection of SC cells in the bank is a voltage spread, which is proposed to be eliminated in present work by means of application of special charging device – equalizer. Different schemes of equalizers are considered, their advantages and disadvantages when using in pulse current generators are described. Relevance of application of energy-saving scheme of equalizer for pulse welding methods is shown. Scheme of such a device is proposed and described and calculation relationships providing analytical description of its operation are presented. A scheme for resistance spot welding, based on equalizer and bank of 6 SC is given as an example and technical characteristics of the proposed device are presented. 7 Ref., 1 Table, 6 Figures.

Keywords: pulse welding, pulse current generators, slope controllers, supercapacitor, bank of supercapacitors, charge-discharge characteristics, equalizer

Application of electric pulse energy storages is extremely efficient in some welding processes. This, first of all, refers to resistance spot welding [1], resistance butt welding [2], stud welding

[3] as well as gas-shielded pulse-arc welding [4], where they are used as pulse slope controllers. The authors of present work have positive experience of application of capacitor storages in arc cutting, where pulse effect, in contrast to air-arc cutting, is created by current pulse, that allows significant equipment simplification.

Simplicity of switching of bank of capacitors during charge and discharge and possibility of strict dosing of accumulated energy due to regulation of level of charge voltage or duration of pulse effect are to be referred to significant advantages of the capacitor storages, that expands their application in pulse technologies. Capacitor banks, based on cells with double-electric layer – supercapacitors (SC) – find more and more application at present time as capacitor storages. Still, SC cells are connected in the banks for receiving of necessary electric characteristics of the storages due to low level of operating voltage of SC cell ($U_{SC} \leq 2.7$ V). However, there are specific difficulties in manufacture of the banks with series SC (BSC) because of technological spread of capacity values of SC in the ranges of one nominal. Figure 1 shows the examples of performance of such BSC for 4 and 6 cells.

Account must be taken of $C_{\Sigma}(n) = C_i/n$, $U_{\Sigma}(n) = nU_i$ (where C_i is the capacity of separate SC; U_i is its operating voltage) in calculation of energy, accumulated in series BSC. Hence, it follows according to known formulae that energy



Figure 1. Examples of assembly of series BSC based on 4 (a) and 6 (b) cells

Characteristics of SC used for series BSC

BSC type	Quantity of cells	C, F	R, μOhm	$\tau = RC, s$	U_{op}, V	W, J
BSC-4	4	750	0.96	0.72	10.8	43,740
BSC-6	6	500	1.44	0.72	16.2	65,610
BSC-10*	10	300	2.44	0.72	27	109,350

*BSC-10 is the structure with series BSC-4 and BSC-6.

$$W(n) = \frac{C_{\Sigma}(n)(U_{\Sigma}(n))^2}{2} = \frac{nC_i U_i^2}{2} = nW_i.$$

Technical characteristics of applied SC are given in the Table.

Voltage is usually non-uniformly distributed in the cell during operation of such banks and it will be in inverse proportion to the values of capacity in circuit of series capacitors: $U_1 C_1 = U_2 C_2 = U_3 C_3 = U_n C_n$. Therefore, factor of non-uniform distribution of voltages in the circuit of series SC should be taken into account in charging of such a bank and stop charging process after achievement of maximum voltage $U C_i = U C_{max}$ by any of capacitors. At that total voltage at capacitor bank will be lower than nominal one: $U_b \leq \leq n U C_{max} = U_{b,max}$ or $\Delta U_{b,max} = U_{b,max} - U_b$.

Experimental investigations of voltage spread in BSC cells in the process of test operation were carried out at test bench, scheme of which is shown in Figure 2. Obtained test results were used for plotting of histograms of distribution of voltage in BSC cells (Figure 3), consisting of 10 series SC of VSAR3000 R270 K05 type. Results of investigation of SC behavior in mode of long-term storage of electric charge are given in Figure 4. Obtained experimental data showed that series connection of power SC provides for problems, related with undercharging of separate elements of BSC, that reduces to significant extent energy efficiency of pulse generator.

This work is dedicated to elimination of given effect and, thus, increase of energy efficiency of pulse generators, made using SC.

Preliminary selection of SC on values of capacity and assembly of banks from SC cells with similar capacity are carried out in order to provide equal voltage at cells and $U_b = U_{b,max}$ in charge of bank of series SC. However, some charge of capacity of SC cells is possible in process of SC operation, that can result in not always uniform distribution of voltages in BSC cells (see Figure 3). At present time, the equalizer type devices are used for voltage adjustment at BSC cells for the purpose of more efficient application of energy properties of SC in the course of the

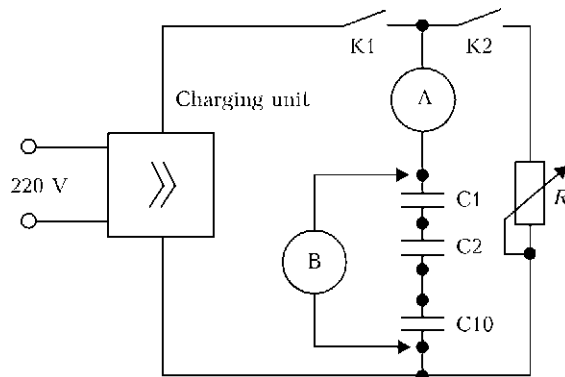


Figure 2. Scheme of experimental bench for verification of BSC: K1, K2 – switching units; C1–C10 – capacitor cells

whole guaranteed period of operation. There are different types of equalizers, i.e. passive dissipative [5], active dissipative [6] and active energy-saving [7].

Designing of systems for SC recharging using the active energy-saving equalizers is proposed

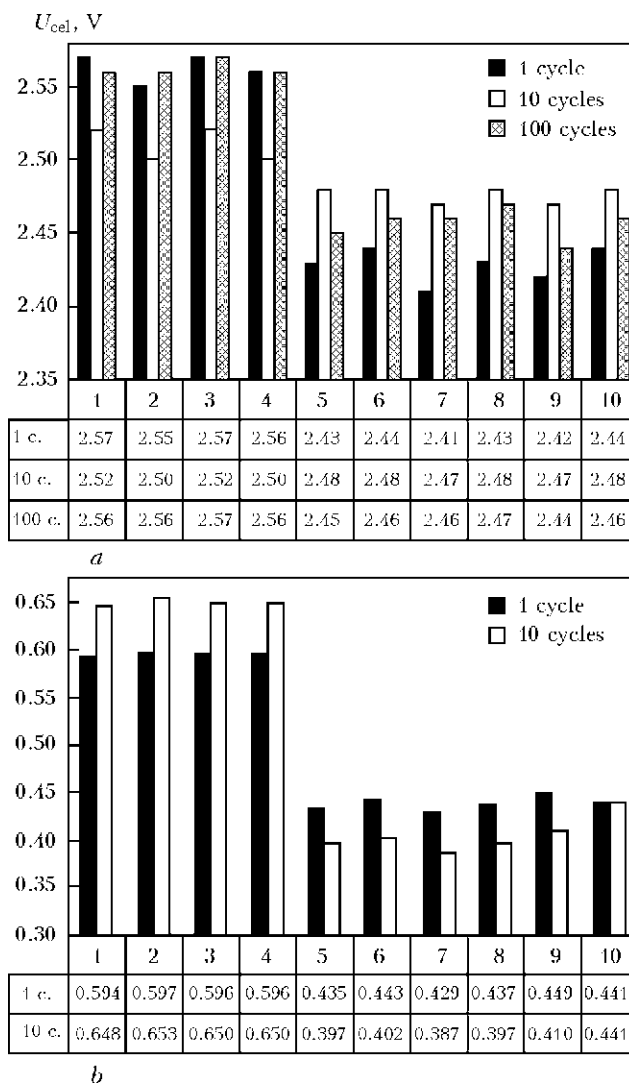


Figure 3. Histograms of distribution of voltages in cells 1–10 of charged (a) and uncharged (b) BSC at different quantity of charge–discharge operating cycles

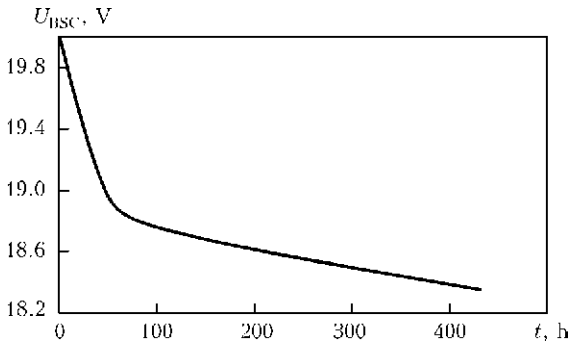


Figure 4. Self-charging of bank from 10 series SC

for consideration due to modern requirements to ecology of energy systems and energy-saving.

Principle of their work is based on application of BSC cell energy-exchanging processes, at that the cells with increased voltage are used for recharging of the cells with reduced one. Uniform distribution of voltages in the circuit, virtually for the whole voltage operating range of the bank, is maintained in BSC as a result of work of such a system in the process of energy exchange between the cells. Earlier similar hardware means [6, 7] were used in operation of power lithium-ion banks in different mobile and aerospace devices. The lithium-ion banks are very similar to BSC

in some characteristics (for example, they are characterized by directly proportional dependence of voltage in cell on charge level), therefore the similar approaches to equalizers can be used for BSC. The example of such adapted equalizer scheme applicable to SC is shown in Figure 5.

The scheme includes a charging supply unit (CSU), designed for formation of BSC charge current from primary mains, series supercapacitors SC1–SCn, where their quantity is determined by the requirements to load supply. Scheme of active equalizer is based on matching transformers Tr1–Tr(n + 1) and electronic power switches T1–Tn. Diodes D1–Dn are integrated in a structure of crystal of electronic power switch. Drivers Dr1–Drn are designed for matching of switch drive circuits T1–Tn with regulation scheme. Regulation scheme of master oscillator (MO) is performed on standard two-phase PWM controller, at that output of the first phase F1 is connected to uneven, and the second F2 to even switchers of the scheme. High-frequency inverter (Inv) is designed for parallel supply of matching transformers for adjustment of voltage between even and uneven groups of cells. In process of device operation the capacitor bank is charged from CSU or discharged into load (L). If voltages at all capacitors are equal, voltage $U_{W2i} = U_{SCi}/2 - \Delta U_{VTi}$ (where ΔU_{VTi} is the overbalance voltage) is supplied to secondary windings W2.1–W2(n + 1) of matching transformers Tr1–Tr(n + 1). Voltage at secondary windings of the transformers is determined from $U_{W2i} \approx U_{BSC}/2n$ condition, when voltage at the primary windings $U_{W1i} = U_{BSC}$.

If voltage at any of the capacitors is more or less than average one ($U_{SCav} \neq U_{BSC}/n$), then equalizing currents start to flow through windings of Tr1–Tr(n + 1) and open switches T1–Tn, resulting in voltage balancing at the capacitors. Matching inverter operates synchronously with switching of T1–Tn switches and in turn carries out recharging of even and uneven groups of capacitors, thus balancing voltages between the groups. Operation of the scheme results in balancing of voltages at SC cells and reduction of values of equalizing currents to the minimum. Currents in primary windings of the transformers are reduced to the values determined by losses of transformer

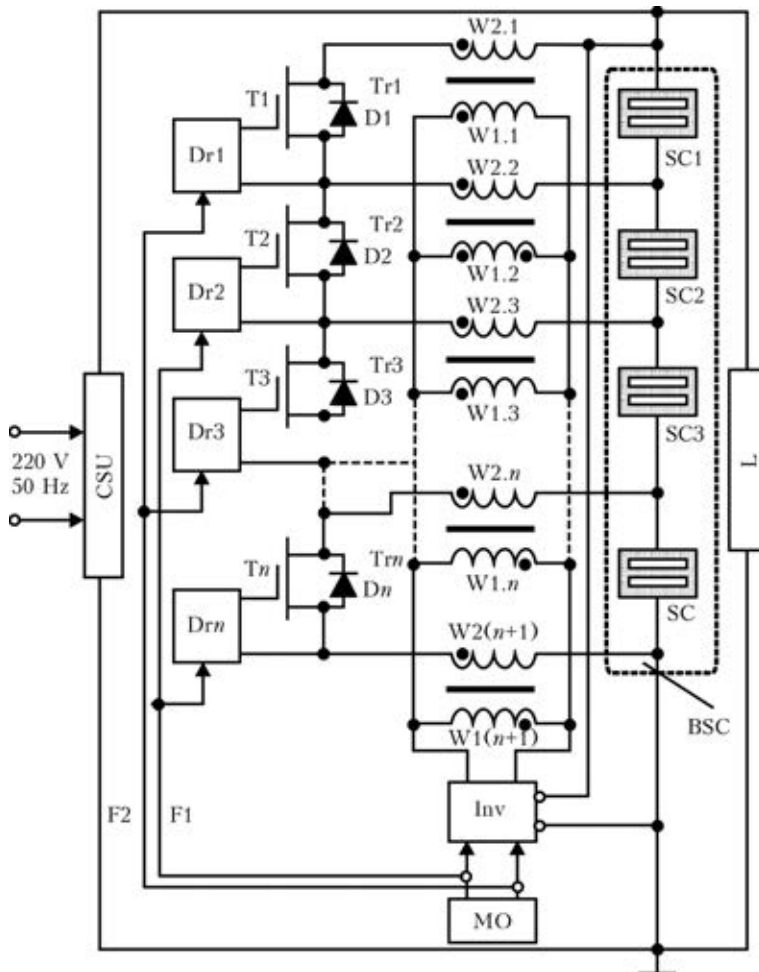


Figure 5. Scheme of BSC equalizer (see designations in the text)

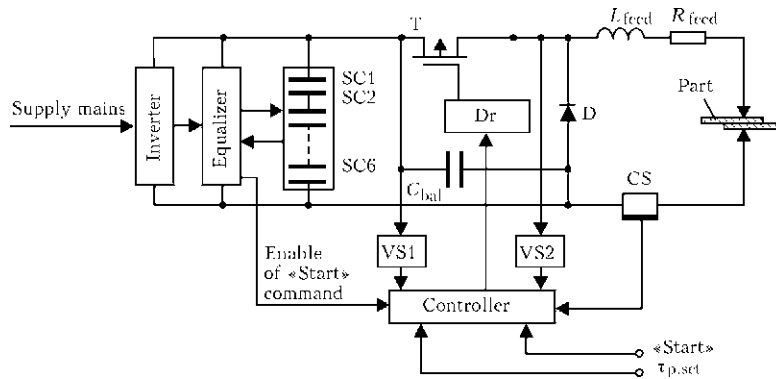


Figure 6. Example of application of equalizer in resistance spot welding device

open-circuit. Balancing of voltages at BSC cells is carried out exactly in such a way.

The peculiarity of this device (see Figure 5), making it different from described in work [7], is application of separate sections of matching transformers for each SC cell as well as replacement of the diodes for synchronous rectifiers (field-controlled transistor), that provided higher rate and accuracy of voltage balancing.

Compare energy parameters of BSC in use of scheme of active equalizer (see Figure 5).

Energy, accumulated in BSC with series capacitor cells, is determined by the expression

$$E_{BSC} = \frac{nC_0U_0^2}{2}, \quad (1)$$

where n is the quantity of cells; C_0 is the nominal capacity; U_0 is the nominal voltage.

If BSC has a capacitor cell with reduced capacity

$$C_i = kC_0, \quad (2)$$

(where $k < 1$ is the coefficient of undercharging of separate cell), charged to nominal voltage $U_{Ci} = U_0$, then voltage at remaining cells with nominal voltage will equal

$$U_x = kU_0(kC_0U_0 = C_0U_x). \quad (3)$$

It follows from this that sum voltage at such a bank with series cells

$$U_{BSC} = U_0k(n-1) + U_0 = U_0(1+k(n-1)). \quad (4)$$

Energy, accumulated by BSC, including one capacitor cell with reduced capacity, will equal

$$\begin{aligned} E'_{BSC} &= \frac{C'_{BSC} U_{op}'^2}{2} = \\ &= \frac{C_0 \frac{k}{1+k(n-1)} [U_0k(n-1) + U_0]^2}{2} = \\ &= \frac{C_0 U_0^2 k(1+k(n-1))}{2}. \end{aligned} \quad (5)$$

Energy accumulated in BSC in use of equalizer, balancing the voltage at capacitor cells, is

$$\begin{aligned} E''_{BSC} &= \frac{C''_{BSC} U_{op}''^2}{2} = \frac{C_0 \frac{k}{1+k(n-1)} (nU_0)^2}{2} = \\ &= \frac{C_0 U_0^2}{2} \frac{kn^2}{1+k(n-1)}. \end{aligned} \quad (6)$$

Comparative analysis of energy efficiency of equalizer application can be carried out with the help of given expressions (4)–(6). If coefficient of efficiency of BSC with similar cells is taken for $K_{ef} = 1$, then efficiency of BSC with cell, having reduced capacity, will be determined by relationship

$$\begin{aligned} K_{ef1} &= \frac{E'_{BSC}}{E_{BSC}} = \frac{kC_0U_0^2[1+k(n-1)]}{nC_0U_0^2} = \\ &= \frac{k^2(n-1)+k}{n}, \end{aligned} \quad (7)$$

and efficiency of BSC with equalizer and cell, having reduced capacity, is

$$K_{ef2} = \frac{E''_{BSC}}{E_{BSC}} = \frac{kn^2}{1+k(n-1)} = \frac{kn}{1+k(n-1)}. \quad (8)$$

Therefore, fractional increase of BSC efficiency with equalizer will be determined by relationship

$$Q = 1 - \frac{K_{ef1}}{K_{ef2}} = 1 - \left(\frac{k(n-1)+1}{n} \right)^2. \quad (9)$$

Use of given calculation relationship (7)–(9) for estimation of energy efficiency of the equalizer allows proving that significant effect is noted even at 10 % deviation of capacity of only one capacitor from nominal value.

It is necessary to outline that application of equalizers in different devices for pulse welding technologies allows reaching not only high energy indices, but providing high stability of weld-

ing-technological indices due to precision BSC charging.

Figure 6 as an example shows a scheme of device for resistance spot welding. Its main difference from known devices [1] is presence of the equalizer. Inverter of charging current after switching of electric supply provides charging of capacitors SC1 and SC6 to a level of voltage, determined by controller, after what the scheme is transformed in a waiting mode. Simultaneously, the equalizer scheme analyzes balancing of voltages in SC cells and, if necessary, carries out active balancing of voltages in BSC cells. «Start» command blocks the operation of charging inverter and regulation pulse is supplied to driver of current switch T. As a result, emergence of pulse of operating current, flowing along circuit: SC1–SC6, T, L_{feed} , R_{feed} , CS, SC1–SC6, is observed. Welding device allows dosing of energy, supplied to contact gap by means of programming of SC1–SC6 voltage and duration of current pulse, determined by switching unit. Duration of current pulse can be varied in the ranges from units to several hundred milliseconds. Also, series of pulses with individual parameters for each pulse in the series is possible. Information, received from current and voltage sensors CS and VS2, is used for control and regulation of energy, supplied to the contact gap of part being welded. High technological indices in given device are achieved due to application of high-speed electron current switching unit, which carries out accurate dosing of energy, supplied to welding zone.

Experimental check of the device for resistance spot welding, assembled on given scheme (see Figure 6), provides for the following results: maximum welding current equals 1200 A; consumed energy makes 2 VA in open-circuit mode, 500 VA in BSC charge mode and 100 VA in welding mode at supply from single-phase mains 220 V. Smoothly regulated duration of welding current pulse is at the level of $0.01 \div 0.5$ s.

In practice the SC cells should be connected in the banks for receiving of necessary and ac-

ceptable load resistance of the capacitor storage. Quantity of series cells in such a bank determines its operating voltage, and number of parallel branches is defined by its maximum operating current and efficiency, that should be considered in BSC designing. Due to the fact that SC has some internal loss resistance R_0 , energy accumulated in it during discharge is released for load resistance R_1 as well as R_0 . Obviously that the higher R_0 in relation to R_1 , the lower is the level of loss in SC and, as a result, the lower is the level of energy-conversion efficiency in load during its operation. Clearly that it is necessary to be assumed in BSC use. Moreover, it is desirable to consider not only the effect of bank and its weight-dimension indices, but environment requirements of electrical consumers as well as economy criterion, determined among other by cost of electric energy and operation expenses, for designing of current welding equipment and other technological equipment using BSC as energy storage.

1. Paton, B.E., Korotynsky, A.E., Drachenko, N.P. et al. (2009) Application of supercapacitors for increase the power efficiency of devices for spot resistance welding. In: *Proc. of Int. Sci.-Pract. Conf. on Power- and Resources-Saving in Industry, Power Engineering and Transport* (Kiev, 2009), 54–58.
2. Kuchuk-Yatsenko, S.I., Lebedev, V.K. (1976) *Continuous flash-butt welding*. Kiev: Naukova Dumka.
3. Paton, B.E., Drachenko, M.P., Kaleko, D.M. et al. *Apparatus for stud welding*. Pat. 92389 Ukraine. Int. Cl. B 23 K 9/20. Publ. 25.10.2010.
4. Korotynsky, A.E. (2002) State-of-the-art, tendencies and prospects of development of high-frequency welding converters (Review). *The Paton Welding J.*, **7**, 44–47.
5. Shurygina, V. (2003) Supercapacitors as the helpers or competitors to battery power sources. *Electronics: science, technology, business*, Vol. 3, 20–24.
6. Cizov, M. (2003) Device for voltage rectification on elements of supercapacitor bank. *Sovr. Elektronika*, **1**, 40–43.
7. Eremenko, V., Vorontsov, K., Varlamov, D. (2007) Hardware methods of increase in power efficiency of high-voltage accumulator bank. *Elektr. Komponenty – Ukraina*, **7/8**, 62–66.

Received 21.10.2013

AUTOMATIC MACHINE FOR WET UNDERWATER WELDING IN CONFINED SPACES*

V.A. LEBEDEV¹, S.Yu. MAKSIMOV¹, V.G. PICHAK¹ and D.I. ZAJNULIN²

¹E.O. Paton Electric Welding Institute, NASU

11 Bozhenko Str., 03680, Kiev, Ukraine. E-mail: office@paton.kiev.ua

²Greenfield Energy Ltd, Great Britain

PWI developed technology and equipment allowing performance of automatic flux-cored wire wet underwater welding of structural elements, reliably insulating the lower part of heat exchanger column. The unique aspect of the work consists in development of an automatic welding machine, capable of operating when immersed into a pipe of 119 mm inner diameter into liquid heat carrier medium at 200 m depth. The semiautomatic machine was designed with application of special torque electric drives for electrode wire feed and welding displacement mechanisms. A special cable with welding and control wires was developed, capable of operating at a large distance from the arc power sources and control system. Cable uncoiler design was also developed, with digital recording of automatic machine position along the pipe length. Approbation results showed that application of special automatic machine allows increasing heat exchanger reliability, reducing time loss during performance of work on its sealing, rational use of site area and reducing financial expenses. 5 Ref., 8 Figures.

Keywords: *wet arc welding, geothermal heat exchangers, sealing, automatic machine, power source, cable uncoiler, control system*

Process of mechanized wet arc welding, equipment and flux-cored wire for its implementation were proposed at PWI [1] and are currently being developed in different spheres. This is repair of ships and vessels, underwater product lines, port underwater facilities, etc [2, 3].

One of the new objects of effective application of wet welding are complexes of Greenfield Energy Ltd Company — technology developer and operator of power efficient Geoscart™ complexes, combining such systems for satisfying production needs as closed-loop heating systems, systems of treatment of consumed hot water for production purposes, refrigeration units and air conditioning systems.

Geoscart™ system was developed to control heat flows of public and commercial buildings and enterprises with continuous high-density energy consumption such as modern supermarkets, higher class hotel business enterprises, stationary hospital complexes, as well as satisfying production needs of food and pharmacological industry. One of the main functional features of Geoscart™ system is the ability to store excess thermal energy up to the moment of this energy deficit. Company uses geothermal heat exchangers

of a special design for fast and efficient transfer of excess or deficit of low-grade thermal energy, using high density and heat capacity of formations located much lower the surface soils. Standard depths for the main transaction of heat-exchange process are the ranges down to 200 m from ground surface level.

At construction of heat exchangers, the quantity of which can reach several tens, depending on facility size, principles similar to methods applied in oil and gas well drilling, but with certain differences in construction technology, are used. In particular, closed-loop heat exchangers require guaranteed insulation of the lower part of insulation column, in order to avoid losses of expensive heat-conducting working liquid, produced from a composition of nonpolluting propylene glycols, extracted from the plant mass. Used for these purposes are plugs of a special design, made from organic uncured rubber. Operation experience of these heat exchangers, however, showed that natural ageing of plug material in service results in a change of its dimensions, and leakage of its working fluid. Mounting a new plug requires shutting down the complex. Considering that heat exchangers are usually located in the territory of vehicle parking areas near the serviced facility, this operation leads to significant financial losses, in addition to losses of op-

*V.K. Zyakhor, I.S. Kuzmin, V.G. Novgorodsky, N.A. Poddubny and I.V. Lendel participated in the work.



Figure 1. Heat exchanger pipe neck and external conditions of work performance

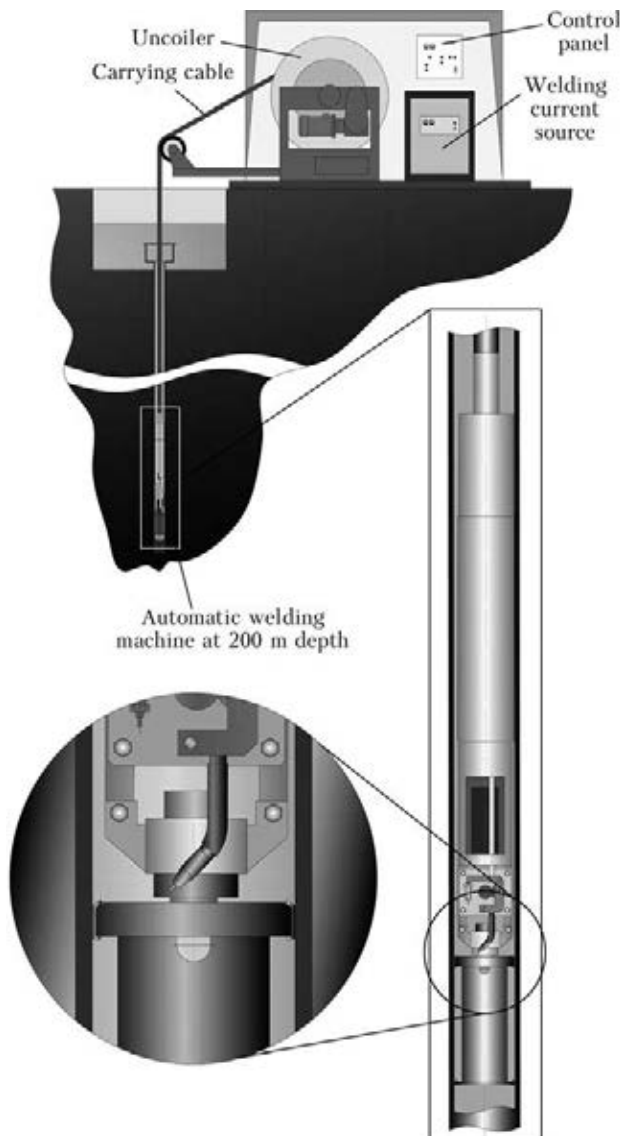


Figure 2. Complex of equipment for automatic welding inside the pipe at great depth

eration effectiveness at lowering of liquid level. As an alternative, PWI proposed a process of heat exchanger tube sealing by placing and welding-on a cap.

The objective of this work was development and introduction of a special automatic welding machine and its application technology for welding-on the plug-cap inside the pipe at down to 200 m depths, that will allow shortening time losses, lowering financial expenses, reducing loss of useful area, and improving heat exchanger reliability.

Pipe neck design and conditions of work performance are shown in Figure 1.

Conditions and environment of welding performance predetermine the complexity of the problem being addressed both in terms of equipment and technology. Development was based on PWI experience on designing mechanized equipment for wet welding with application of special flux-cored electrode wires. However, rather great welding depths, extremely confined conditions (pipe inner diameter is not more than 120 mm), as well as the medium (25 % water solution of polyethylene glycol) required a large scope of additional research both on individual components of welding equipment, and on welding technology and welding consumables, as experience of equipment design and its application in the automatic welding mode for these conditions is lacking either at PWI or in the world practice.

Development of the automatic machine proper for cap welding-on at great depth is just part of the complex, which should include welding current source of a special design (remoteness of welding site with inevitable voltage drop in the cable), special load-carrying cable with power conductors and control wires, as well as a device for automatic machine lowering and lifting. The entire equipment set and its application conditions are shown in Figure 2.

Algorithm of welding performance envisages that the cap of a special design to be welded on is placed into the automatic welding machine clamp before immersion, and is disengaged from it after welding and beginning of automatic machine lifting.

Considering that none of the complex components without exception could be selected from commercially manufactured equipment, features of their development and design are of interest.

Let us consider ADSP-200 automatic machine for wet welding at great depth in a confined space. The automatic machine is a tubular metal structure, combining the following main compo-

nents: module of electrode wire feed, module of welding head rotation (of feed mechanism), module of contact components. Feed module and rotation module are based on gearless computerized DC electric drives incorporated into commutatorless electric motors with bevel drive to feed roller. Feed module consists of the device of electrode wire pressing down, nozzle with guide channel and current-conducting tip. Module further includes nozzle oscillator, as well as the assembly of cap fixing with fixation force regulator for guaranteed disengagement of the cap from the automatic machine after the welding cycle, as well as sliding contact component of welding voltage current transfer (return wire «-»). Addition of nozzle oscillator to the module is due to presence of quite large gaps between the cap being welded-on and pipe inner surface, on the one hand, and impossibility of essentially increasing the welding modes, because of the possible overheating of automatic machine components and pipe wall burn-through. The guide channel, accommodating the electrode wire stock required for a single welding cycle, is made of plastic with a low coefficient of friction. Channel length is 15–18 m. Considering the confined conditions, electrode wire is not wound on the spool, as it is usually done, but is in the straightened state. Two effects are achieved here: space saving for automatic machine systems, and essential reduction of feeding force. To provide protection from the liquid medium, feed mechanism electric motor is placed into a water-tight box filled with insulating-lubricating fluid and having a compensating diaphragm, as well as special sealed connector for control cable connection.

Main difficulties in development of automatic welding machine ADSP-200 consisted in selection of layout solutions in an extremely confined space, with performance of a large scope of experimental studies, with development of welding equipment mock-ups and simulation of welding conditions. This enabled effective solution of the problem of development of nozzle oscillator of an ingenious design, where the drive is combined with electrode wire feed drive and, as a result, increase of the required moment on drive electric motor shaft. The impossibility of mounting sensors of nozzle position relative to the butt being welded determined the search for engineering solutions in two directions. Before the automatic machine lifting the nozzle is oriented by the future gap relative to the cap fixed in the clamp. The start and end of welding is possible from any point and is pre-programmed by controller-based control system of rotation module, with analysis

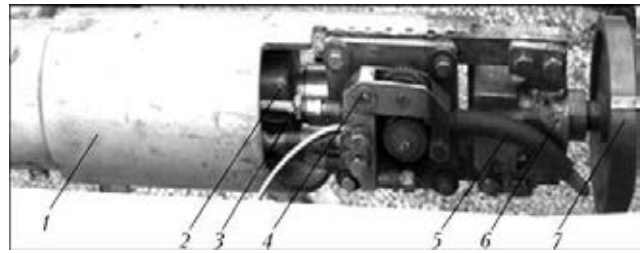


Figure 3. Automatic machine for welding in confined conditions at great depth: 1 – case; 2 – rotation mechanism; 3 – guide channel; 4 – feed mechanism with nozzle oscillator; 5 – nozzle; 6 – fixtures and elements of current transfer to the cap; 7 – cap

of path covered by nozzle, and then the operation of weld closing by automatic machine is performed by a similar algorithm.

Figure 3 shows the ADSP-200 automatic welding machine in the position before immersion for welding.

The complexity of the task of connecting and sealing the welding cables and control wires should be noted. The great length predetermined the need to develop engineering solutions for their fast connection to automatic machine systems and sealing. This also involves special deep-water connectors, and couplings filled with low-melting dielectrics.

Welding current source of VDU 25-506 MP type. It is obviously impossible to implement the welding process with the required characteristics at considerable distance from the object of welding, by using traditional welding current sources with flat external volt-ampere characteristics (VAC). This follows from experimental investigations and conclusions of [4]. Source VAC in the arcing zone changes significantly because of great lengths of welding cables of a limited section (ohmic resistance of outer circuit rises and, hence, voltage drop in the cable becomes higher). Here, compensation of voltage drop in the outer circuit due to voltage rise, does not yield the required result. Inductance of source–arc system changes noticeably, that has a negative effect on the nature of arcing and electrode metal transfer. In order to solve these problems, specialized VDU 25-506 MP source for mechanized and automatic welding at large distance of feed mechanism (of automatic machine) from power source was designed and manufactured, in particular, for wet automatic welding at 200 m depth. Figure 4 shows the appearance of VDU 25-506 MP source.

To ensure high quality of welding at application of various kinds of electrode wire, the source enables adjustment of dynamic characteristics to establish the rate of current rise, required for a specific wire type. Ability to perform such additional adjustments is ensured through application



Figure 4. Source of welding current for working with remote objects

of Moller programmable logic controller (Germany). Application of the principle of proportional plus integral plus derivative control of welding contour dynamics to ensure the required power source characteristics at operation with long welding cables allows guaranteeing its stable performance in the entire adjustment range and repeatability of the selected adjustment parameters.

Cable. As shown by results of experiments on possibilities of transfer of welding current, control and adjustment signals, the only correct engineering solution for operation under confined conditions is combining all the electric circuits

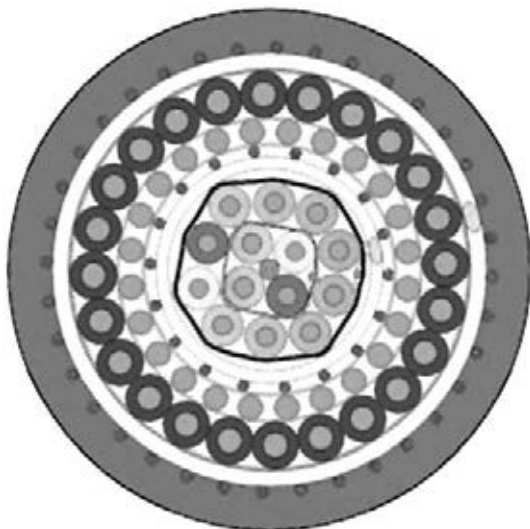


Figure 5. Section of cable for underwater automatic welding

in one cable, which, in addition to that, should also be carrying, i.e. should be able to support the automatic machine weight, its own weight, as well as overcome the hydrostatic resistance of the environment at immersion and lifting stages.

Industry lacks cables, capable of satisfying such a set of requirements. It turned out to be possible to solve the above-defined problems at purposeful development of a cable, which was given the technical name «Cable flexible armored strengthened submersible for electric welding KGBUPES 2×95+(4×2.5)e+(10×2.5)e» [5].

Cable specification

Design weight of 1 km of cable, kg	3850
Cable outer diameter	47.5
Tensile force, N	not less than 20,000
Minimum radius of inner loop of cable bending in outer cable diameters	not less than 8

It should be noted that all the conductors with rational layout of cores and conductors to ensure reliable insulation and flexibility are made of copper. Power and control conductors are shielded. Measuring (with one meter spacing) marks are made on the cable for additional control of the length of its unwinding or winding. Figure 5 shows the cross-section of cable of complex design KGBUPES 2×95+(4×2.5)e+(10×2.5)e. Cable strength at considerable tensile force is ensured by additionally incorporated flexible enclosing steel elements, including flexible armour. Additional strengthening was provided by a large number of mylar filaments of different diameter. Insulation of each conductor and conductor layer was performed with application of reliable modern insulating materials, such as PET-E film, folsan, etc., with multiple (3–4 times) overlapping.

Cable uncoiler. Cable uncoiler is designed for storage, transportation, lifting and lowering of automatic welding machine into the pipe to 200 m depth and its subsequent removal, and is a drum of lattice-rod design, mounted on rotator drive shaft. On the other end the shaft is additionally supported by roller support adjustable by its position (backrest). Rotary motion of the shaft with drum with adjustable frequency is provided by variable frequency electric drive with asynchronous electric motor, connected to drum shaft through a reduction gear. Drum design envisages availability of a special cable box for fast connection of welding and control cables. The entire structure of the drum, rotator and roller support is mounted on a welded bed.

Uncoiler incorporates its own local system of control and adjustment, allowing control of both the direction of drum rotation, and its rotation



Figure 6. Appearance of cable uncoiler

frequency. For convenience of automatic machine immersion or lifting, the uncoiler has a remote control panel. More over, uncoiler incorporates automatic guide roller, ensuring stable advance of the cable into the pipe to the welding area. The roller is fitted with rubber-bonded bush, ensuring roller engagement with the cable at its uncoiling. The roller is also connected to incremental encoder (digital converter of cable movement), ensuring calculation of length of uncoiled cable (lowered to welding area) with result digitizing. Figure 6 shows the considered uncoiler in the position of automatic machine readiness for immersion.

Main technical characteristics of cable uncoiler

Minimum drum diameter, mm	100
Nominal rotation frequency, rpm	0.267
Range of rotation frequency adjustment	1:10
Nominal moment, N·m	40095

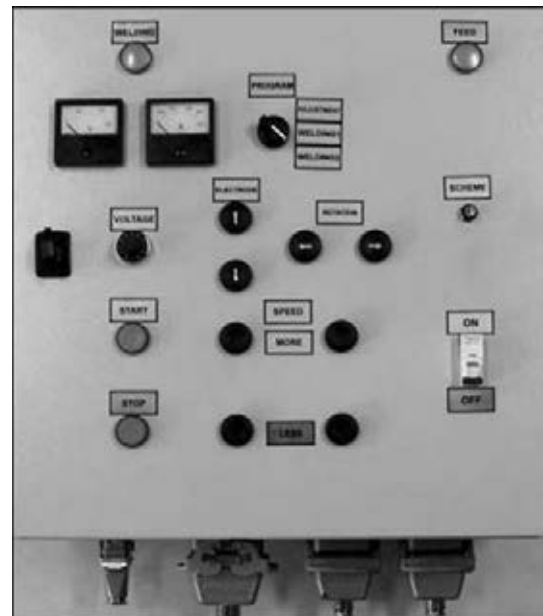


Figure 7. Appearance of control panel of ADSP-200 automatic machine

System of control and adjustment of automatic machine ADSP-200. The system is designed for adjustment control of direction of rotation of electric motors of electrode wire feed and rotation mechanisms, setting the rates of wire feed and welding displacement (feed mechanism rotation). System of control and adjustment is based on welding cycle control module, several of which can be used and which differ by the method of arc excitation and weld crater welding up. The model is based on a programmable controller. This system further includes modules of controllerized control of automatic machine electric motors with the possibility of setting and monitoring their shaft rotation frequencies, as well as welding cycle control. Each of the modules is fitted with its own power stabilizer block. All the above-mentioned is installed on a special control

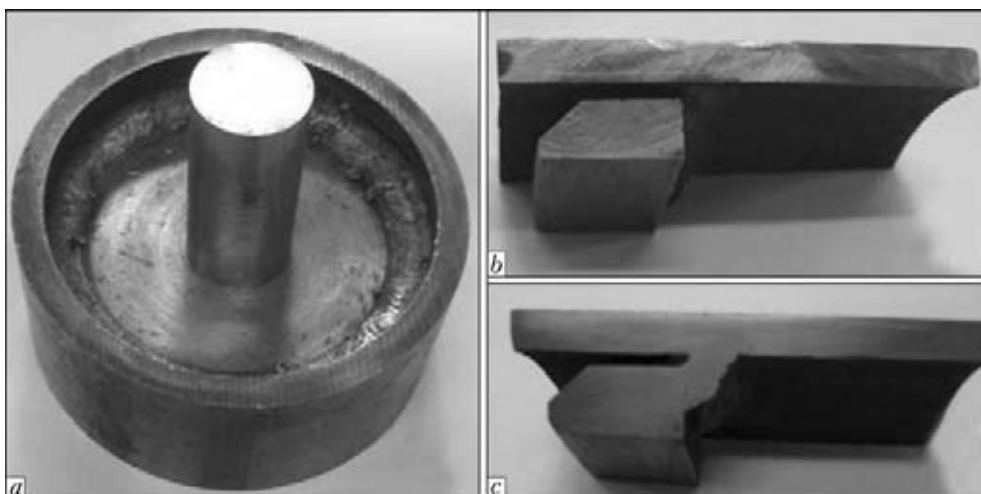


Figure 8. Results of welding the cap to pipe inner surface: *a* – circumferential weld with overlapping; *b* – actual gap between the cap and pipe; *c* – welded joint shape

panel with sealing elements (Figure 7). The same panel separately accommodates matching equipment, for instance, decoupling relays for remote control of welding current source. Front control panel carries signaling devices, elements for protection from overloads and short-circuit currents, control and adjustment elements, as well as dial monitoring instruments. Connection with the objects of control is provided through a number of connectors.

For testing and adjustment of both individual components of ADSP-200 automatic machine, and the complex as a whole, PWI developed a specialized facility, where basic technology was optimized. Deep-water technological experiments were performed in a special pressure chamber. Some test results are shown in Figure 8. Note that the welding cycle consists of two stages: cap fixing with application of the arc process preventing rotation of automatic machine with the cap relative to the pipe, and welding performance around the contour of the fixed cap with weld overlapping.

The complex has passed production trials at GFE facility (London). Obtained results showed that application of special automatic welding machine allows heat exchanger reliability to be increased, time losses for performance of work for

its sealing to be reduced, site area to be rationally used and financial losses to be reduced.

Conclusions

1. Technology and equipment are proposed, allowing performance of flux-cored wire wet automatic arc welding of structural elements, reliably insulating the lower part of heat exchanger column.

2. Automatic welding machine has been designed, which is capable of operation when immersed into a pipe of 119 mm inner diameter into liquid heat carrier at 200 m depth.

1. Savich, I.M., Smolyarko, V.B., Kamyshev, M.A. (1976) Technology and equipment for semiautomatic underwater welding of metal structures. *Neftepromysl. Stroitelstvo*, **1**, 10–11.
2. Kononenko, V.Ya., Rybchenkov, A.G. (1994) Experience of wet mechanized welding with self-shielded flux-cored wires in underwater repair of gas-and-oil pipelines. *Avtomatich. Svarka*, **9/10**, 29–32.
3. Kononenko, V.Ya., Gritsaj, P.M. (1994) Mechanized wet welding in repair of ship hulls. *Morskoj Flot*, **11/12**, 21–22.
4. Lebedev, V.K., Uzilevsky, Yu.A., Savich, I.M. et al. (1980) Analysis of possibility of self-adjustment system compensating typical disturbances of arc length in mechanized underwater welding. In: *Underwater welding and cutting of metals*, 10–23. Kiev: PWI.
5. Martinovich, V.N., Martinovich, N.P., Lebedev, V.A. et al. (2010) High-quality hose packs for underwater welding and cutting. *The Paton Welding J.*, **9**, 33–35.

Received 02.04.2014

SANITARY-HYGIENIC EVALUATION OF NOISE IN MANUAL ARC WELDING WITH COVERED ELECTRODES

O.G. LEVCHENKO¹, V.A. KULESHOV¹ and A.Yu. ARLAMOV²

¹E.O. Paton Electric Welding Institute, NASU

11 Bozhenko Str., 03680, Kiev, Ukraine. E-mail: office@paton.kiev.ua

²NTUU «Kiev Polytechnic Institute»

6/2 Dashavskaya Str., 03056, Kiev, Ukraine

Presented are the results of measurements of noise characteristics at working place at the distance of 0.55 m from welding arc using covered electrodes designed for welding carbon and low-alloyed steels. It was established that the equivalent level of sound is 83–86 dBA, and the maximum level does not exceed 93 dBA. It is shown that in welding with covered electrodes the noise level is linearly increased with increase of welding current, here the noise at the working place is mainly contributed by welding process, and the noise from current generator and ventilation equipment is in the ranges of measurements error. The data are given, which can be used for sanitary-hygienic evaluation of noise level at the working place in definite processes of arc welding. 13 Ref., 7 Tables, 1 Figure.

Keywords: electric arc welding, steel, electrodes MR-3, UONI-13/55, ANO-4, ANO-12, ANO-36, noise level, sanitary-hygienic evaluation

Welding and allied technologies remain the sources of many dangerous and harmful industrial factors, including an acoustic noise [1, 2]. From the psycho-physiological and social-economical point of view the noise is any kind of sound, harmful for health, interfering the reception of useful signals and reducing the labor efficiency of a human [3]. In the structure of professional deceases this kind of «noise decease» as deafness together with deceases of breathing organs, locomotor apparatus and with vibration decease compose the main group of deceases of industrial workers [4].

Among the 80 welding technologies in accordance with ISO 857-1:1998 [5] the excessive noise exceeding the limiting allowable level (LAL) [6] is typical of many welding processes. Thus, among methods of fusion welding the gas, laser, plasma and electric arc welding, magnetic-pulsed, percussion, ultrasonic and explosion welding from methods of pressure welding, and resistance welding from combined welding are distinguished. However, in the national publications the quantitative data about acoustic noise in welding production, as a rule, are not given [1].

The aim of the present work was the investigation of noise environment at the working place during manual arc welding with covered electrodes (MR-3, UONI-13/55, ANO-4, ANO-12,

ANO-36), designed for welding carbon and low-alloyed steels.

Methods of investigation. The levels of noise were determined in the process of manual surfacing with 4 mm diameter electrodes, having different types of coatings (Table 1), on St.3 steel plate, arranged on welding table at the operating local exhaust ventilation of 1700 m³/h efficiency and 2 kW power. Welding rectifier VDU-506 was used as a power source. Distance from the place of arcing to the nearest wall was not less than 0.5 m. The working place of a welder was at the distance of 0.55 m from welding arc.

The noise parameters were measured by integrating meter of noise level of the first class of accuracy (Bruel&Kjaer noise meter of 2230 model), the functional and technical characteristics of which are in compliance with the requirements of the interstate standards (GOST 17187–2010) of CIS countries [7]. Noise meter has a verification certificate and allows determining the noise characteristics of up to 1 dB accuracy.

Table 1. Characteristics of electrodes applied for determination of level of noise in manual surfacing

Grade	Type of coating	I_w , A
MR-3	Rutile	140–220
UONI-13/55	Basic	130–160
ANO-4	Rutile	140–210
ANO-12	Basic	140–210
ANO-36	Rutile-cellulose	130–180

Table 2. Level of background noise at the working place of welder at the distance of 0.55 m from the arc

Parameters of noise, dBA								
L_{eq}			$L_{op\ max}$			$L_{op\ min}$		
Number of measurements								
1	2	3	1	2	3	1	2	3
69.1	69.1	69.2	78.4	78.7	78.9	66.9	66.8	66.5

The measurements and sanitary-hygienic evaluation of noise at the working place were carried out in accordance with the requirements of GOST 12.1.003–83, GOST 12.1.050–86 and DSN 3.3.6.037–99 [8–10]. Duration of measurement was equal to duration of electrodes burning (about 60 s). Each measurement was three times repeated. As a component of technological noise the noise generated by the current generator and equipment of air ventilation was taken. Measurement of background noise, generated by auxiliary equipment, was made before the beginning of electric arc surfacing process. At all the measurements the noise levels with a frequency correction A (dBA), required for finding the temporary nature of noise and carrying out of sanitary-hygienic evaluation, were recorded [6]: the equivalent level of sound L_{eq} , maximum $L_{op\ max}$ and minimum $L_{op\ min}$ levels of sound pressure.

Results of investigations. The measured levels of background and technological sound at the working place of operators are given in Tables 2 and 3. Surfacing with each type of electrode was made at current almost at the level of maximum allowable welding current (see Table 3).

Let us apply the obtained results for evaluation of noise in welding L . The recorded noise is composed of noise L_w , generated by arc welding process, and background noise L_b , generated by operation of auxiliary equipment. By using the principle of additivity of power flows in the point

of measurement [11], the measuring level of noise can be determined as

$$L = L_w + 10 \lg (1 + 10^{L_b - L_w/10}). \quad (1)$$

If $L_w - L_b \geq 10$, then $L \approx L_w$, as the addition is not more than 0.4 dB and commensurable with the error of measurements. It follows from the analysis of obtained data (see Tables 2 and 3) that this condition is fulfilled for all the measurements. Consequently, the contribution of background noise can be neglected and the measuring noise as a welding one should be considered.

Let us determine the accuracy of obtained results [12]. The best estimate of measurements N of the same value L is equal to their average value:

$$\bar{L} = \sum_{i=1}^N L_i / N.$$

It can be expected that the true meaning of measuring value lies in the ranges of $\bar{L} \pm \delta\bar{L}$. The full error consists of instrumental or systematic error of noise meter $\delta L_{instr} = \pm 1$ dBA and random component of error $\delta\bar{L}_r$ whose source, in the first turn, is the non-uniformity of the technological welding process. The random error is equal to the error of mean value:

$$\delta\bar{L}_r = \sigma_{\bar{L}} = \frac{\sigma_L}{\sqrt{N}},$$

where the standard or mean-square deviation of single measurement is equal to

$$\sigma_L = \sqrt{\frac{1}{N-1} \sum_{i=1}^N (L_i - \bar{L})^2}.$$

Then the full error shall be

$$\delta\bar{L} = \sqrt{(\delta L_{instr})^2 + (\delta\bar{L}_r)^2}.$$

By assuming that $L = L_{eq}$ and $L = L_{op\ max}$ we shall find the values of appropriate errors for the data given in Table 3 (Tables 4 and 5).

Table 3. Level of technological noise at the working place of welder at the distance of 0.55 m from the arc during surfacing using electrodes of different grades

Grade of electrode	I_w, A	Parameters of noise, dBA								
		L_{eq}			$L_{op\ max}$			$L_{op\ min}$		
		Number of measurements								
		1	2	3	1	2	3	1	2	3
MR-3	200	83.1	83.4	82.7	89.6	90.1	89.9	68.3	68.4	67.9
UONI-13/55	150	82.4	82.8	82.4	90.5	90.3	91.9	68.7	69.3	69.0
ANO-4	200	86.0	85.9	86.1	89.3	90.0	90.4	70.2	69.8	70.1
ANO-12	200	84.6	84.2	84.7	92.8	92.7	93.0	69.5	69.5	69.4
ANO-36	170	83.5	83.4	83.2	92.1	89.9	91.9	68.0	67.9	68.1

Table 4. Error in measurements of equivalent level of sound, dBA

Grade of electrode	Measured L_{eq}			\bar{L}	δL_{instr}	$\bar{\delta L}_r$	$\bar{\delta L}$	Error of L_{eq} measurement
	Number of measurements							
	1	2	3					
MR-3	83.1	83.4	82.7	83.1	1	0.2	1	83 ± 1
UONI-13/55	82.4	82.8	82.4	82.5	1	0.1	1	83 ± 1
ANO-4	86.0	85.9	86.1	86.0	1	0.1	1	86 ± 1
ANO-12	84.6	84.2	84.7	84.5	1	0.2	1	85 ± 1
ANO-36	83.5	83.4	83.2	83.4	1	0.1	1	83 ± 1

Table 5. Error in measurements of maximum level of sound, dBA

Grade of electrode	$L_{op\ max}$			\bar{L}	δL_{instr}	$\bar{\delta L}_r$	$\bar{\delta L}$	Error of $L_{op\ max}$ measurement
	Number of measurements							
	1	2	3					
MR-3	89.6	90.1	89.9	89.9	1	0.1	1.0	90 ± 1
UONI-13/55	90.5	90.3	91.9	90.9	1	0.5	1.1	91 ± 1
ANO-4	89.3	90.0	90.4	89.9	1	0.3	1.0	90 ± 1
ANO-12	92.8	92.7	93.0	92.8	1	0.1	1.0	93 ± 1
ANO-36	92.1	92.0	89.9	91.3	1	0.5	1.1	91 ± 1

Table 6. Level of noise at the working place of welder at the distance of 0.55 m from the arc during surfacing using electrodes of different grades

Grade of electrode	Type of coating	I_w , A	I_s , A	L_{eq} , dBA	$L_{op\ max}$, dBA
MR-3	Rutile	140–220	200	83 ± 1	90 ± 1
UONI-13/55	Basic	130–160	150	83 ± 1	91 ± 1
ANO-4	Rutile	140–210	200	86 ± 1	90 ± 1
ANO-12	Basic	140–210	200	85 ± 1	93 ± 1
ANO-36	Rutile-cellulose	130–180	170	83 ± 1	91 ± 1

Table 7. Level of noise at the distance of 1 m from the arc in welding using electrodes MR-3 at different welding current

I_w , A	Noise parameters, dBA								
	L_{eq}			$L_{op\ max}$			$L_{op\ min}$		
	Number of measurements								
	1	2	3	1	2	3	1	2	3
150	79.8	80.3	80.2	85.9	88.9	84.9	73.6	76.4	72.1
180	81.3	81.1	81.1	85.1	85.4	85.8	79.0	78.6	78.4
210	82.7	82.4	82.4	86.0	85.9	85.6	80.3	80.3	80.1
	L_b , dBA								
	68.1	68.0	68.3	73.8	74.6	75.1	66.9	67.5	68.0

It follows from Tables 4 and 5 that the measurements error is completely determined by value of instrumental error and, consequently, the further increase in number of measurements (more than 3) will not lead to decrease of full error. As the error is equal to ± 1 dBA, the noise level is presented at an accuracy of up to 1 dBA. The total results of analysis of all the obtained data are summarized in Table 6.

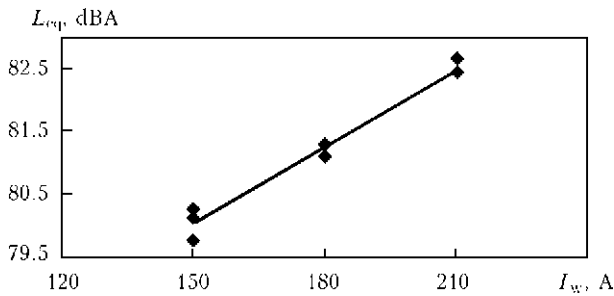
Let us consider the nature of dependence of noise level on welding current within the ranges

of its rated values for electrode MR-3, used in the widest range of welding current values (see Table 1). Results of noise measurements at the distance of 1 m from the arc are given in Table 7.

Using the least squares method [12] the following linear relationship between the obtained data was found (Figure):

$$L_{eq} = 0.04I_w + 74.056. \quad (2)$$

The square of linear correlation value $R^2 = 0.9705$ indicates the high degree of validity of



Dependence of noise level on welding current in surfacing with electrodes MR-3

the established linear dependence of noise level on welding current value. However, it is evident from the results of carried out investigations that quantitative increase in current strength has a negligible effect on noise level. Thus, the current increase by 40 % led to growth of noise level only by 2.5 %. It is clear that the level of generated noise in surfacing with electrodes of other types and at other distances from the source of noise will also depend linearly on current value, as the physical principle of occurrence and spreading of acoustic noise in arc welding at different modes is one and the same, namely: the noise level is determined by the arcing stability.

Sanitary-hygienic evaluation of noise. In accordance with the requirements of GOST 12.1.003–83 [8] let us determine the temporary nature of noise and appropriate limits for the level of acoustic parameters being examined. As the change in sound level during all the measurements exceeds 5 dBA (see Tables 2 and 3), the noise at electric arc welding should be classified as non-constant. For the non-constant noise the LAL are accepted for L_{eq} and $L_{op\ max}$. The LAL depends on kind of activity with account for difficulty and labor intensity. In the given work the manual arc welding is regarded as a physical work connected with accuracy, concentration or periodical aural control. For this kind of labor the safe L_{eq} level for personnel during 8 h working day should not exceed 80 dBA, and the maximum sound level at the working place should not exceed 110 dBA. As it follows from the measured values (see Table 6), the latter condition is fulfilled, while the noise level exceeds the standard LAL. However, it is not right to state that the LAL was exceeded [13], as the comparison should be made at a single time base equal to 8 h. However, we had a single measurement, continued only 1 min. In practice, the processes of surfacing and welding are running with intervals. Moreover, the duration of noise episodes can be much lower than 8 h, and the noise

level here is much higher than 80 dBA. The standards admit operation under the conditions of increased (more than 80 dBA noise level), but its duration should be, respectively, decreased according to the procedure regulated by GOST 12.1.050–86 [9].

Conclusions

1. It was found that electric arc process of welding with covered electrodes mainly contributes to the noise at working place and the contribution of noise generating by current generator and ventilation equipment is negligibly low and is in the ranges of measurements error.

2. The level of generated noise is growing linearly with increase of welding current value, but change of level in the range of rated current values is negligible.

3. The equivalent level of sound is in the ranges of 83–86 dBA, and the maximum level does not exceed 93 dBA. The levels of recorded noise exceed officially the LAL (80 dBA) regulated by the standard documents for this kind of labor activity at 8 h working shift. However, for the correct sanitary-hygienic evaluation it is necessary to carry out comparison at a single time base.

4. The given data can be used for sanitary-hygienic evaluation of noise episodes of definite processes of electric arc welding.

1. Levchenko, O.G. (2010) *Labor protection in welding production*: Manual. Kyiv: Osнова.
2. Encyclopedia of ILO. Welding and flame cutting. <http://base.safework.ru/iloenc>
3. Yudin, E.Ya., Borisov, L.A., Gorenshtejn, I.V. et al. (1985) *Noise control in production*: Refer. Book. Moscow: Mashinostroenie.
4. Kononova, I.G. (2010) Occupational disease of workers of machine-building enterprises. *Ukr. Zhurnal Problem Med. Pratsi*, 21(1), 9–14.
5. ISO 857-1:1998: Welding and allied processes – Vocabulary. Pt 1: Metal welding processes. Publ. 12.01.98.
6. Levchenko, O.G., Kuleshov, V.A. (2013) In-plant noise. Pt 1. *Svarshchik*, 2, 36–41.
7. GOST 17187–2010: Noise dosimeter. Pt 1: Specifications. Introd. 01.11.2012.
8. GOST 12.1.003–83: Safety general requirements. Introd. 01.07.84.
9. GOST 12.1.050–86: Methods of noise measurement on workplace. Introd. 01.01.87.
10. DSN 3.3.6.037–99: Sanitary codes of in-plant noise, ultrasound and infrasound. Introd. 01.12.99.
11. Grinchenko, V.T., Vovk, Sh.V., Matsipura, V.T. (2007) *Principles of acoustics*. Kiev: Naukova Dumka.
12. Taylor, J. (1985) *Introduction to theory of errors*. Moscow: Mir.
13. Levchenko, O.G., Kuleshov, V.A. (2013) In-plant noise. Pt 2. *Svarshchik*, 3, 44–48.

Received 17.02.2014



The 55th Anniversary of the Experimental Design Technological Bureau of the E.O. Paton Electric Welding Institute

In May, 1959 the Experimental Design Bureau (currently the State Enterprise «The Experimental Design Technological Bureau of the E.O. Paton Electric Welding Institute» – PWI EDTB) was founded with the purpose of development of new welding equipment and technologies, design-technological provision of research works and acceleration of implementation of scientific and technical developments into the national economy. EDTB was founded on the basis of developments of the design department of the Institute in prewar, further war and postwar times. The principle «laboratory–design bureau–pilot production» established by Evgeny O. Paton during foundation of the Institute, was fully realized. This close relation with practice, production, readiness to solve any tasks, put forward by the national economy, allowed EDTB to participate efficiently in creation of reliable welded structures and implementation of mechanized and automated welding processes.

Within close cooperation with the PWI scientists and specialists, branch institutes and other leading enterprises during 55 years EDTB has been designing equipment for different mechanized welding methods, testing of equipment and technology of welding, implementing the completed research developments of the Institute into industry. The main attention is paid to the complex mechanization of welding production, creation of highly-efficient machines and automated production lines.

The welding machines, developed by the EDTB designers and produced in tens of thousands by many plants, were used in such branches as construction, machine and ship building, pro-

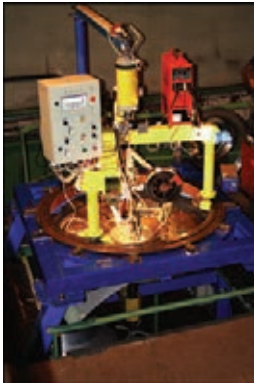


duction of pipes for main pipelines, nuclear power engineering, etc.

In different periods five Doctors and more than forty Candidates of Techn. Sci. were working at EDTB. Twenty six works, in which together with the scientists of the Institute the EDTB colleagues were participating, were awarded with two Lenin Prizes, eight USSR State Prizes, nine Prizes of the Council of Ministers of the USSR and six Prizes of the Council of Ministers of the Ukrainian SSR. 29 specialists of EDTB have a title of laureates of these prizes. Many colleagues of the EDTB were also awarded with other state prizes.

EDTB during its 55 years of activity was headed by the following members: Dr. P.I. Sevbo, a team-mate of E.O. Paton; Profs A.I. Chvertko, V.F. Moshkin, as well as S.I. Pritula and V.S. Romanyuk. During many years Dr. Vladimir E. Paton talented designer, worked as the chief of the department and later as the





EDTB Deputy Chief. At the present time EDTB is headed by G.V. Zhuk.

EDTB carries out works on the following main directions:

- technology and equipment for arc and resistance welding;
- materials, technology and equipment for mechanized surfacing and thermal spraying of wear-resistant materials;
- mechanization and automation of assembly-welding works;
- technology and equipment for welding in building and bridge construction;
- development and manufacture of automated systems for ultrasonic and eddy-current control;
- working out of design documentation and manufacture of non-standard equipment for welding production;
- complex mechanization and auxiliary equipment;
- development and manufacture of control systems for welding and surfacing equipment.

Today the welding equipment, created by the EDTB designers and technologists, is operating in on-land and underground conditions, in space and under water. This equipment is used to perform most of the technologies in welding, surfacing and spraying of different steels, cast iron, nonferrous metals, which are known to the modern science.

In close cooperation with the PWI research departments and PWI Pilot Plant of Welding Equipment, the EDTB designers and technologists in the period of 2000–2013 designed, manufactured and implemented the equipment for welding and surfacing of wide range of metals and alloys. These works were performed on the orders of enterprises and organizations of

Ukraine, the countries of near and far abroad and also order of the NAS of Ukraine and «Gosinformnauka».

EDTB during many years has been closely cooperating with many educational establishments of Ukraine, including NTTU «Kiev Polytechnic Institute». The EDTB specialists deliver lectures on welding equipment, conduct practical classes, supervise industrial and pre-graduation practice of students, head the State examination boards on defense of diploma projects.

In most cases in welding equipment, designed by EDTB, the modern design and technological solutions are applied, which allowed authors to receive hundreds of author certificates, dozens of patents and awards for the participation in national and international exhibitions. The EDTB specialists published the results of their work in hundreds of information letters and articles in the journal «Avtomaticeskaya Svarka» and other leading technical journals and, finally, the catalogue-guidebook «Welding equipment» in eleven volumes, created at EDTB, the first volume of which was published in 1968.

From the day of its foundation up to the present time the EDTB staff has always been feeling and still feels the continuous and active support of Prof. Boris E. Paton, Director of the Institute, the President of the National Academy of Sciences of Ukraine, who made great contribution to the foundation of EDTB, its formation and development.

Today EDTB is a mobile friendly team, where immense experience of veterans gained during decades, maturity of high-skilled specialists of middle-aged generation and thirst for knowledge of talented youth are closely combined.

G.V. Zhuk, PWI EDTB



Paton Turbine Technologies — new name of a well-known company

History of emergence of Paton Turbine Technologies Company, which before April 2014 operated under the name of Pratt&Whitney-Paton, dates back to the beginning of 1993. This is exactly when the E.O. Paton Electric Welding Institute (PWI) of the NAS of Ukraine and Pratt&Whitney — Division of United Technologies Corporation (UTC), USA, one of the leading world manufacturers of aircraft engines, signed an Agreement on establishing in Kiev a joint venture, which has been successfully operating for more than 20 years in the world market.

This resulted in formation of a modern high-technology company, involved both in deposition of protective coatings on blades for aviation and industrial gas turbines, and manufacturing of commercial EB-PVD equipment, evaporation materials, as well as repair of blades and other parts of various purpose turbines.

Intensive activities of the staff, as well as long-term joint work with our US partners allowed the company reaching world-class level of pro-

duction, which has been evaluated as «Silver» in ACE system of UTC competitiveness assessment that is a quite high mark.

With support and very direct involvement of Pratt&Whitney, the JV has been certified to all the necessary international standards, that allowed it to successfully operate in the world markets of aviation and power gas turbine construction.

Company customers include such well-known names as Pratt&Whitney (USA), Siemens (Sweden), Honeywell (USA), Rolls Royce (UK), Turbine Overhaul Services (Singapore), Kawasaki Heavy Industries (Japan), Permskie Motory (Russia), Mayer Tools (USA), Glen Group (USA) etc., as well as Ukrainian enterprises operating in the field of gas turbine construction, aircraft repair and gas transportation.

In March, 2014 United Technologies Corporation, one of the founders, left Pratt&Whitney-Paton JV, in connection with global change of its business strategy, which was followed by the



Protective coating shop



Paton Turbine Technologies Certificates ISO 9001:2008 and AS 9100C-JISQ 9100:2009

Company changing its name to Paton Turbine Technologies (PTT). Company sphere of activity, standards and management system, including quality management system, and customers, remained the same.

Quality management system (QMS) is based on the requirements of international general technical standard ISO 9001, as well as international aerospace standard AS9100, which is harmonized with EN 9100 and JIS Q 9100 standards. The Company is certified as overseas repair station for compliance with US Federal Aviation Regulations CFR FAR145. Availability of such a certificate allows performance of work on maintenance

of aviation equipment, registered in the USA. Starting from 2006 the Company takes part in the US National Program on accreditation and qualification of processes in the defense and aerospace industries – Nadcap. In July 2014, PTT successfully passed the regular audit on this Program, that once more confirmed the high international technical level of organization of production in the Company.

Company personnel are highly-qualified workers, engineers, researchers and office workers, who continuously improve their skills and performance through various courses and training programs. Program of personnel training in keep-



Designed and manufactured at Pratt&Whitney-Paton EB unit for deposition of protective coatings on aircraft gas turbine blades at customer facility



ing with the requirements of US Federal Aviation Agency has been introduced and is running in the Company.

PTT now manufactures products and provides services with optimum price-quality ratio in the following business segments:

- EB deposition of metal and ceramic coatings on blades of various-purpose gas turbines;
- design, manufacture and servicing of EB equipment for coating deposition;
- production of consumable materials (ceramic and metal ingots) for deposition of EB coatings;
- comprehensive reconditioning of gas turbine engine components with application of classical (welding, brazing, microplasma) and original (EB PVD) repair technologies;
- engineering of processes, materials and equipment.

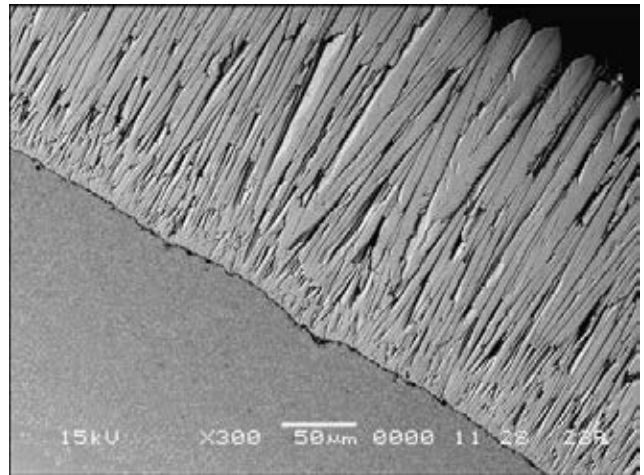
Thermal barrier coatings of up to 200 μm thickness proposed to customers by PTT are applied by EB PVD of ceramic ingots, mainly of zirconium dioxide. Coatings have columnar structure with specified thickness distribution over the cross-section, that ensures excellent performance of coatings on turbine parts exposed to both mechanical and temperature cyclic loads.

It should be noted that achieving the specified distribution of coating thickness on turbine blades is a complex engineering problem that is successfully solved due to many years of experience of our staff.

The Company developed technology of deposition of coatings based also on other oxides that appears to be promising for protection of aircraft turbine parts with increased working temperatures.

Application of protective ceramic coating requires presence of a bond coat on the part surface that ensures both adhesion of thermal barrier ceramic layer to part surface, and its protection from the impact of turbine aggressive working environment. Technologies developed in the Company (surface preparation, heat treatment, EB deposition, etc.) allow deposition of both only the ceramic coating on parts, which already have a bond coat, and of two-layer coating (metal + ceramic). The most wide-spread combinations are bond coat from nickel aluminide (or platinum), as well as nickel, cobalt and chromium alloys, doped by aluminium and yttrium (MCrAlY). Deposition of purely metal protective coatings of various composition is also performed.

Procedures of deposition of structural coatings, for instance from titanium alloys, to restore the shape of worn fan blades have been mastered.



Typical microstructure of thermal barrier coating

In this case, EB PVD technology with ionization of evaporation metal can be applied that allows an abrupt increase of coating adhesion to the base of the parts being reconditioned.

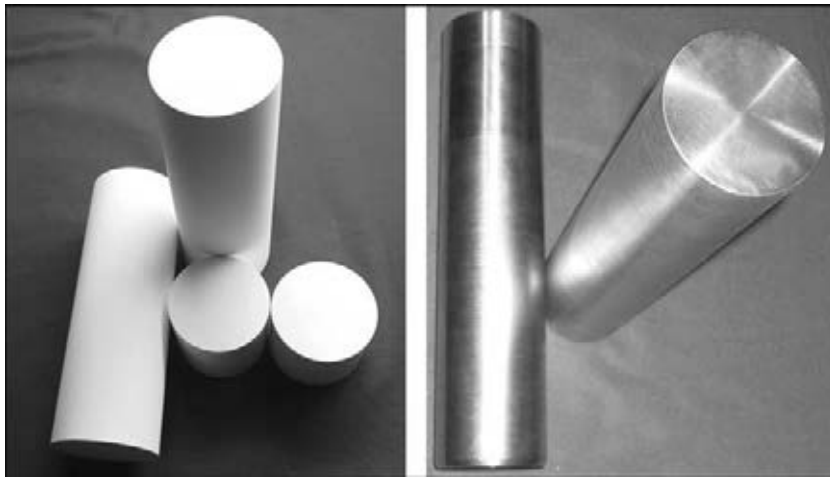
Over many years of working in the market, the Company has acquired experience of coating deposition on parts of various types of gas turbines, including their aircraft, land and navy variants. Here are some of them: PW4000, JT9D-7Q, JT9D-7R4, PW4090, CF6-80C2, G61, CFM56-5B, CFM56-7B, GTX100, PS90A, PS90GP, V84.3A2, V94.3A2, etc.

PTT Company can rightfully be regarded as one of the reliable producers of world-class commercial EB PVD equipment for deposition of ceramic and metal coatings. Our equipment is running successfully in the US and Singapore. We provide servicing of our equipment and supply spares and consumables.

As was noted above, PTT produces high-quality ceramic and metal ingots, which are both used



Commercial gas turbine blade with thermal barrier coating



Ceramic (*left*) and metal (*right*) ingots

in its own production, and are supplied to customers as a separate product.

Ceramic ingots are made by special methods of compacting oxide powders of the required composition with subsequent high-temperature sintering. The most widely accepted type of materials is zirconium dioxide, partially stabilized by yttrium oxide ($ZrO_2-6-8\% Y_2O_3$). Manufacturing technology ensures ingot density on the level of $3.6-4.2\text{ g/cm}^3$.

Metal ingots are made by vacuum-induction melting with double EB remelting that provides high quality of billets for subsequent evaporation in vacuum. Ingot manufacturing to customer specification is possible.

The Company has been developing technology and performing repair of components of aircraft and land gas turbine engines starting from 2001. Many years of practical experience of operation and high professional level of personnel, application of high technologies and unique specialized equipment, high quality standards and efficient management system allow the Company to satisfy customer requirements to the maximum both in terms of quality, and in terms of economic

efficiency (terms, volume, price). Nowadays customers are offered a complete range of repair operations, including those with application of EB technology of deposition of high-temperature MeCrAlY and thermal barrier $ZrO_2-7\% Y_2O_3$ coatings.

Availability of an up-to-date laboratory of metallographic examination, directly integrated into the technological process, equipment and instruments applied for nondestructive and destructive testing, in addition to highly qualified personnel, enables PTT maintaining and developing reliable manufacturing with invariably high product quality. Company laboratory has been certified in the LCS system, applied at UTC, and has confirmed its compliance to the requirements of Nadcap Program.

One can see from the above-said that Paton Turbine Technologies Company is a reliable partner, which successfully operates in Ukraine in compliance with the best world business practices.

*Prof. G.S. Marinsky,
Director of PTT Company
www.patontt.com*